

# Structural Performance Evaluation of Interlocking Concrete Pavement Crosswalk Designs

by

Sudip L. Adhikari

A thesis  
presented to the University of Waterloo  
in fulfillment of the  
thesis requirement for the degree of  
Master of Applied Science  
in  
Civil Engineering

Waterloo, Ontario, Canada, 2008

©Sudip L. Adhikari 2008

## **AUTHOR'S DECLARATION**

I hereby declare that I am the sole author of this thesis. This is a true copy of the thesis, including any required final revisions, as accepted by my examiners.

I understand that my thesis may be made electronically available to the public.

## **Abstract**

Interlocking Concrete Pavements (ICP) have been successfully used in many pavement applications all across the world. ICP design and analysis methods, construction practices and materials specifications have been developed. However, there is very limited field data to quantify structural performance with respect to traffic and environmental loadings. The interaction between traffic loadings and environmental factors needs to be explored in order to improve relationships between pavement performance and response.

Pavement performance prediction in terms of fatigue cracking and surface rutting are essential for any mechanistically-based pavement design method. The estimation of the expected fatigue performance in the field is based on the quantification of the maximum tensile strain in bound base layers and the expected rutting performance is based on maximum vertical stress/strain in granular layers.

This thesis presents an innovative research project involving the design, construction, instrumentation, performance modeling and distress evaluation of seven ICP crosswalks with four different design assemblies. The research projects were constructed at the Centre for Pavement and Transportation Technology (CPATT) test track and at the University of Waterloo ring road. Each of the test sections is instrumented with structural and environmental sensors of sensors to monitor the pavement performance under heavy truck traffic, typical municipal loadings and to quantify environmental effects. A database is generated and the measured stress, strain, temperature and moisture measurements are analysed to evaluate the expected long-term performance of the structural components of ICP crosswalk designs.

## **Acknowledgements**

First of all I would like to express my sincere gratitude to my supervisor Professor Susan Tighe, for her invaluable guidance, full support and constant encouragement throughout this research.

I would like to express my deepest appreciation to Interlocking Concrete Pavement Institute (ICPI) for providing funding to this study. I would also like to convey my special thanks to Robert Burak, Director of Engineering of ICPI for his constructive suggestions and continuous encouragement. In addition, special appreciation is extended to Ross Yantzi, Steve Lange, Jason Bell from Ross Yantzi's Pavestone Plus Limited, Gary Kosar from the University of Waterloo Plant Operations, and Cameron Becker from Steed and Evans for their assistance in construction and instrumentation.

Many thanks to CPATT co-op students Eugene Kim, Xin Xu, Vimi Henderson and Rabiah Rizbi and graduate students Fazal Mabood, Alauddin Ahammed and James Smith for their support during construction and instrumentation.

My special thanks Jodi Norris, CPATT research technician and Terry Ridgway, Civil Engineering technologist for helping with field work and data collection. Many thanks to fellow graduate students at Transportation Group for their friendship and support.

Finally, I would like to thank my wife Jyoti Sharma for her unconditional love, support and patience.

## Table of Contents

List of Figures .....	vii
List of Tables .....	xi
Chapter 1 Introduction.....	1
1.1 Background .....	1
1.2 Research Scopes and Objectives .....	1
1.3 Methodology .....	2
1.4 Thesis Organisation .....	3
Chapter 2 Literature Review .....	4
2.1 ICP Components.....	4
2.1.1 Interlocking Concrete Paver (ICP) .....	4
2.1.2 Laying Patterns.....	5
2.1.3 Bedding Sand and Jointing Sands .....	6
2.1.4 Edge Restraints .....	7
2.1.5 Geotextile .....	7
2.1.6 Drainage .....	8
2.1.7 Base .....	8
2.1.8 Subbase.....	8
2.1.9 Subgrade.....	9
2.2 Interlocking Concrete Pavement Design .....	9
2.3 Performance Criteria .....	11
2.3.1 Parameters Influencing ICP Performance .....	13
Chapter 3 Construction of Test Sections .....	17
3.1 Description of the Test Sites.....	17
3.1.1 CPATT Test Track .....	17
3.1.2 University of Waterloo Ring Road.....	34
Chapter 4 Instrumentation .....	49
4.1 CPATT Test Track .....	49
4.1.1 Moisture Probe .....	50
4.1.2 Earth Pressure Cells.....	52
4.1.3 Temperature Probe .....	52
4.1.4 Vibrating Wire Strain Gauges .....	53

4.1.5 Data logger Installation.....	59
4.2 University of Waterloo Ring Road .....	60
4.2.1 Data Logger Installation.....	65
4.3 Sensors Validation .....	65
Chapter 5 Data Analysis .....	66
5.1 Data Collection .....	66
5.1.1 Traffic .....	66
5.1.2 Horizontal Strain.....	66
5.1.3 Vertical Stress .....	67
5.1.4 Temperature .....	67
5.1.5 Moisture .....	68
5.2 Pavement Response .....	68
5.2.1 Test Track .....	68
5.2.2 UW Ring Road.....	74
5.3 Prediction Models .....	77
5.3.1 CPATT Test Track.....	78
5.3.2 UW Ring Road.....	83
Chapter 6 Pavement Distress Condition Evaluation .....	86
Chapter 7 Conclusions and Recommendations .....	101
7.1 Conclusions.....	101
7.2 Recommendations.....	102
References.....	103

## List of Figures

Figure 1: Typical Components of Interlocking Concrete Pavements (Chung, 2005) .....	5
Figure 2: Typical ICP Laying Patterns .....	15
Figure 3: Region of Waterloo Waste Management Facility, CPATT Test Track and Crosswalk .....	18
Figure 4: CPATT Test Track.....	18
Figure 5: Existing CPATT Test Track Cross Section .....	19
Figure 6: Layout of CPATT Test Track Crosswalk Projects .....	20
Figure 7: SSCBCH Crosswalk Cross Section .....	21
Figure 8: SSABSH Crosswalk Cross Section .....	22
Figure 9: BSCBCH Crosswalk Cross Section.....	23
Figure 10: Sailor Course with 45 Herringbone Pattern .....	24
Figure 11: Soldier Course with 45 <sup>0</sup> Herringbone Pattern.....	24
Figure 12: Excavation of Existing Asphalt Pavement.....	26
Figure 13: Concrete Placement on BSCBCH.....	27
Figure 14: SSCBCH Base Section .....	28
Figure 15: SSABSH Base Section.....	28
Figure 16: Formworks, Drain Pipes and Reinforcement Bars for BSCBCH .....	29
Figure 17: Bedding Sand and Non-Woven Geotextile .....	30
Figure 18: Physical Characteristics of a Concrete Paver.....	31
Figure 19: ICP Placement.....	31
Figure 20: On-site Concrete Air-Void Testing.....	32
Figure 21: A Cylinder after Compressive Strength Testing .....	33
Figure 22: Compressive Strength Testing Results .....	33
Figure 23: UW Ring Road and Crosswalks Project Location (Source: Google Earth).....	34
Figure 24: UW Ring Road Cross Section.....	35
Figure 25: Layout of Crosswalk Sections at UW Ring Road.....	36
Figure 26: SSCBCH Crosswalk Section .....	37
Figure 27: BSCBCH Crosswalk Section .....	38
Figure 28: SSABAH Crosswalk Section.....	39
Figure 29: SSGBCH Crosswalk Section .....	40
Figure 30: Formworks, Drainage Pipes and Reinforcement Bars for SSCBCH Section .....	43
Figure 31: Concrete Placement on SSCBCH Section .....	44

Figure 32: Concrete Base Section.....	45
Figure 33: Asphalt Base Construction .....	45
Figure 34: Granular Base Construction .....	46
Figure 35: Interlocking Concrete Pavers Placement.....	47
Figure 36: On Site Concrete Slump Testing .....	48
Figure 37: Compressive Stress Testing Results.....	48
Figure 38: Moisture Probes.....	51
Figure 39: Moisture Probes Installation.....	51
Figure 40: Earth Pressure Cells Installation.....	52
Figure 41: Temperature Probe Installation .....	53
Figure 42: Vibrating Wire Asphalt Strain Gauge .....	54
Figure 43: Vibrating Wire Concrete Strain Gauge .....	54
Figure 44: Vibrating Wire Asphalt Strain Gauge Installation .....	55
Figure 45: Vibrating Wire Concrete Strain Gauge Installation .....	55
Figure 46: Profile View of Instrumented SSCBCH.....	56
Figure 47: Instrumented View of SSABSH.....	57
Figure 48: Profile View of Instrumented BSCBCH .....	58
Figure 49: Conduit and Data Logger Layout .....	59
Figure 50: Profile View of Instrumented SSCBCH.....	61
Figure 51: Profile View of Instrumented BSCBCH .....	62
Figure 52: Profile View of Instrumented SSABAH .....	63
Figure 53: Profile View of Instrumented SSGBCH.....	64
Figure 54: Conduits and Data Logger Layout .....	65
Figure 55: Sensors Functionality Validation .....	65
Figure 56: Measured Vertical Stress and Moisture Variation in Subbase of SSCBCH.....	69
Figure 57: Accumulation of Horizontal Strain and Temperature Variation in Base of SSCBCH.....	69
Figure 58: Accumulated Vertical Stress and Moisture Variation in Subbase of SSABSH .....	70
Figure 59: Accumulated Horizontal Strain and Temperature Variation in Base of SSABSH.....	71
Figure 60: Accumulation of Vertical Stress in Subbase of BSCBCH .....	72
Figure 61: Accumulation of Horizontal Strain in Base of BSCBCH.....	72
Figure 62: Accumulated Vertical Stress in Subbase in All Crosswalks .....	73
Figure 63: Accumulated Horizontal Strain in Base in All Crosswalks.....	73

Figure 64: Accumulated Horizontal Strain and Temperature and Moisture Variation in SSCBCH....	74
Figure 65: Accumulated Horizontal Strain and Temperature and Moisture Variation in BSCBCH....	75
Figure 66: Accumulated Horizontal Strain and Temperature and Moisture Variation in SSABAH....	76
Figure 67: Accumulated Horizontal Strain in All Crosswalk Sections .....	76
Figure 68: Vertical Stress Prediction Model of SSCBCH.....	79
Figure 69: Fatigue Cracking Prediction Model of SSCBCH.....	79
Figure 70: Vertical Stress Prediction Model of SSABSH.....	81
Figure 71: Fatigue Cracking Prediction Model of SSABSH.....	81
Figure 72: Vertical Stress Prediction Model of BSCBCH .....	82
Figure 73: Fatigue Cracking Prediction Model of BSCBCH .....	82
Figure 74: Fatigue Cracking Prediction Model for SSCBCH .....	83
Figure 75: Fatigue Cracking Prediction Model of BSCBCH .....	84
Figure 76: Fatigue Cracking Prediction Model of SSABAH .....	85
Figure 77: Rut Profile along Sailor Course in SSCBCH.....	91
Figure 78: Rut Profile along Southbound Wheelpath in SSCBCH .....	91
Figure 79: Depressions, Ruttings and Joint Sand Loss and in SSCBCH .....	91
Figure 80: Longitudinal Profile along Sailor and Soldier Courses in SSABSH .....	92
Figure 81: Rut Profile in Southbound Wheelpath in SSABSH .....	92
Figure 82: Depressions, Ruttings and Joint Sand Loss in SSABSH .....	92
Figure 83: Rut Profile along Sailor and Soldier Courses in BSCBCH.....	93
Figure 84: Rut Profile in Southbound Wheelpath in BSCBCH .....	93
Figure 85: No Distresses in BSCBCH.....	93
Figure 86: Rut Profile along Sailor Courses in SSCBCH .....	96
Figure 87: Rut Profile in Wheelpaths in SSCBCH.....	97
Figure 89: Depressions, Ruttings and Heaves in SSCBCH.....	97
Figure 90: Profile along Sailor and Soldier Courses in BSCBCH .....	97
Figure 91: Rut Profile in Wheelpaths in BSCBCH.....	98
Figure 92: No Visual Distresses in BSCBCH .....	98
Figure 93: Rut Profile along Sailor and Soldier Courses in SSABAH.....	98
Figure 94: Rut Profile in Wheelpaths in SSABAH .....	99
Figure 95: Depressions and Ruttings in SSABAH.....	99
Figure 96: Rut Profile in Sailor and Soldier Courses in SSGBCH .....	99

Figure 97: Rut Profile in Wheelpaths in SSGBCH..... 100  
Figure 98: Uniform Deformations and Cracks on Concrete Headers in SSGBCH ..... 100

## List of Tables

Table 1: Summary of Construction .....	25
Table 2: Gradation of Bedding Sand .....	30
Table 3: Summary of Construction .....	41
Table 4: Summary of Instrumentation.....	49
Table 5: Summary of Instrumentation.....	60
Table 6: Summary of Permissible ESLAs, Stress and Strain .....	80
Table 7: Summary of Permissible ESALs and Strain.....	85
Table 8: Summary of Pavement Condition Evaluation in Test Track Sections .....	88
Table 9: Summary of Pavement Condition Evaluation in Ring Road Sections .....	94



# Chapter 1

## Introduction

### 1.1 Background

In many parts of the world Interlocking Concrete Pavement (ICP) is rapidly gaining popularity for roads, airports and industrial pavements. The history of ICP dates back to 19<sup>th</sup> Century when paving stones were used in European countries for construction of roads serving as footpaths and tracks for steel-wheeled vehicles. The use of small stone elements to create a hard surface for roads or pavements is an ancient tradition dating back to Greek and Roman times. The successful use of ICP occurred in post war Holland in the late 1940's as a replacement for clay brick streets. From the 1950s onwards there was a steady evolution of this technology and much of the development took place in Germany. For the past 50 years, significant research activities for the development is going on in many countries, including Argentina, Australia, Canada, France, Germany, Israel, Japan, the Netherlands, New Zealand, South Africa, the UK and the USA (Panda, 1999).

ICP was introduced in North America in the mid 1970s and have been successfully used in many pavement applications. Currently, there are approximately 60 million square meters and 300 million square meters of concrete pavers are produced annually in North America and Europe respectively (Tighe, 2004). There are a wide range of ICP applications including city streets, driveways, crosswalks, sidewalks, parking areas, ports, container terminals, and airports.

ICP have several advantages, including resistance to freeze-thaw and deicing salts, high abrasion and skid resistance, no need for heavy construction equipment, ease of maintenance and low maintenance cost, no thermal expansion and contraction of concrete pavers, instant opening to traffic, accommodates higher elastic deflections without failure, access to utilities, protection from fuel and oil spillage, and environmentally friendly technology.

### 1.2 Research Scopes and Objectives

This research is carried out in a partnership between the Interlocking Concrete Pavement Institute (ICPI) and the Centre for Pavement and Transportation Technology (CPATT) located at the University of Waterloo.

Although the interlocking concrete pavers have provided many benefits, there is some evidence of early failures with respect to use in crosswalks. There have been varying failure modes noticed and there needs to be a better understanding of the various design aspects of using ICP in crosswalks.

The main objectives of the research project are:

- To define the mechanics of failure for ICP crosswalk designs with various bases and setting beds
- To quantify the threshold value for type and/or number of axle loads (ESALs) for various crosswalk assemblies.
- To validate current industry crosswalk designs and recommend new designs (or modifications to existing designs) as needed based upon the load/traffic/environment/failure modes from the study.
- To offer the designer/city/municipality/DOT at a higher level of confidence on long term crosswalk performance.

In short the research will offer design professionals with guidance on design protocols and performance of ICP crosswalks for various loading conditions.

### **1.3 Methodology**

For the purpose of assessing structural performance of different crosswalk designs of ICP, seven crosswalks with different bases and bedding layers were constructed at two locations in Waterloo. The first three sections are located at the Centre for Pavement and Transportation Technology (CPATT) test track in the south east corner of the Regional Municipalities of Waterloo Waste Management Facility. The second test site with four test sections is located at North Campus Gate intersection on the University of Waterloo Ring Road. The test sections are instrumented with four sets of sensors at test track and three sets of sensors on Ring Road, to monitor the pavement performance under heavy truck traffic, typical municipal loadings and to quantify environmental effects. The sensors include vibrating wire strain gauges, earth pressure cells, and temperature and moisture probes. Data is collected at four hour intervals and includes stresses, strains and temperature. Moisture data is collected on weekly basis. A database is being generated for all seven sections and the measured stress, strain, temperature and moisture measurements are analysed to evaluate the expected long-term performance of the structural components of ICP crosswalk designs. Traffic data

at test track was obtained from Region of Waterloo waste management automation system. Pavement predictive models are developed based on measured structural and environmental parameters to describe the pavement performance.

In addition, routine performance testing including distress (type, severity, density) survey was carried out on a regular basis on accordance with Interlocking Concrete Block Pavement Institute Distress Guide developed by ICPI. The total of eleven types of surface distresses evaluated separately for each test sections. The degree of distress is rated high, medium, or low based on Pavement Condition Index (PCI) numerical indicator.

## **1.4 Thesis Organisation**

This thesis consists of seven chapters, and the contents of each chapter are explained as follows:

CHAPTER 1: This introductory chapter highlights the background of the development of Interlocking Concrete Pavement (ICP) throughout world. The chapter also summarises the objective, and scope and methodology of assessment of the study.

CHAPTER 2: This chapter presents a literature review that covers the components of ICP, design methodology, and the parameters affecting the performance of the pavement.

CHAPTER 3: Chapter three explains the site description, pavement structure, and the construction process of seven test sections at two locations.

CHAPTER 4: Chapter four discusses the instrumentation types and installation effort.

CHAPTER 5: This chapter presents the data collection, monitoring and analysis. This chapter also explains pavement response under traffic and environmental loadings.

CHAPTER 6: Chapter six details the pavement distress condition survey, surface distress types and severity and the rating results.

CHAPTER 7: This chapter summarizes the main conclusions of this research and recommendations.

## **Chapter 2**

### **Literature Review**

Interlocking Concrete Pavement (ICP) differs from other forms of pavement in that the wearing surface is made from small paving units bedded and jointed in sand rather than continuous paving. Beneath the bedding sand, the substructure is similar to that of a conventional flexible pavement. The material of concrete block pavement is rigid, but the construction is flexible pavement (Hasanan, 2005).

In ICP, the blocks are a major load-spreading component which is comprised of concrete blocks bedded and jointed in sand. Interlock has been defined as the inability of an individual paver to move independently of its neighbours and has been categorized as having three components: horizontal, rotational, vertical. Interlock is of major importance for the prevention of movement of pavers horizontally when trafficked (Knapton, 1979).

#### **2.1 ICP Components**

An ICP is a flexible pavement in which the surfacing consists of concrete pavers laid on a thin layer of sand referred to as the laying course or bedding sand (Beauty, 1992). The base layer can be constructed using untreated aggregate, asphalt treated base or cement treated base. If either an asphalt base or cement treated base is used a granular subbase layer maybe placed underneath the treated base layer. A typical ICP cross-section of an ICP is shown in Figure 1.

##### **2.1.1 Interlocking Concrete Paver (ICP)**

Interlocking concrete paver is a unique material, exhibiting important differences to other small element paving such as stone and clay, as well as to form-less materials such as asphalt and in-situ concrete. It provides a hard surface which is good to look at, comfortable to walk on, extremely durable and easy to maintain. It adds a richness, complexity and human scale to any setting (Bin, 2006). The pavers are structural elements designed to be placed together with paver to paver joints filled so as to develop frictional interlock.

The concrete paving blocks used typically are 200 mm to 250 mm long and 100 mm to 112 mm wide. The thickness of the blocks used ranges from 60 mm to 100 mm, depending on the traffic intensity. The paving blocks are typically installed on a sand bed 20 mm to 40 mm thick, separated by sand joints of 2 mm to 4 mm (Koon, 2000).

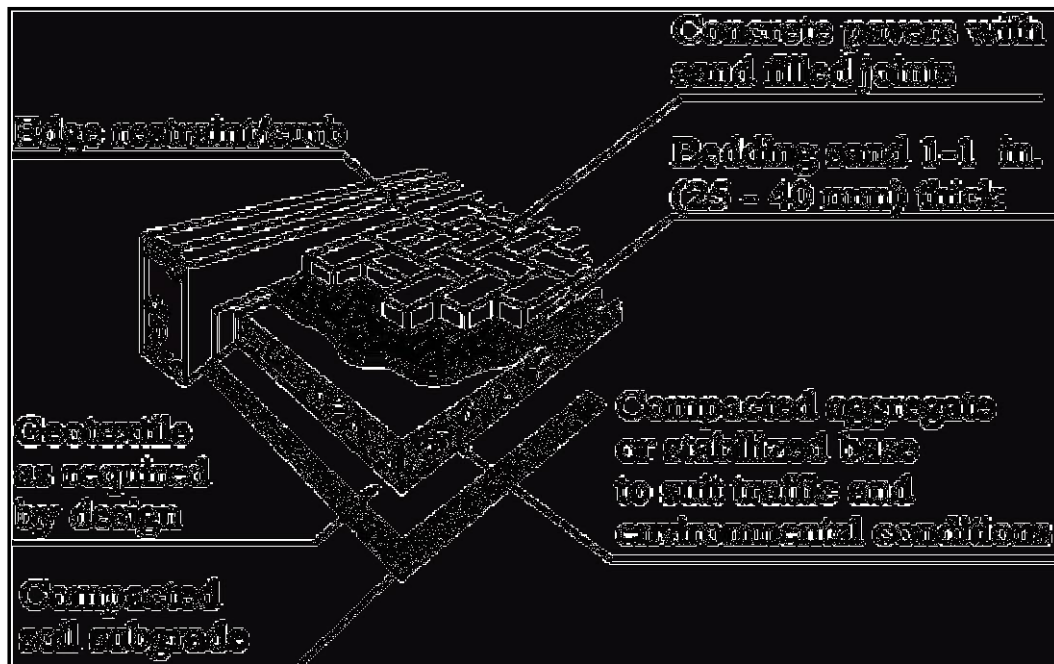


**Figure 1: Typical Components of Interlocking Concrete Pavements (Chung, 2005)**

Accelerated trafficking studies in Australia, South Africa, Japan, France and the USA have shown that pavement performance is influenced by the shape of the pavers in respect of both horizontal and vertical deformations (Shackel, 1979). The pavers may be rectangular or one of more than two hundred proprietary shapes. Three categories of paver shape have been recognized (Morrish, 1980). Category A comprises dentate blocks which key into each other on all four faces. Category B comprises dentated blocks which key into one another on two faces only and category C comprises non-dentated blocks which do not key together geometrically.

The rectangular concrete pavers consist of spacer bars to secure a space between adjoining paver units which protrude not more than 2mm from the sides of the pavers. The spacers ensure that there is a minimum joint width and allows joint sand to enter and reduces the likelihood of edge spalling. The spacer bars are recommended to extend the full height of the paver, i.e., from bottom to the top (ICPI, 2004).

### **2.1.2 Laying Patterns**

The laying pattern chosen for the ICP to support traffic loads should be resistant to horizontal creep. Many of the paver shapes can be installed in a variety of patterns. The most commonly used patterns are herringbone, stretcher, basket-weave and parquet bonds. Accelerated trafficking tests

have been used to compare the performance of these patterns. In general, the best level of performance is found in pavements laid herringbone bond, where as the greatest deformations are associated with stretcher bond pattern (Shackel, 1980). The Herringbone pattern can have three orientations relative to the direction of traffic. It should be laid at  $45^{\circ}$  to the traffic to resist the traffic shear stresses. Sailor and soldier courses can be placed against edge restraint to further prevent the surface from the formation of shear plane.

### **2.1.3 Bedding Sand and Jointing Sands**

It has been demonstrated that the bedding and jointing sands play a crucial role in controlling the response of interlocking concrete pavement. The bedding sand layer in ICP is included to provide a smooth, level running surface for placing the paver sand act as a barrier against the propagation of cracks from the base to the pavement surface. The horizontal forces developed between the paving blocks from repeated loading cause the sand to dilate. Thus the load is distributed to the adjoining paving blocks and the paving blocks behave as a load-bearing layer (Koon, 2000).

European practices (Eisenmenn 1988; Lilley 1988; Hurmann 1997) specify a bedding sand thickness after compaction of 50 mm, whereas compacted bedding sand thickness of 20 to 30 mm is used in the United States (Rada, 1990) and Australia (Shackel, 1993). Simmons (1979) recommended a minimum compacted sand depth of 40 mm to accommodate free movement of paving units under initial traffic. Mavin (1980) specified a compacted bedding sand depth of  $30 \pm 10$  mm, keeping 10 mm tolerance on sub-base.

Jointing sand is the main component of ICP, and plays a major role in promoting load transfer between blocks ultimately in spreading the load to larger areas in lower layers. Spacing between pavers showed a significant influence on the structural performance of block surfacing. Pavers laid too close together become overstressed and spall when in contact. However, the structural capability of the surfacing decreases if the joint width exceeds 5 mm (Lilley, 1994). For optimum load spreading by friction, it is necessary to provide uniform, narrow, and fully filled joints of widths between 2 and 4 mm (Shackel, 1993; Hurman, 1997). Knapton and O'Grady (1983) recommended joint widths between 0.5 and 5 mm for better pavement performance. Joint widths ranging from 2 mm and 8 mm are often used, depending upon the shape of pavers, laying pattern, aesthetic considerations, and application areas.

In most of the pavements, the sand used for bedding course is also used in joint filling (Lilley, 1980; Hurmann, 1997). As reported by Shackel (1980), a finer jointing sand having a maximum particle size of 1.18 mm and less than 20 % passing the 75 µm sieve has performed well.

Barber and Knapton (1980) have reported that, in an ICP subjected to truck traffic, a significant proportion of the initial deformation occurred in the bedding sand layer which had a compacted thickness of 40 mm. similar results have been reported by Seddon (1980). These investigations tend to confirm the findings of the earlier Australian study (1989) which demonstrated that a reduction in the loose thickness of the bedding sand from 30 mm to 50 mm was beneficial to the deformation (rutting) behaviour of ICP.

#### **2.1.4 Edge Restraints**

Edge restraints are a key part of ICP, are used at the interfaces with asphalt or concrete pavements. Edge restraints resist lateral movement, prevent rotation of the pavers under load and restrict loss of bedding sand material at the boundaries. Edge restraints are designed to remain stationary while receiving impacts during installation, from traffic loads and freeze-thaw cycles.

Edge restraints should be laid at all boundaries of the paved area or between the joints of the edge restraints. There are two general types of edge restraints. Those made elsewhere and installed at the site include precast concrete, plastic, cut stone, aluminum and steel. Restraints formed on-site are made of poured-in-place concrete (ICPI, 2006).

The concrete edge restraints generally extend the depth of the base materials. However, partial depth precast concrete may be used for residential and light duty commercial applications. Precast concrete and plastic edge restraints must be firmly anchored on a compacted base with steel spikes. L-shaped aluminum or steel edging can be used to provide smooth vertical surface against pavers and additional stability and should be anchored with stakes or spikes into the base course. Poured-in-place concrete edge restraint is suitable for pavers subjected to pedestrian traffic and for residential driveways and should extend well below the sand bedding layer. Exposed concrete edge is trimmed to reduce the likelihood of the chipping.

#### **2.1.5 Geotextile**

If there is a possibility of sand loss from beneath the pavers, geotextile is recommended to prevent its migration. As a separation layer, they prevent soil from being pressed into base under loads,

especially when saturated, thereby reducing the likelihood of rutting (ICPI, 2003). The filter cloth is can be applied along the base and turned up along the dies of the edge restraints. The geotextile generally is not required across the entire surface of an aggregate base, nor should it be placed on the top of the bedding sand (ICPI, 2006).

### **2.1.6 Drainage**

Drainage pipes should be installed perpendicular to the road surface at the lowest level of the concrete and asphalt bases before the construction of headers, curbs and bases. The pipes are filled with pea gravel and covered with geotextile to prevent the loss of bedding materials. Their purpose is to remove excess water from the base course. The drainage pipes are not required for the aggregate base pavement design.

### **2.1.7 Base**

The base is the main structural element in an ICP. A wide range of materials are suitable for use as the base in ICP. The base layer can be constructed using untreated aggregate, asphalt concrete, cement stabilized granular materials and lean concrete.

Comparisons have been made of the performance under traffic of ICP laid on various types of bases. For identical base and pavement thickness the best levels of performance are usually achieved by using cement-treated bases followed by the use granular base (Shackel, 1980).

The surface of the bas is shaped to the required finished profile of the road surface, including a minimum crossfall for surface drainage of 2.5% and the tolerance on the finished surface should be +/-15mm (Beaty, 1992).

### **2.1.8 Subbase**

The layer directly below the base is known as subbase. Its purpose is to transfer traffic imposed loads from overlying structures to the supporting embankment. The subbase layer is usually consists of an unbound layer, although cement bound materials are sometimes used. In some situations, where the subgrade has a high load bearing capacity or where anticipated traffic loading is reasonably light the subbase may be omitted.

### **2.1.9 Subgrade**

The strength of the subgrade is a key factor in the design of ICP. The characteristics and behavior of subgrade soils have a major influence in the design and performance of flexible pavement systems. In general, the weaker the subgrade, the greater the thickness of pavement required. Many procedures for establishing this design factor are available: e.g., estimates made by the engineer based on experience, soil-type-to-strength correlations, laboratory tests, and in situ evaluation methods such as dynamic deflection tests (Rada, 1990). The method most widely used to characterize the bearing capacity of subgrade is the California Bearing Ratio (CBR) test.

## **2.2 Interlocking Concrete Pavement Design**

Several methods for designing ICP for roads and streets are presently available. Most of the methods are the extensions of flexible pavement design methods because the load distribution and failure modes of ICP and flexible pavement are very similar: permanent deformation from repetitive loads. There are a number of limitations associated with each, including inadequate characterization of the subgrade soil and paving materials, lack of pavement performance prediction capabilities, and inability to specify desired pavement failure and reliability level (Rada, 1990). All recognize the need to consider the subgrade soil, paving materials, environment, and anticipated traffic.

Shackel (1980) has summarised the various design procedures developed around the world. These methods can be divided into four categories as follows:

### ***1. Design on the basis of experience***

In this method, the pavement thickness is selected on the basis of experience of road construction. The design catalogues are developed according to subgrade conditions or traffic loads

### ***2. Ad-Hoc Modification of Conventional design Methods***

In this method, concrete pavers are substituted for part of existing flexible pavement. The pavers have been reported as being equivalent to 2.1 and 2.9 times their thickness of crushed stones and to be between 1.1 and 1.5 times more efficient than asphalt concrete (Shackel, 1978). Several design curves were developed by using this method and adopted by the Asphalt Institute and Corps of Engineers in their design procedures.

### ***3. Mechanistic Methods of Design***

This method followed the design procedures used for the design of flexible pavement. The method involved the calculation of maximum tensile strain in bound base for defining the fatigue life and the calculation of subgrade stress or strain for predicting rutting life (Knapton, 1979). After analysing the stresses and strains distributions caused by traffic and environmental loadings, the progressive adjustment of thicknesses until the predicted stresses and strains can be deemed to be insufficient to cause failure within the required service life of the pavement (Shackel, 1986).

### ***4. Empirical Methods of Design***

This method was developed on the basis of observed pavement response of actual interlocking concrete pavement under traffic. The test was conducted at the University of New South Wales in 1978 and several design curves were developed (Shackel, 1980). The major drawback of these curves was that they had not been evaluated at subgrade CBR values less than 16 (Sharp, 1986).

There are a number of limitations associated with the above mentioned design procedures. These design methodology lacked the pavement performance prediction capabilities and materials and subgrade characterisation. Rada (1990) developed a new methodology to overcome these limitations. The AASHTO flexible pavement design methodology (AASHTO, 1986) was used as the fundamental framework for developing this procedure. The AASHTO method was modified for the application to the design of ICP. In particular, a strength characterisation for concrete pavers was developed and alternate procedures for characterising the environment, traffic, subgrade, and the materials were also developed.

The design methodology developed by Rada (1990) is based on the evaluation of four primary factors and their interactive effects. They are environment, traffic, subgrade soils and materials. The evaluation will determine the final pavement thickness and material.

#### ***1. Environment***

The main environmental factors affecting pavement are temperature and moisture. Moisture adversely affects the load-bearing capacity of the pavement by reducing the strength of subbase and the subgrade. Moisture also causes the differential heaving and swelling of certain soils (ICPI, 2006). Temperature can contribute to a decreased load

bearing capacity, particularly for asphalt stabilized layers. Moisture and freezing temperatures working together will lead to freeze-thaw cycles in the pavement structure, thus causing heaving of certain layers and reduced bearing capacity during thaw periods.

## **2. *Traffic***

The amount of anticipated traffic over its design life is determined based on AASHTO design procedure which is represented using the Equivalent Single Axle Load (ESAL) concept.

## **3. *Subgrade Support***

A crucial step in any pavement design procedure is to characterize the strength of subgrade. The typical resilient modulus ( $M_r$ ), R-value, or soaked California Bearing Ratio (CBR) laboratory tests should be conducted to evaluate the subgrade soil strength. In the absence of laboratory tests, typical resilient modulus ( $M_r$ ) values are assigned to each soil type defined in the United Soil Classification System (USCS) or AASHTO soil classification systems (ICPI, 2006).

## **4. *Pavement Materials***

The type, strength and thickness of all paving materials are established and all feasible material type and layer-thickness combinations that provide sufficient structural capacity are developed.

This method is also being used by ICPI for the structural design of interlocking concrete pavement for roads and parking lots. A set of structural design curves are developed for use with ICP to determine the thickness of various types of bases. The thickness values are seen to be a function of the subgrade strength ( $M_r$ ) and design traffic loading (ESALs). In this methodology environmental effects are incorporated through the characterisation of the subgrade soil and pavement materials. Stiffer bases such as cast-in-concrete and stabilized aggregates are recommended for roads and parking lots to compensate the stress concentration on the subgrade and base.

## **2.3 Performance Criteria**

ICP differ from conventional flexible pavements primarily in their superior load distribution characteristics and the high strength abrasion resistant surfacing (Rollings, 1986). However, load transmitting behavior of the ICP is very similar to the flexible pavements. It requires a base and

subbase to distribute loads to the subgrade. Two criteria are commonly used to assess the in service performance of flexible pavements. Permanent deformations, especially rutting of ICP was considered as the principal mode of distress. To control the rutting subgrade strain criterion is applied. For pavements with cement and asphalt bound bases two criteria were applied: the subgrade strain criterion, and the fatigue cracking criterion for bound bases.

A study of the literature shows that ICP like asphalt pavements, exhibit non-recoverable or rutting deformations under traffic. In the case of ICP most of the deformation occurs early in the loading history prior to the development of lock-up. For conventional asphalt pavements, the terminal levels of rutting generally range between 10 mm to 40 mm (Shackel, 1986).

In order to understand the development of rutting in ICP, insight into the development of permanent strains in substructure is needed. The development of these strains heavily depends on the stresses in the substructure due to traffic load. The rate of accumulation of permanent strain strongly depends on the stress. The larger this stress the stronger the permanent strain accumulation. Currently, there are several different types of vertical subgrade strain criteria in the literature. These criteria are based on the magnitude of the vertical compressive subgrade strain and used to predict load repetitions to failure.

The early deformation occurring very early in the life of the pavement and well before final lock-up can be arrested by recompaction of the pavement prior to lock up (equilibrium). The national Institute for Transport and Road Research has carried out many specialized tests, including Heavy Vehicle Simulator tests on many pavement types. These tests have shown that all pavement types including ICP behave similarly during settling-in period when pavement subjected to traffic and environmental loadings. The structural properties of the pavement layers are improved after the initial settling-in period. The settled in condition of the pavement is capable of supporting design loads with less accumulative rutting than immediately after construction as is shown Figure 2.

In the case of bound bases, a fatigue failure criterion is adopted for the design evaluation of ICP. The tensile strains developed in bound base layers are used for defining the fatigue life. Having computed the distribution of stresses and strains, the numbers of load repetitions of those stress and strain magnitudes that the pavement can withstand prior to failure are calculated in accordance with the failure/damage criteria.

### **2.3.1 Parameters Influencing ICP Performance**

Many parameters seem to affect the performance of interlocking concrete pavement. The principal factors which contribute the performance of the pavements under traffic are as follows:

#### ***1. Traffic***

The main traffic associated factors which affect the ICP response are the axle loads, types and the number of load repetitions. Excessive deformation is caused by heavy traffic, causing differential settlement and rutting. Severe loads can also cause the bond between individual pavers in jointing sand to be broken and the pavement becomes more subject to water ingress and then rapid deterioration (Clifford, 1984).

#### ***2. Subgrade***

ICP have been successfully installed over a wide range of subgrade types and strengths. The bearing capacity of the sub-grade (or natural ground) must be determined as a basis for the overall design. In weak subgrades, those exhibiting CBR values less than 5%, consideration should be given to the installation of sub-surface drains or to subgrade improvement either by using cement or lime or by the use of appropriate geofabric (Shackel, 1988).

#### ***3. Base and Subbase***

The principal factors influencing the performance of the base and subbase courses are the base thickness, type of material used, and quality (Shackel, 1984). With respect to the thickness, the variation in elevation of its finished surface must be very low. In fact, a high variation can cause variations in thickness of the sandy bed, which could become a cause of future failure. Strains, deflections, and stresses in the base layer decrease considerably with the increase in thickness of concrete blocks.

Most materials used as base and subbase courses in flexible pavements have also been successfully used in ICP. For the base course cement stabilized materials, lean concrete, crushed rocks, selected gravels and asphalt treated bases have been used whereas granular materials are used for subbase courses. For identical base and pavement thickness the best levels of performance are usually achieved by using cement-treated bases closely followed by the use of crushed rocks (Shackel, 1982).

#### **4. *Bedding Sand***

The correct choice and installation of the bedding and jointing sands is to achieving good performance in ICP. The thickness and the grading, angularity and the moisture content of the sand have been shown to be critical in influencing the behavior of ICP. Studies in Australia and South Africa have shown that, if the sand thickness is reduced from 50mm to 30mm, the rutting deformations of the pavement also decrease (Shackel, 1980). European practices (Eisenmenn, 1988) specify a bedding sand thickness after compaction of 50 mm, whereas compacted bedding sand thickness of 20 to 30 mm is used in United States (Rada, 1990) and Australia (Shackel, 1993).

#### **5. *Jointing Sand***

Jointing sand is the main component of CBP, and it plays a major role in promoting load transfer between blocks ultimately in spreading the load to larger areas in lower layers. For optimum load spreading by friction, it is necessary to provide uniform, narrow, and fully filled joints of widths between 2 mm and 4 mm (Shackel, 1993). Knapton and O'Grady (1983) recommended joint widths between 0.5 mm and 5 mm for better pavement performance. Joint widths ranging from 2 mm and 8 mm are often used, depending upon the shape of blocks, laying pattern, aesthetic considerations, and application areas.

#### **6. *Edge Restraint***

Edge restraints resist lateral movement, maintain interlock and prevent loss of bedding sand materials at the boundaries. Edge restraints are designed to remain stationary while receiving impacts during installation, from traffic and from freeze-thaw cycles. Improper edge restraint will allow lateral movement, loss of bond and pavement failure.

#### **7. *Paver Shape***

Cement and Concrete Association of Australia has divided paving units into three categories based on the shape. A study conducted in France and Australia has shown that paver shape also influences the development of horizontal creep. Tests showed that for a given laying pattern, rectangular pavers are associated with greater horizontal creep than the dentate paving units. Accelerated trafficking studies in Australia, Japan, South Africa and the USA showed that pavements laid in dentated pavers tended to exhibit smaller deformations than pavement using rectangular pavers (Shackel, 1979). In general, shaped

(dents) blocks exhibited smaller deformations as compared with rectangular and square blocks (Panda, 2003).

#### 8. *Paver Thickness*

Several studies show that increasing the thickness of blocks reduces strains, deflections, as well as the stress transferred to lower layers. Thicker blocks provide a higher frictional area. Thus, load transfer will be high for thicker blocks (Panda, 2003).

#### 9. *Laying Pattern*

There are many ways of laying down the blocks. Accelerated trafficking tests have been used to compare the performance of ICP installed in herringbone, stretcher and basketweave bonds. The best levels of performance are found in pavements laid in herringbone pattern whereas the greatest deformations are associated with stretcher bond patterns (Shackel, 1985).

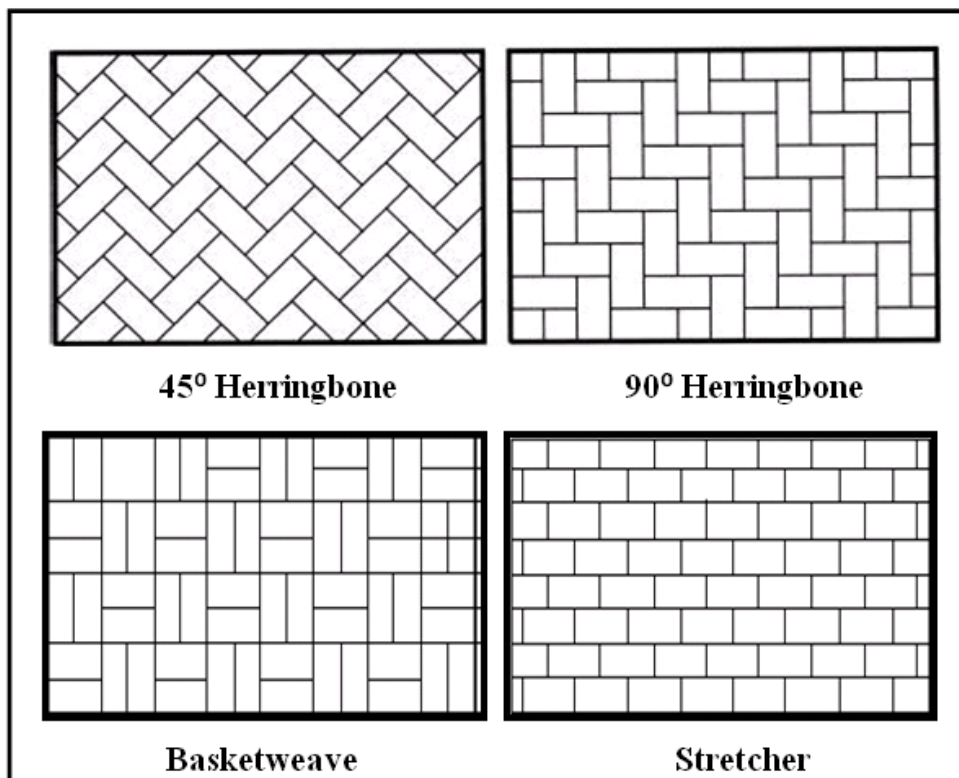


**Figure 2: Typical ICP Laying Patterns (Leong, 2005)**

## ***10. Drainage***

Inadequate drainage is likely to result in failure following subgrade softening and excessive rutting. Rainwater entering the pavement was also a contributing factor in this failure.

## ***11. Compaction***

Adequate compaction is required to minimize the settlement of ICP. The laying course material and blocks should be compacted using a vibrating plate compactor. Some blocks may require a rubber or neoprene faced sole plate to prevent damage to the block surfaces (Interpave, 2004).

The block paved area should be fully compacted as soon as possible after the full blocks and cut blocks have been laid, to achieve finished pavement tolerances from the design level of  $\pm 10$  mm under a 3 m straightedge. The surface elevation of pavers should be 3 to 6 mm above adjacent drainage inlets, concrete collars or channels to help compensate for possible minor settling normal to pavement (ICPI, 2004). Normally two cycles of compaction are applied. The first cycle compacts the bedding sand and cause this material to rise up the joints and the second cycle is applied once joint sand is brushed into the joints.

## Chapter 3

### Construction of Test Sections

#### 3.1 Description of the Test Sites

There are two locations selected for the construction of the test sections considering the traffic composition. The first site is located at the Centre for Pavement and Transportation Technology (CPATT) test track in the south east corner of the Regional Municipalities of Waterloo Waste Management Facility, located in the City of Waterloo as shown in Figure 3. The CPATT test track is a 880 m long and 8 m wide road. This site is comprised of three crosswalks with different bases and bedding materials are constructed in June 2007. The pavement is subjected to heavy truck traffic primarily loaded garbage trucks. The construction detail of this site is presented in Chapter 3.1.3.

The second test site is located at the North Campus Gate intersection on the University of Waterloo Ring Road. Four crosswalk sections with different designs are built during the reconstruction of the ring road in July and August, 2008. The road is similar to a typical city/municipal road. The construction procedure of this site is presented in Chapter 3.2.3.

##### 3.1.1 CPATT Test Track

The first series of crosswalks is situated at the Centre for Pavement and Transportation Technology (CPATT) test track in the south east corner of the Regional Municipalities of Waterloo Waste Management Facility, located at 925 Erb Street West in the City of Waterloo as noted in Figure 3. This site is comprised of three crosswalks with different bases and bedding materials are constructed in June 2007. The pavement is subjected to heavy truck traffic primarily loaded garbage trucks.

There are three crosswalks with different bases and bedding materials located at the first section of test track. The center line of the first crosswalk is located at 0+070, the second is at 0+080, and the third is at 0+090 of the test track as shown in Figure 4.



**Figure 3: Region of Waterloo Waste Management Facility, CPATT Test Track and Crosswalk Projects (Source: Google Earth)**

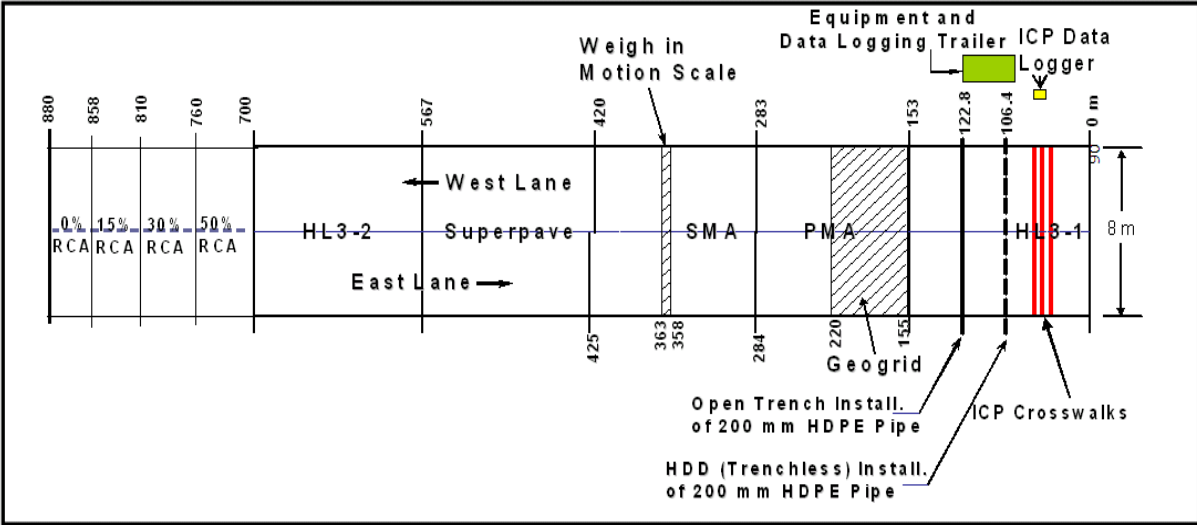


**Figure 4: CPATT Test Track**

### 3.1.1.1 Pavement Structural Designs

The proposed project is retrofitted on existing HL3 asphalt pavement. The structural components of the existing pavement are shown in Figure 5.

A typical interlocking concrete paver crosswalk consists of concrete pavers placed on top of a layer of bedding sand over a base and sub-base layers. Three different designs selected for this study are as follows and are shown in Figure 6, 7, 8 and 9. In addition, the sections have two border details- sailor versus soldier course as shown in Figure 10 and 11.

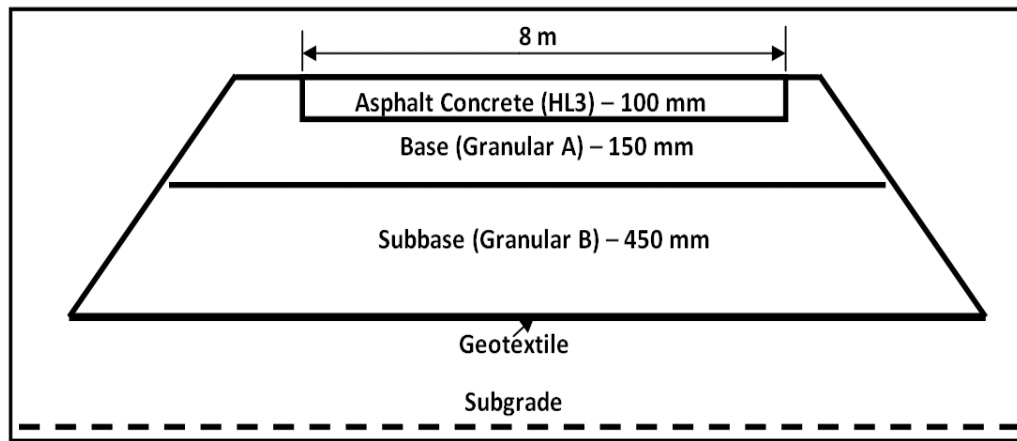


**Figure 5: Existing CPATT Test Track Cross Section**

- a) Crosswalk One - Sand Set Concrete Base Concrete Headers (SSCBCH)
- b) Crosswalk Two - Sand Set Asphalt Base Steel Headers (SSABSH)
- c) Crosswalk Three - Bituminous Set Concrete Base Concrete Headers (BSCBCH)

The first crosswalk design is composed of 80 mm interlocking concrete paver on the top of 25 mm bedding sand layer, 200 mm thick concrete base is built on the top of 400 mm granular subbase as shown in Figure 7 and is called Sand Set Concrete Base Concrete Header (SSCBCH). The 150 mm wide concrete header is placed and continues as a restraint on the transverse sides. Note that in a typical construction there would be a curb edge on each side but this is not the case at the test track so it was necessary to form a concrete restraint on the transverse ends of all of the test track sections.

The second crosswalk design is comprised of 80 mm interlocking concrete paver on the top of 25 mm bedding sand layer. The 100 mm thick asphalt base is built on the top of 50 mm granular A and 400 mm granular B subbase as shown in Figure 8 and is called Sand Set Asphalt Base Steel Header

(SSABSH). Two concrete curb restraints along the edge of the road are parallel to the road centerline while the L-shaped iron angle edge restraint with dimension of 95 mm x 95 mm x 6 mm are designed on top of the asphalt base on the both sides parallel to the center line of the crosswalk section.

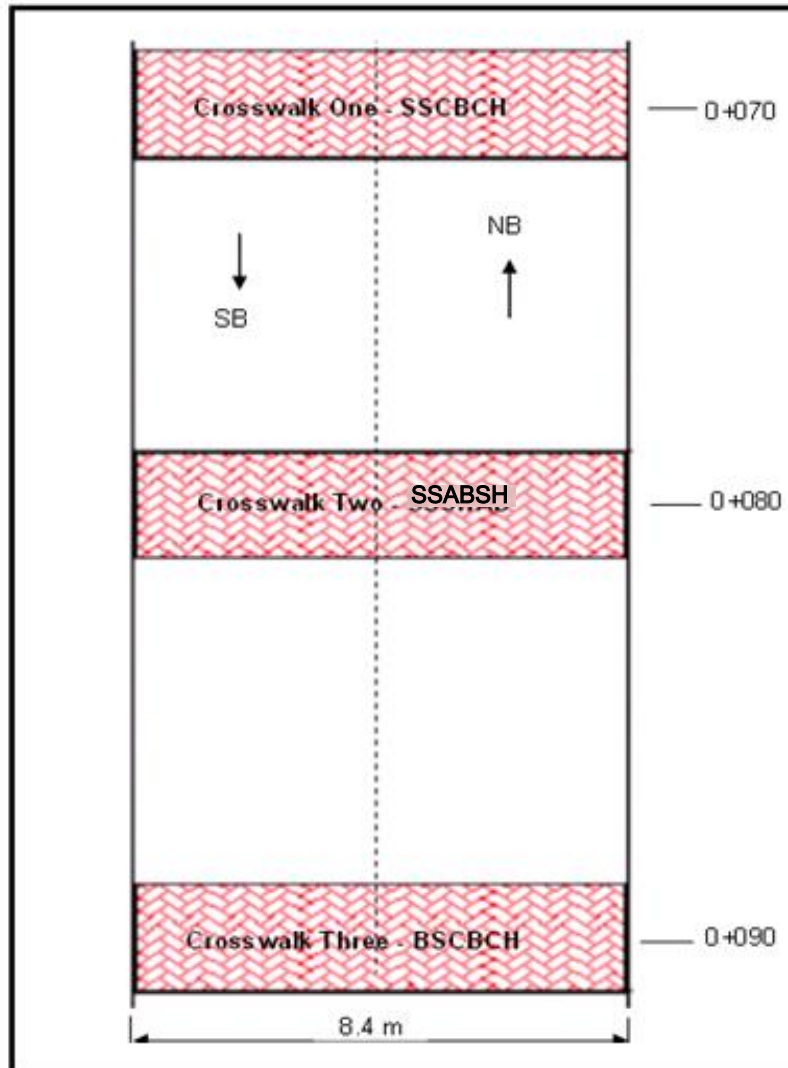
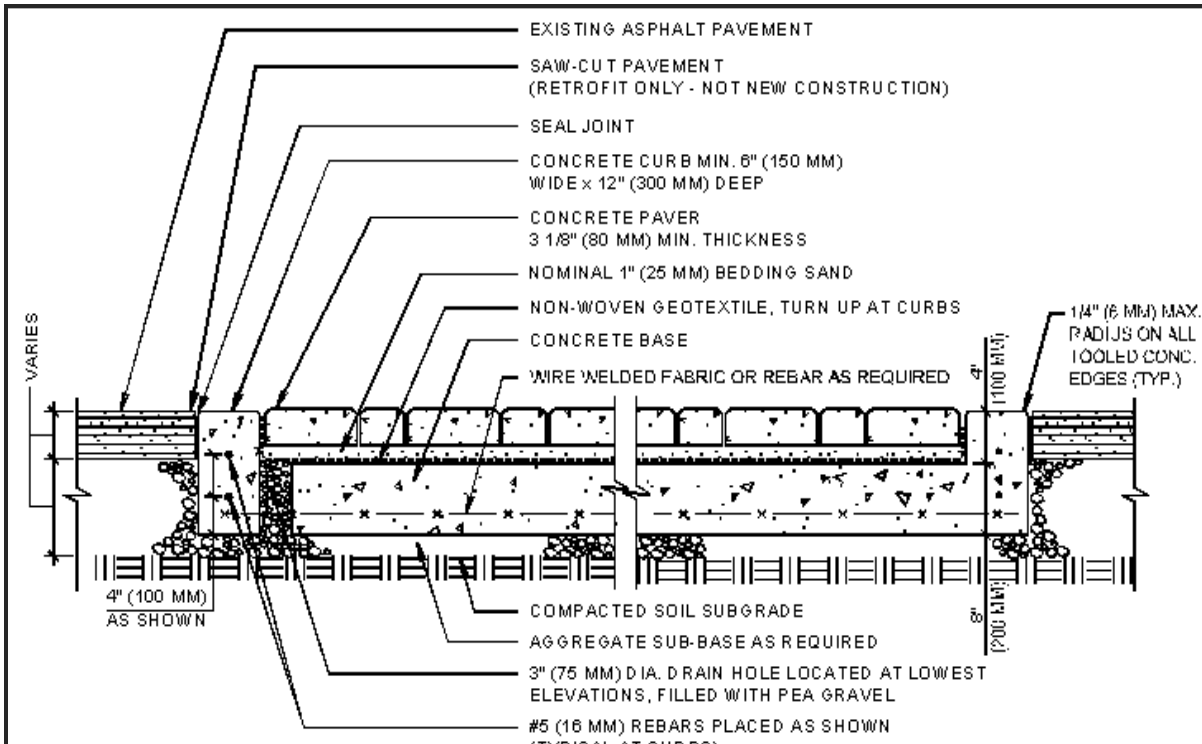
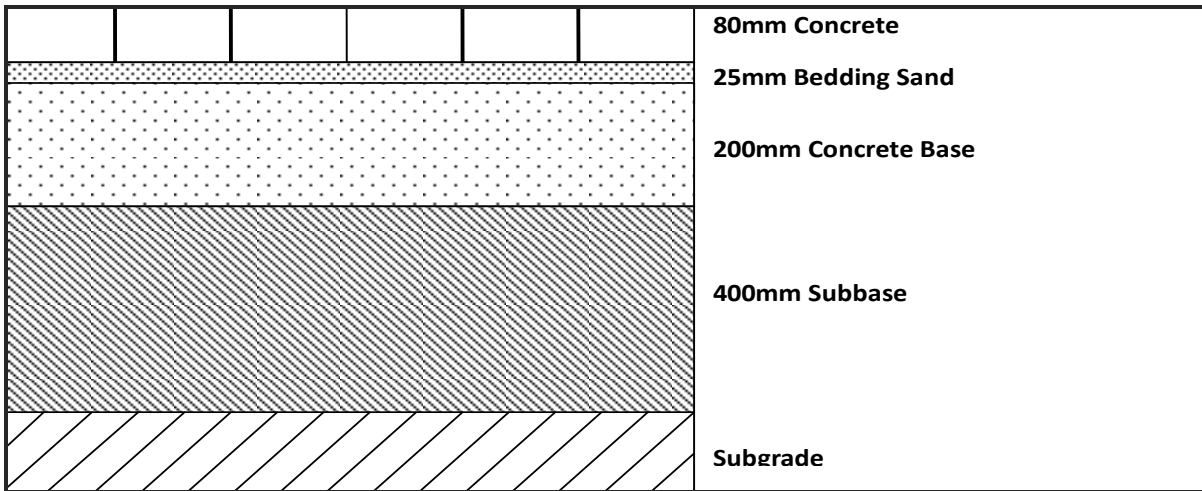


**Figure 6: Layout of CPATT Test Track Crosswalk Projects**

The third crosswalk design is composed of 80 mm interlocking concrete paver on the top of 25 mm bituminous sand layer. Concrete base with 200 mm thickness is built on the top of 400 mm granular subbase as shown in Figure 9 and is called Bituminous Set Concrete Base Concrete Header (BSCBCH). The 150 mm wide concrete header is placed and continues as a restraint on the transverse sides.



- NOTES:
1. BASE THICKNESS AND REINFORCING VARIES WITH TRAFFIC, CLIMATE, AND SUBGRADE CONDITIONS.
  2. CONCRETE BASE MINIMUM 2% SLOPE FROM CENTERLINE TO CURB.
  3. DO NOT PROVIDE DRAIN HOLES TO SUBGRADE WHEN WATER TABLE IS LESS THAN 2 FT. (0.6 M) FROM TOP OF SOIL SUBGRADE. PROVIDE DRAIN HOLES TO CATCH BASINS.
  4. DRAIN HOLES SPACED AT 2 FT. (600 MM).
  5. CONCRETE CURB AND BASE TO BE POURED MONOLITHICALLY.

 <b>CROSSWALK ON CONCRETE BASE</b> <b>ICPI/U OF W RESEARCH PROJECT</b>	DRAWING NO. X - A
	SCALE NO SCALE

Figure 7: SSCBCH Crosswalk Cross Section

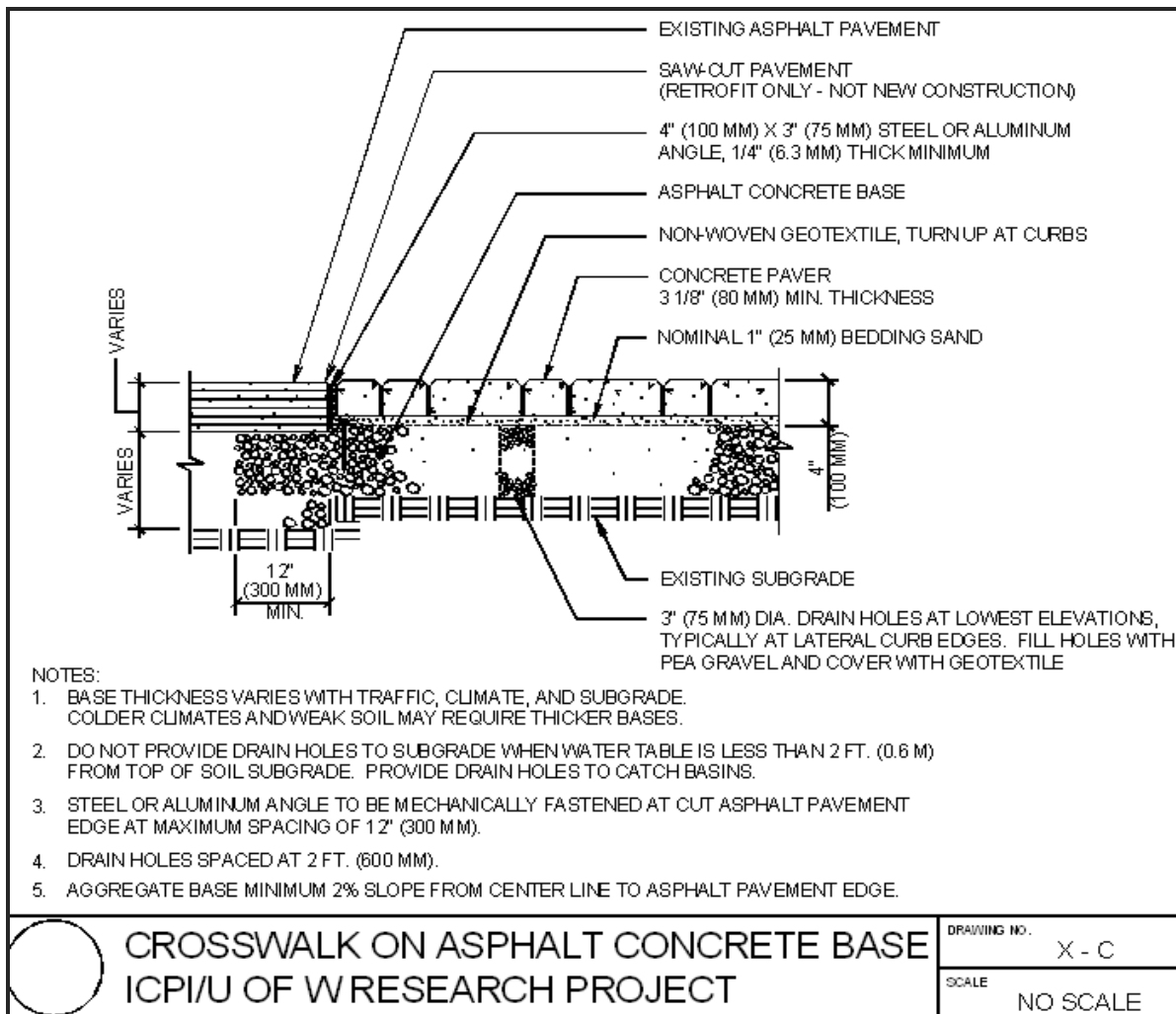
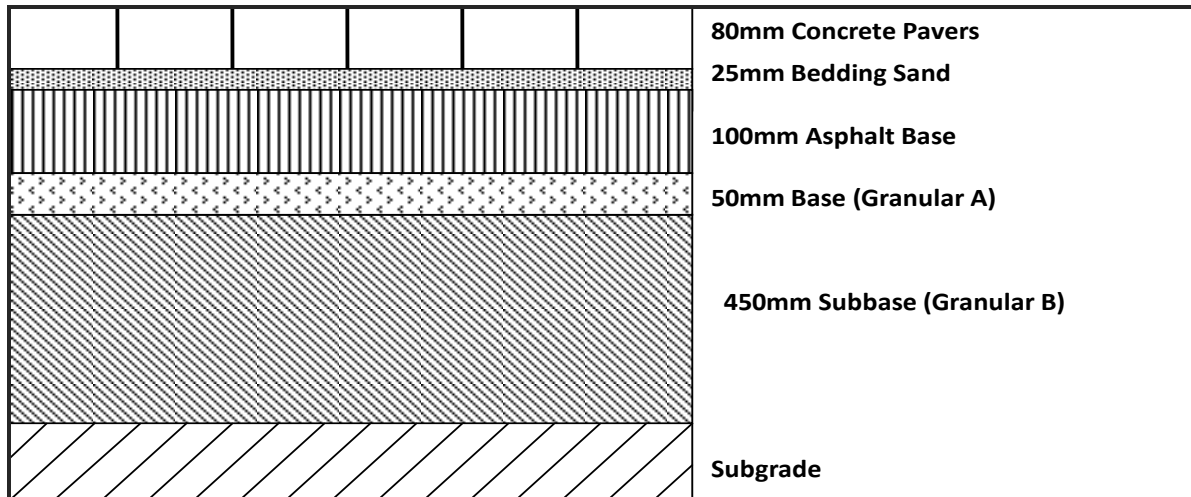


**Figure 8: SSABSH Crosswalk Cross Section**

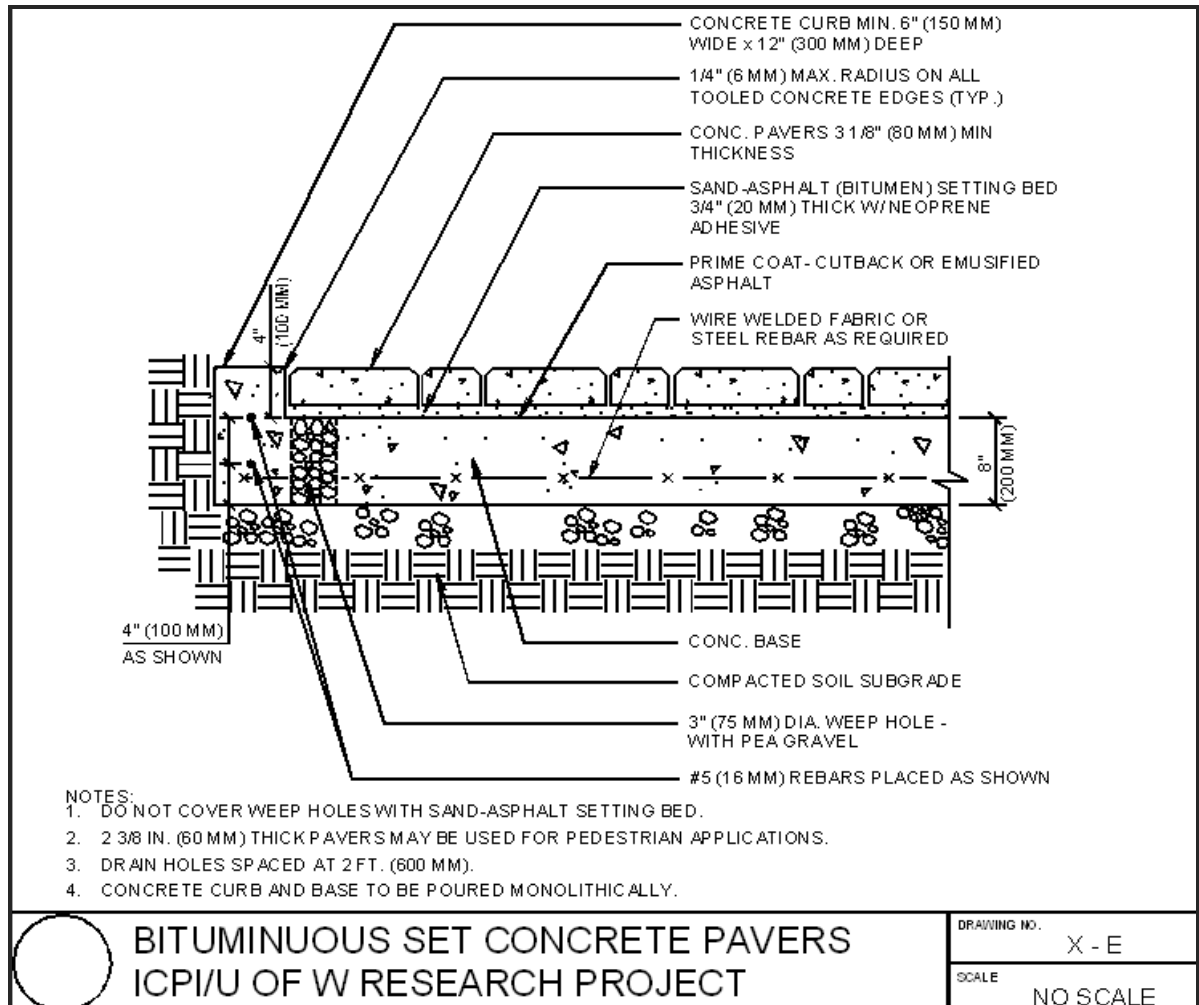
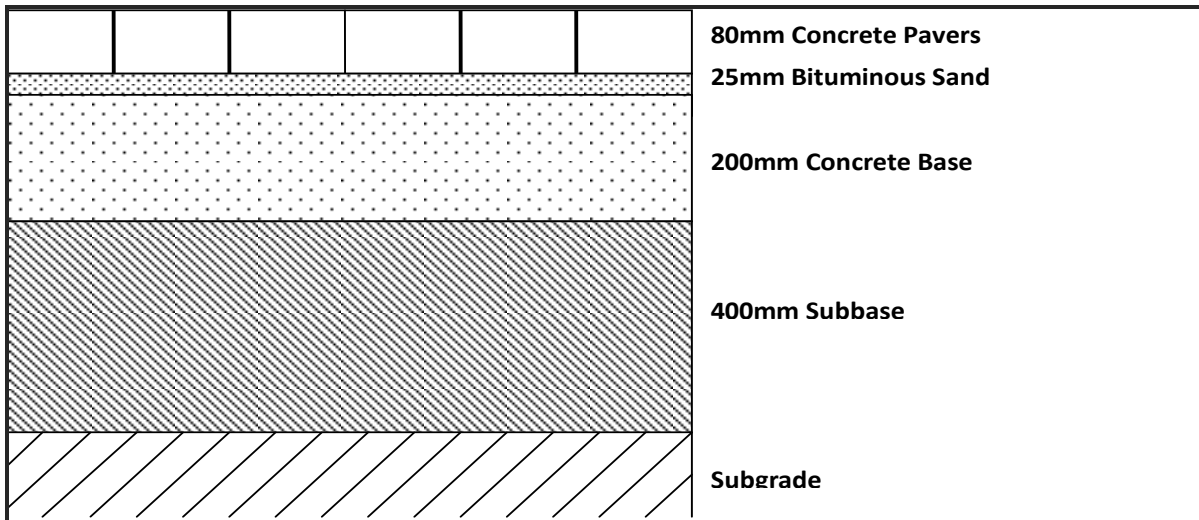
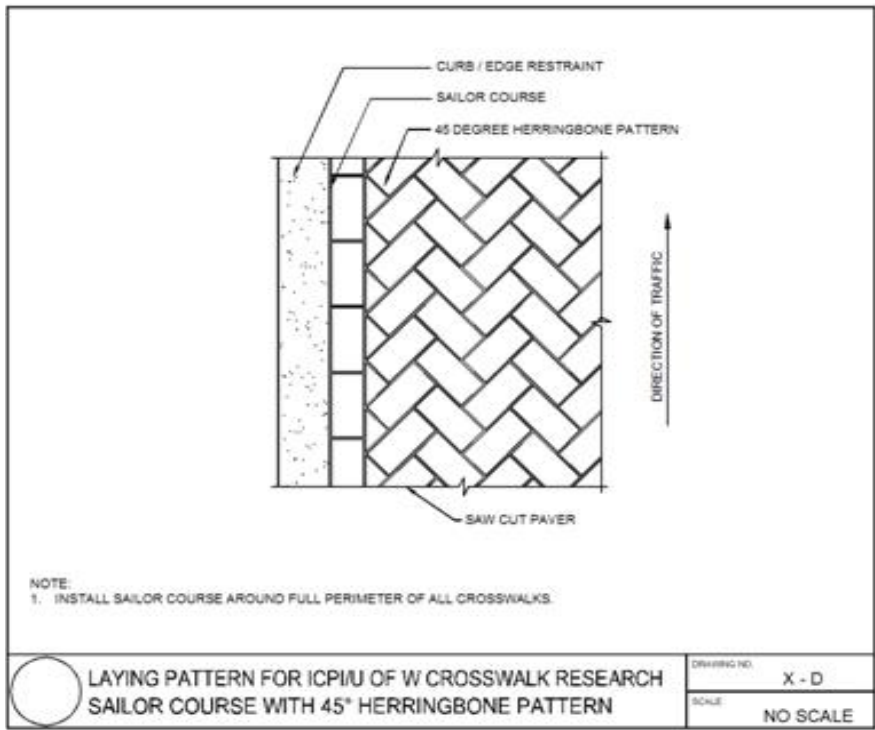
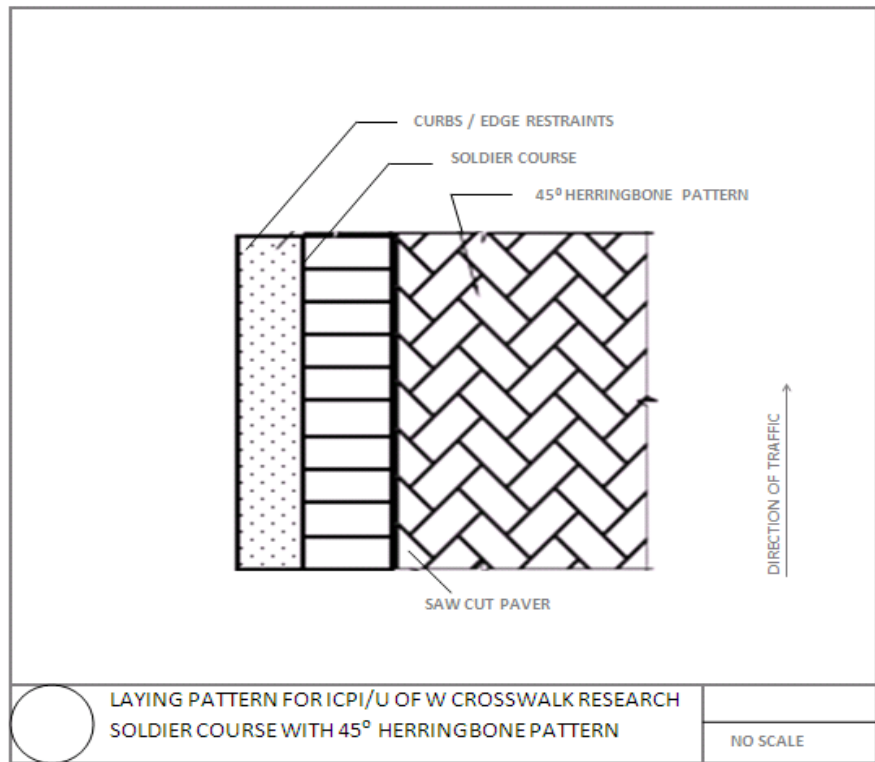


Figure 9: BSCBCH Crosswalk Cross Section



**Figure 10: Sailor Course with 45° Herringbone Pattern**



**Figure 11: Soldier Course with 45° Herringbone Pattern**

### 3.1.1.2 Construction Phase

The construction of the interlocking concrete crosswalks at the CPATT test track was carried out by Ross Yantzi’s Pavestone Plus Limited in June, 2007. The interlocking concrete pavers were supplied by NAVA STONE in Cambridge, Ontario. The entire construction phase lasted approximately seven days. Each of the crosswalks is 3 m in width and 8.3 m in length. The centerline of the first crosswalk (SSCBCH) is located at 90 m south from the north end of the test track. The second crosswalk (SSABSH) is located at located 10 m south from the SSCBCH, centre to centre. Similarly the third crosswalk (BSCBCH) is located at 10 m centre to centre from the SSABSH as shown in Figure 6. The summary of activities is presented in Table 1.

**Table 1: Summary of Construction**

<b>Crosswalk</b>	<b>Date</b>	<b>Construction Activity</b>
<b>1</b> (SSCBCH)	June 18, 2007	Excavation of asphalt pavement
	June 19, 2007	Compaction of subbase course and formworks for curbs and headers
	June 20, 2007	Reinforcement rebars and drainage pipes placement
	June 21, 2007	Concrete placement
	June 22, 2007	Non-woven geotextile installation and spreading and screeding of bedding sand
	June 22, 2007	Installation of ICP
	June 22, 2007	Spreading and sweeping of joint sands and final compaction
<b>2</b> (SSSHAB)	June 18, 2007	Excavation of asphalt pavement
	June 19, 2007	Compaction of subbase course
	June 22, 2007	Asphalt paving
	June 25, 2007	Installation of Angle iron edge restraint
	June 26, 2007	Non woven geotextile installation and spreading and screeding of bedding sand
	June 26, 2007	Installation of ICP

	June 22, 2007	Spreading and sweeping of joint sands and final compaction
3 (BSCBCH)	June 18, 2007	Excavation of asphalt pavement
	June 19, 2007	Compaction of subbase course and formworks for curbs and headers
	June 20, 2007	Reinforcement rebars and drainage pipes placement
	June 20, 2007	Concrete placement
	June 25, 2007	Non woven geotextile installation and spreading and screeding of bituminous sand
	June 25, 2007	Installation of ICP
	June 25, 2007	Spreading and sweeping of joint sands and final compaction

**3.1.1.2.1 Excavation of Existing Asphalt Pavement**

The first phase in the CPATT crosswalk construction involved excavating the existing asphalt pavement as shown in Figure 12. The carpenter square was used to mark the section to be cut.



**Figure 12: Excavation of Existing Asphalt Pavement**

### **3.1.1.2.2 Base Construction**

Within the three crosswalk test sections, SSCBCH and BSCBCH have a concrete base underneath the ICP while SSABSH has an asphalt base underneath the ICP. The subbase course was leveled and compacted with a 20 kN/4500 lbs vibrating plate compactor after the excavation of the trench. Wooden forms were installed around the perimeter of the crosswalk for curbs and headers. Welded wire fabric having mesh size of 150 mm/150 mm was placed on the top of the subbase course before the concrete placement as shown in Figure 13. High Early concrete from Dufferin Concrete's Forwell Plant in Kitchener was used for the bases, headers and curbs construction.



**Figure 13: Concrete Placement on BSCBCH**

The length of the concrete base is 8.3 m including curbs and the width is 3 m including the headers on both sides. The thickness of the concrete bases is 200 mm. Each base has curb and headers around the perimeter, the width of the curb/header is 150 mm. Exposed concrete headers edges are trimmed to 3 mm radius to reduce the likelihood of chipping. Three control joints for shrinkage were provided at three locations throughout the base.

The construction of 100 mm thick asphalt base was carried out in two lifts. The HL3 mix was spread, screeded, and compacted with a 20 kN plate compactor. The mix temperature on arrival to the site was 114°C and 106°C before compaction of the first lift. Similarly, the mix temperature of the second lift before the compaction was 72°C.



**Figure 14: SSCBCH Base Section**

The asphalt base also has two concrete curbs similar to ones for the concrete bases along its two edges that are parallel to the test track and these curbs were constructed using high early concrete.



**Figure 15: SSABSH Base Section**

### ***3.1.1.2.3 Drainage***

Prior to the concrete placement of the base, eight ABS pipes with diameter of 75 mm and length of 300 mm were installed perpendicular to the road surface at the lowest level of the base course as shown in Figure 16. The pipes are filled with pea gravel and covered with geotextile to prevent the loss of bedding materials. Their purpose is to remove excess water from the base course. Since the

road base is constructed with two percent slope towards the edge, four pipes were installed along the two outer edges of the bases. With one set of four drainage pipes are located in northbound lane and another set at located in southbound lane. The distance between adjacent drainage pipes (centre to centre) is approximately 80 cm and the first drainage pipe of each set is 20 cm offset from the edge of the base.



**Figure 16: Formworks, Drain Pipes and Reinforcement Bars for BSCBCH**

#### ***3.1.1.2.4 Bedding Material Placement***

Prior to placing the interlocking concrete pavers, a layer of bedding material was placed in the base of each section. The thickness of the bedding sand is 25 mm. The CSA requirements and actual gradation of the bedding sand is provided in Table 2. Micro-Deval test was also performed before the placement as per ICPI Tech Spec Number 17. An 8.9% Micro-Deval degradation loss was calculated which is slightly greater than maximum recommended value 8%.

For SSCBCH, a layer of non woven geotextile was placed in the constructed base and a layer of bedding sand with the thickness of 25 mm was spread and screeded on top of the non woven geotextile as shown in Figure 17.

For SSABSH, L-shaped iron angle were installed on top of the asphalt base and along the cut pavement edge as edge restraint instead of concrete headers. The angle iron is 9.5 cm wide and 9.5 cm high and 6 mm thick. Nails and screws were drilled through the angle iron and into the asphalt

base in every 60 cm to fasten the angle iron onto the base. On top of the angle iron and the asphalt base, a similar layer of non woven geotextile and bedding sand as SSCBCH were placed.

**Table 2: Gradation of Bedding Sand**

CSA Requirements		Actual	
Sieve Size (mm)	Percent Passing (%)	Sieve Size (mm)	Percent Passing (%)
10 mm	100	9.5 mm	100
5 mm	95-100	4.75 mm	99.9
2.5 mm	80-100	2.36 mm	86.6
1.25 mm	50-90	1.18 mm	71.1
0.630 mm	25-65	0.600 mm	53.2
0.315 mm	10-35	0.300 mm	26.3
0.160 mm	2-10	0.150 mm	6.2
0.075 mm	0-1	0.75 mm	1.1

For BSCBCH, the concrete base surface was prepared with an emulsified asphalt tack coat. A hot-sand asphalt mix was brought to the site and spread and compacted to 25 mm thick layers. After the asphalt cooled, a thin coating of asphalt-neoprene adhesive was applied across the surface.



**Figure 17: Bedding Sand and Non-Woven Geotextile**

### 3.1.1.2.5 Interlocking Concrete Pavers (ICP) Installation

The interlocking concrete pavers were laid in 45° herringbone pattern in all sections. Installation was started from the corner with securing 45° string lines on the bedding course as shown in Figure 19. Edge pavers are saw-cut to fit against the sailor and soldier courses. The sailor and soldier of interlocking concrete pavers were placed in such a way that SSABSH and BSCBCH have three sides (one long side and two short sides) with sailor course and one long side with soldier course. In contrast, SSCBCH has sailor courses on the both sides. After the installation, the surface was compacted with a vibratory plate roller to compact the bedding sand, seat the pavers in it and force the bedding sand into the joints at the bottom of the pavers. Figure 18 provides the physical characteristics of the paver. The final elevation of the surface course was kept 6 mm above the adjacent asphalt pavement to accommodate any future settlement.

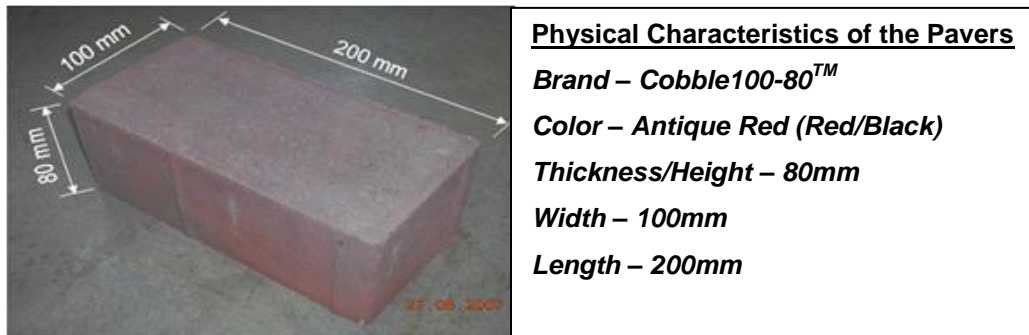


**Figure 18: Physical Characteristics of a Concrete Paver**



**Figure 19: ICP Placement**

### ***3.1.1.2.6 Joint Sands Placement and Compaction***

After initial compaction of the pavers, dry joint sand was spread on the surface and compacted with a vibratory compactor to ensure that the spaces between pavers are filled. Excess joint sand was then removed.

### ***3.1.1.2.7 Quality Control and Assurance***

Extensive testing was performed throughout the construction of the research project. Samples were taken from the original Granular A, Granular B, concrete and HL3 mix. Twelve concrete cylinders were casted to perform the laboratory compressive strength testing. In addition, the mix temperature of the HL3 and sand asphalt were also measured during the placement and before compaction. Slump and air-void testing were carried out for every batch of the concrete as shown in Figure 20.



**Figure 20: On-site Concrete Air-Void Testing**

During the concrete placement, twelve 100 mm x 200 mm concrete cylinders from each concrete mix were made. Two cylinders from each section were crushed on compressive strength testing equipment at the 18 hrs, 24 hrs and on 2 day, 3 day, 7 day, 14 day, and 28 days after placement as shown in Figure 22. The 28 day compressive strength for cylinders from both sections did not meet the 28 days compressive strength requirement (32 MPa).



Figure 21: A Cylinder after Compressive Strength Testing

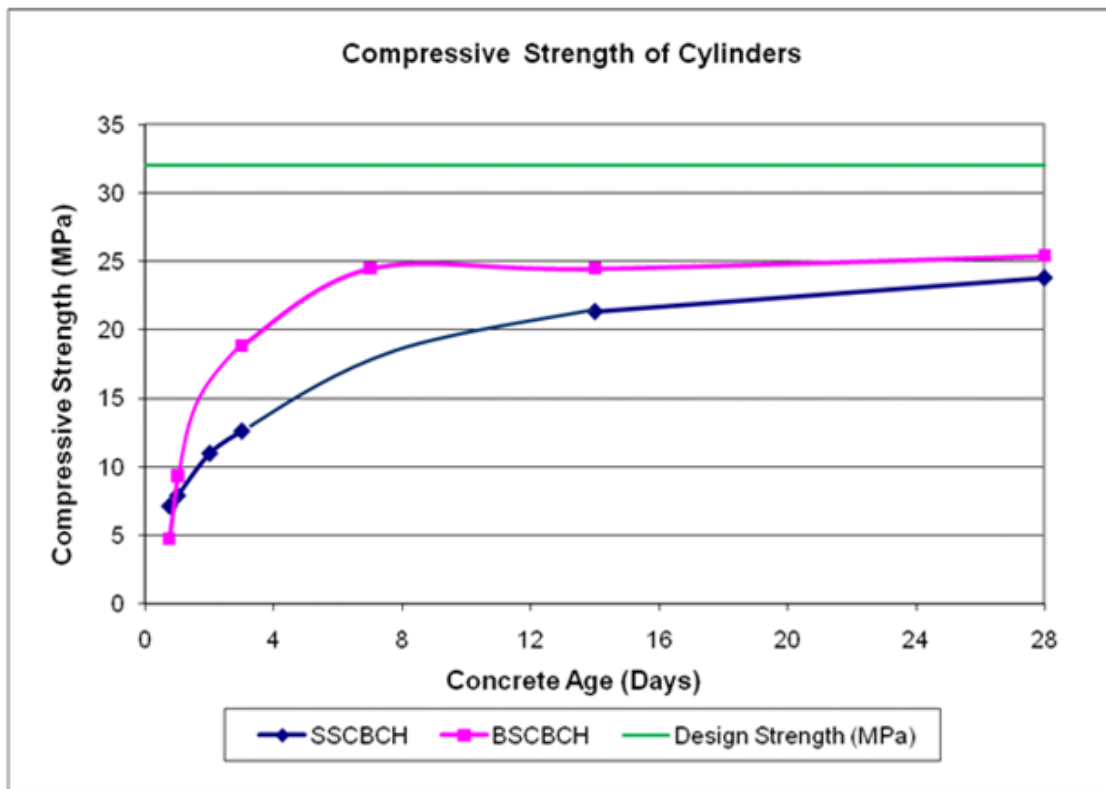


Figure 22: Compressive Strength Testing Results

### 3.1.2 University of Waterloo Ring Road

The second series of crosswalks are situated at the University of Waterloo Ring Road as noted in Figure 23. There are four crosswalks with different bases and bedding materials located at UW north campus gate. The Sand Set Concrete Base Concrete Header (SSCBCH) is installed at station 2+010 Northbound, Bituminous Set Concrete Base Concrete Header (BSCBCH) is at station 2+010 Southbound, the Sand Set Asphalt Base Aluminum Header (SSABAH) is at station 1+140 and the Sand Set Granular Base Concrete Header (SSGBCH) is at station 1+095 as presented in Figure 25.

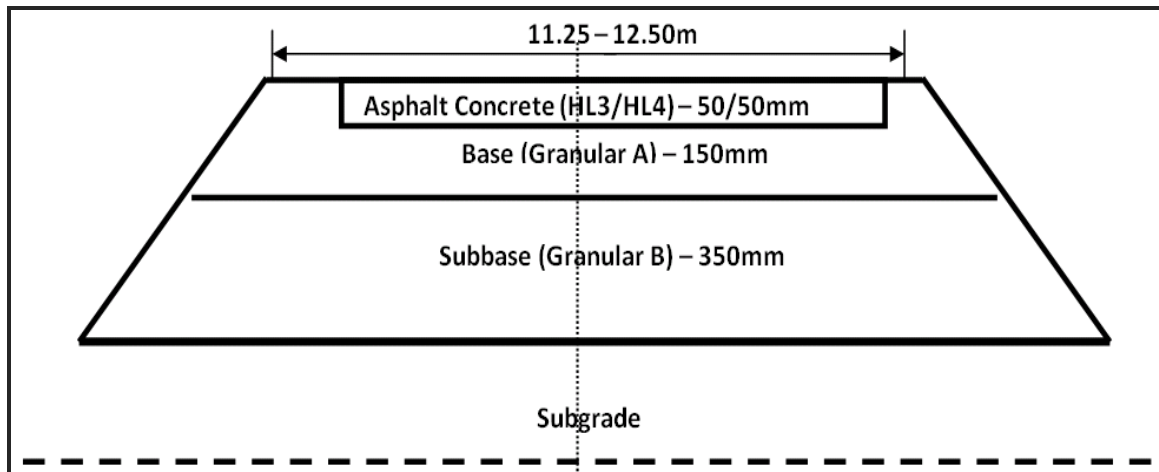
The research projects were constructed during the reconstruction of UW ring road in July and August, 2007. The length of asphalt base and aggregate base crosswalks are 12.5 m and concrete base sections are 11.25 m. The width of all sections is 2.635 m. The installation of the interlocking concrete pavers was done manually by a crew of two to three members.



Figure 23: UW Ring Road and Crosswalks Project Location (Source: Google Earth)

#### 3.1.2.1 Pavement Structural Designs

The crosswalk projects were constructed during the reconstruction of UW ring road. The structural components of the existing pavement are shown in Figure 24.



**Figure 24: UW Ring Road Cross Section**

The following four crosswalk sections were constructed at this location. The layout and the structural designs of the sections are shown in Figures 26-29. The laying and border patterns are similar to the CPATT test track site as shown in Figure 10 and 11.

- a) Crosswalk One - Sand Set Concrete Base Concrete Headers (SSCBCH)
- b) Crosswalk Two - Bituminous Set Concrete Base Concrete Headers (BSCBCH)
- c) Crosswalk Three - Sand Set Asphalt Base Aluminum Headers (SSABAH)
- d) Crosswalk Four - Sand Set Granular Base Concrete Headers (SSGBCH)

Crosswalk One, Sand Set Concrete Base Concrete Headers (SSCBCH), is 11.25 m long and 2.635 m wide and composed of 80 mm interlocking concrete paver on the top of 25 mm bedding sand layer. The 200 mm thick concrete base is built on the top of 300 mm granular subbase as shown in Figure 26. The detail includes 150 mm wide concrete headers and curb and gutter at the transverse ends as shown in Figure 26.

The second crosswalk design, Bituminous Set Concrete Base Concrete Headers (BSCBCH) is 11.25 m long and 2.635 m wide and is comprised of 80 mm interlocking concrete paver on the top of 25 mm bituminous sand layer. The 200 mm thick concrete base is built on the top of 300 mm granular B subbase as shown in Figure 27. The detail includes 150 mm wide concrete headers and curb and gutter at the transverse ends.

The third crosswalk design, Sand Set Asphalt Base Aluminum Headers (SSABAH) is 12.5 m long and 2.635 m wide and is comprised of 80 mm interlocking concrete paver on the top of 25 mm

bedding sand layer. The 100 mm thick asphalt base is built on the top of 50 mm granular A base and 350 mm granular B subbase as shown in Figure 28. The detail includes curb and gutter at the transverse ends parallel to the road centerline while the L-shaped aluminum angle edge restraint are designed on top of the asphalt base on the both sides parallel to the center line of the crosswalk section.

The fourth crosswalk design, Sand Set Granular Base Concrete Header (SSGBCH) is 12.5 m long and 2.635 m wide and is comprised of 80 mm interlocking concrete paver on the top of 25 mm bedding sand layer. The 150 mm thick aggregate base is built on the top of 350 mm granular B subbase as shown in Figure 29. The detail includes 150 mm wide concrete headers and curb and gutter at the transverse ends.

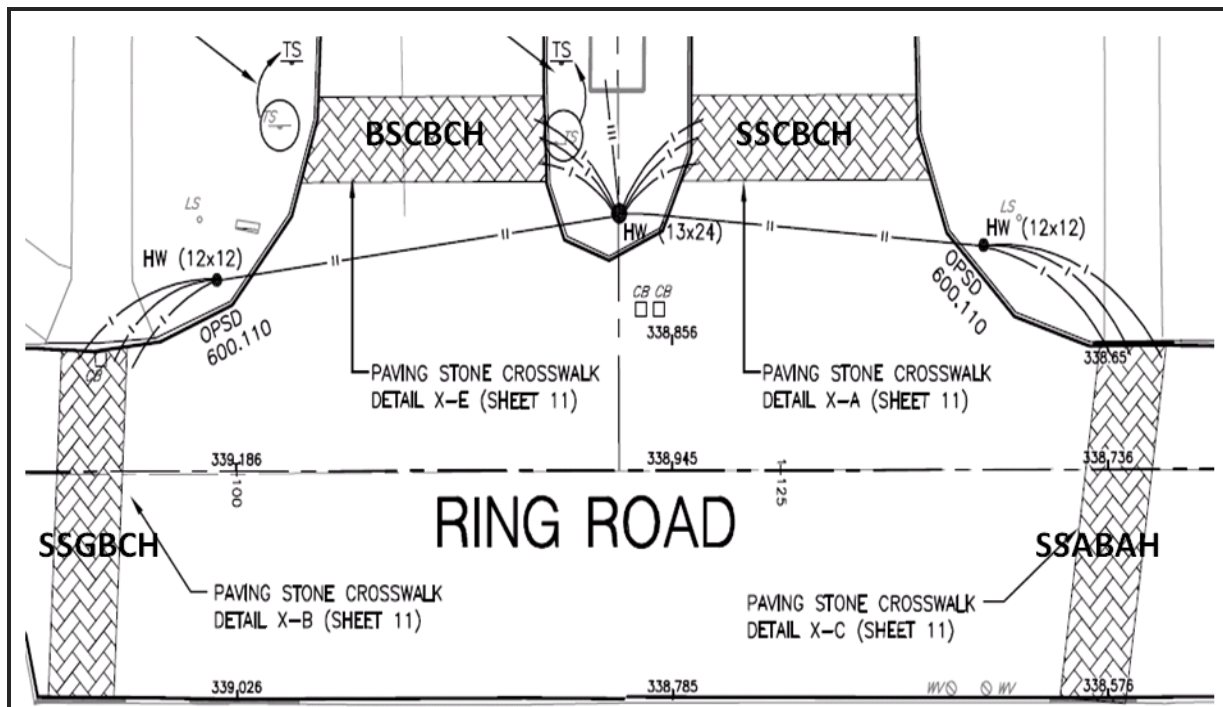


**Figure 25: Layout of Crosswalk Sections at UW Ring Road**

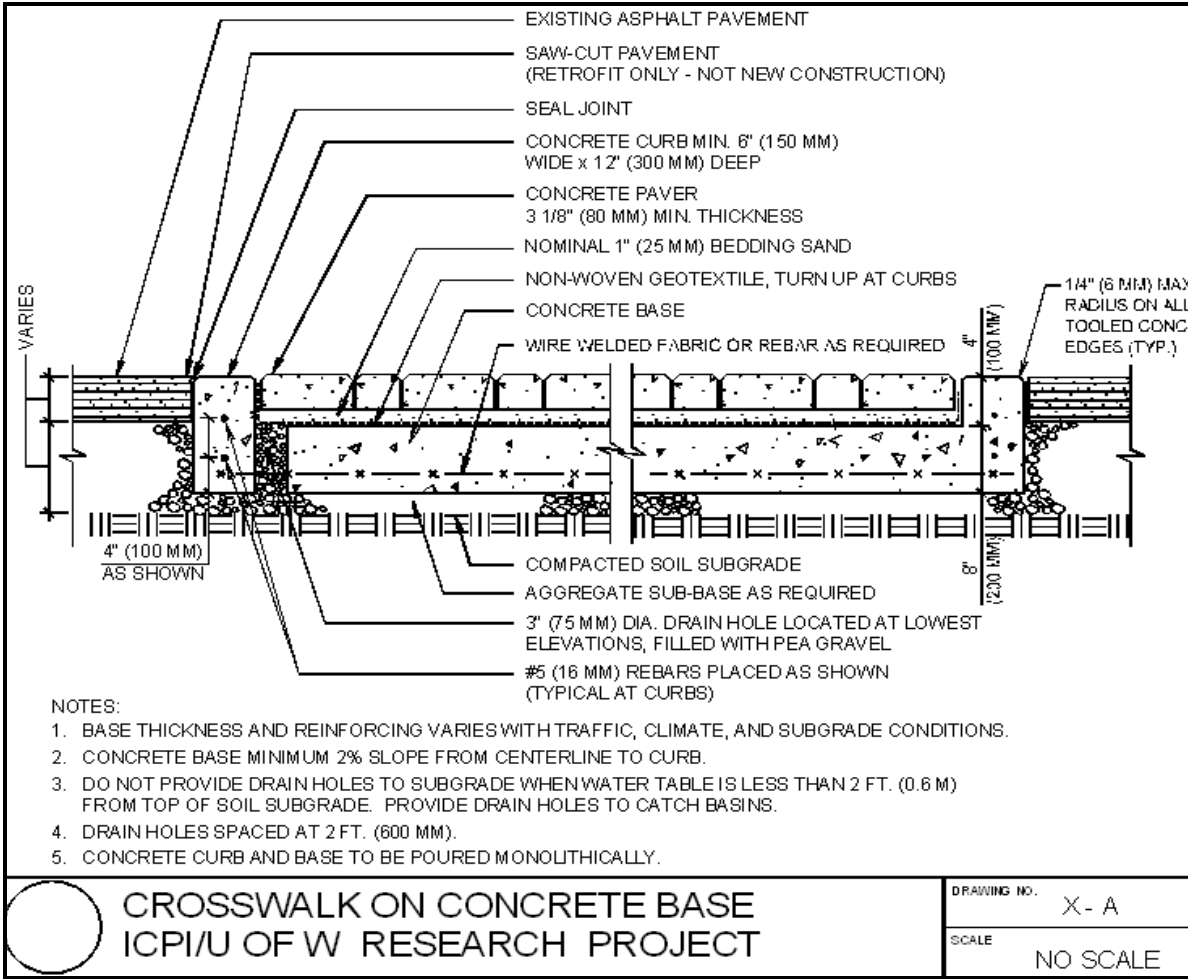
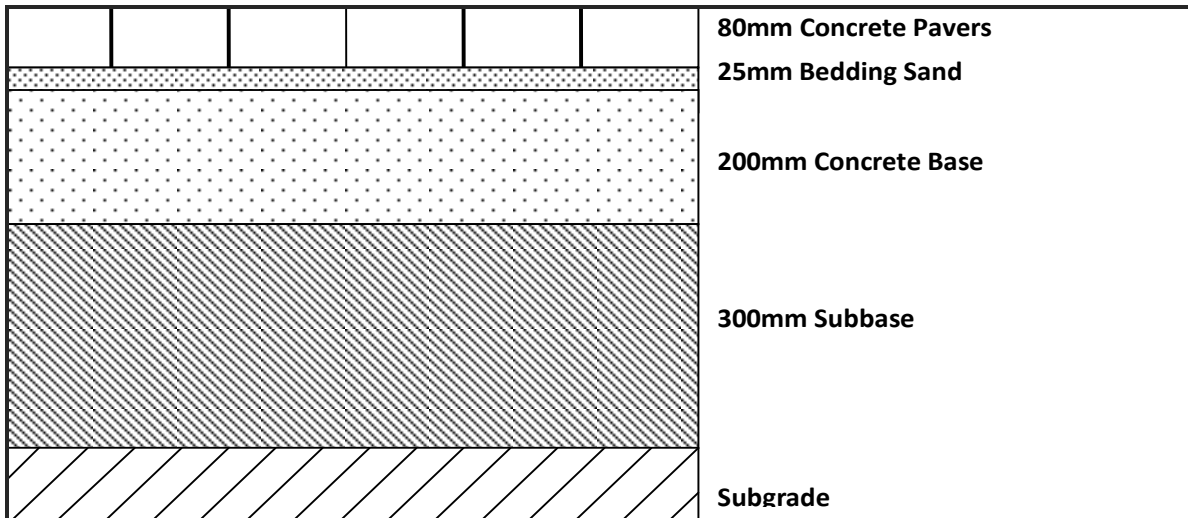
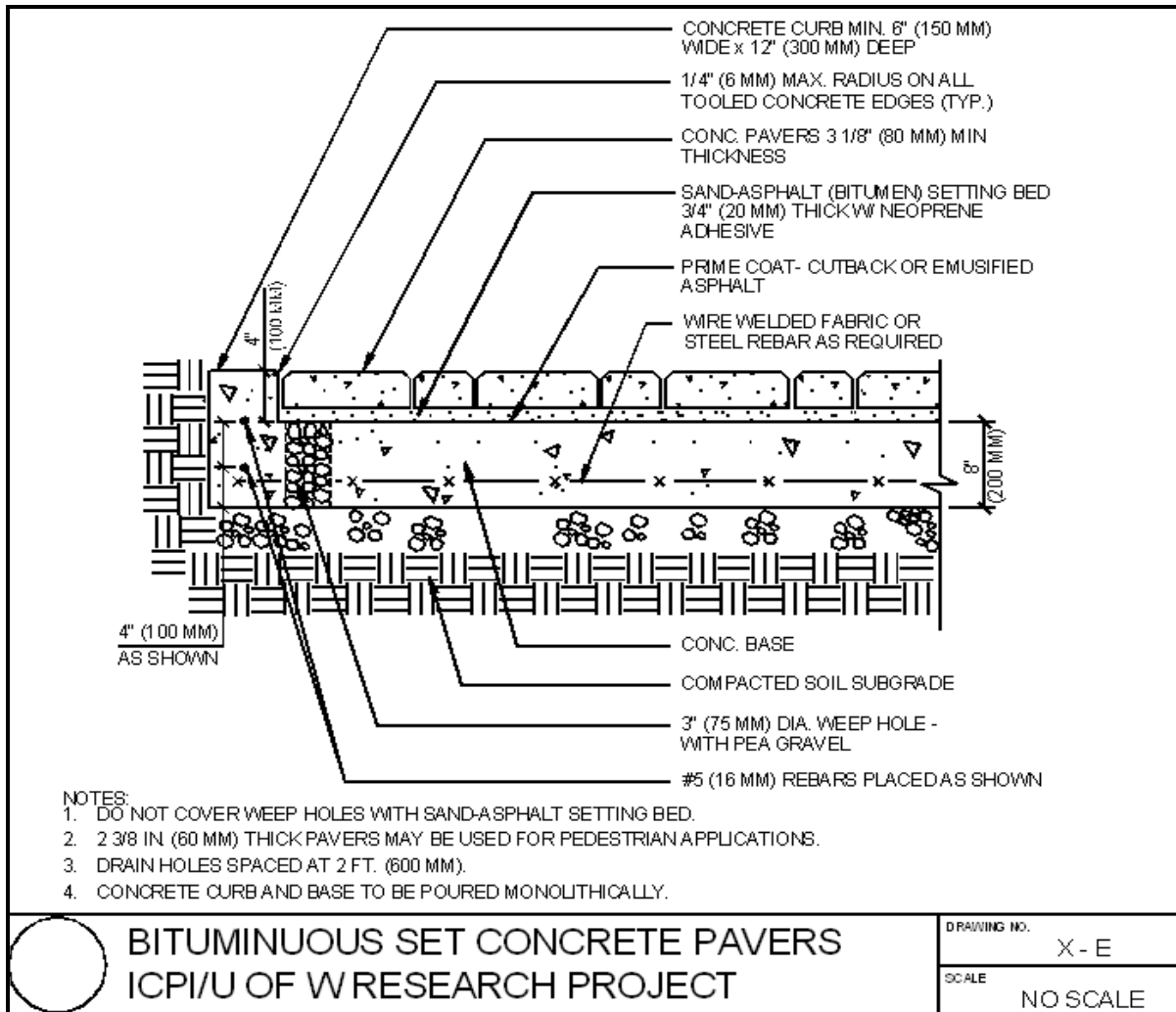
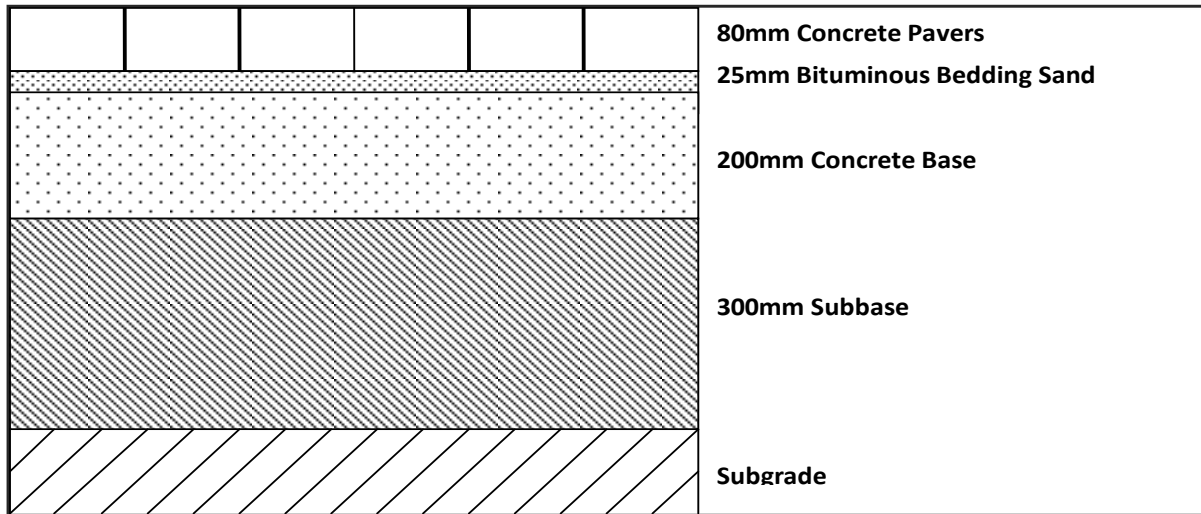


Figure 26: SSCBCH Crosswalk Section



**Figure 27: BSCBCH Crosswalk Section**

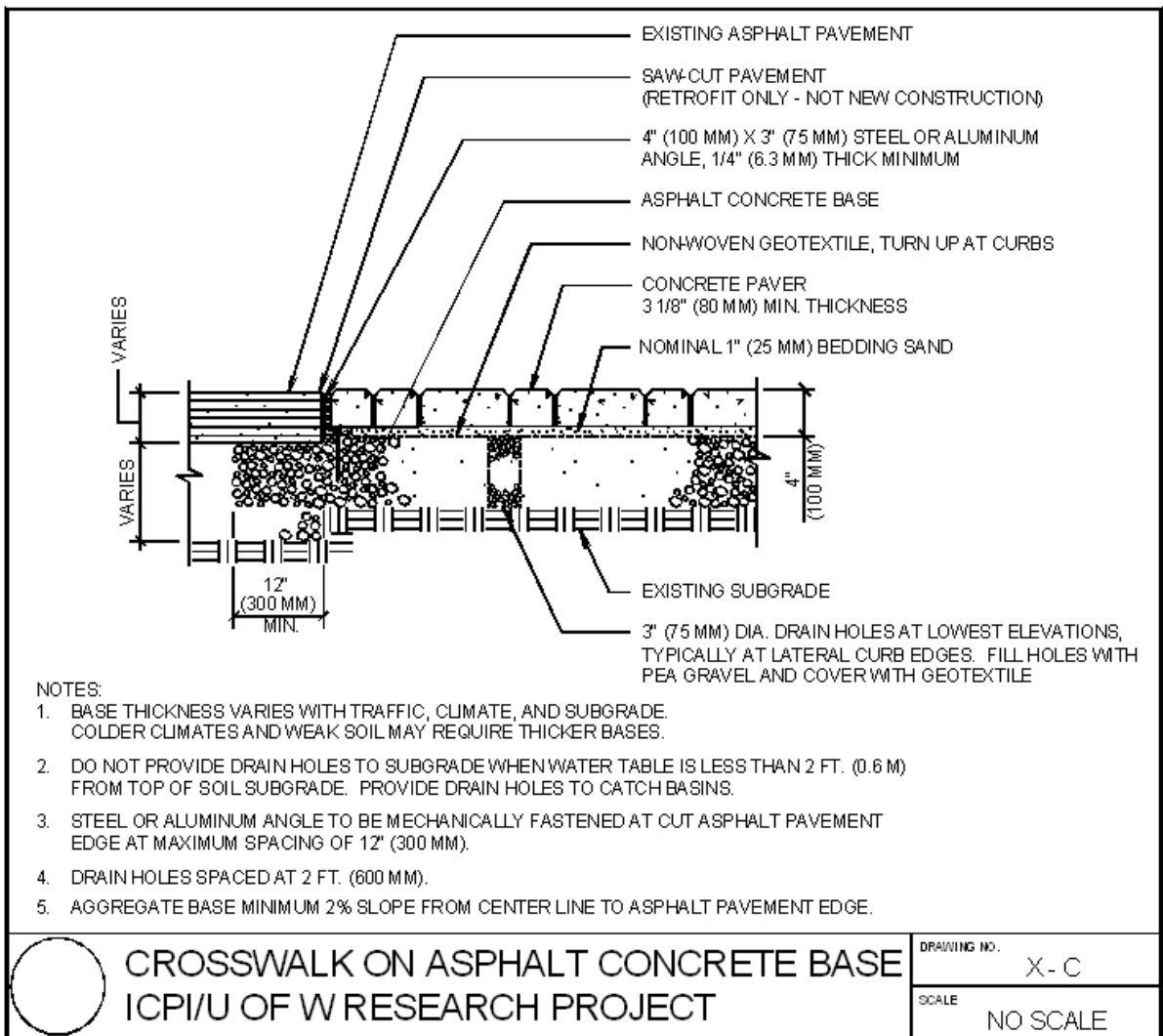
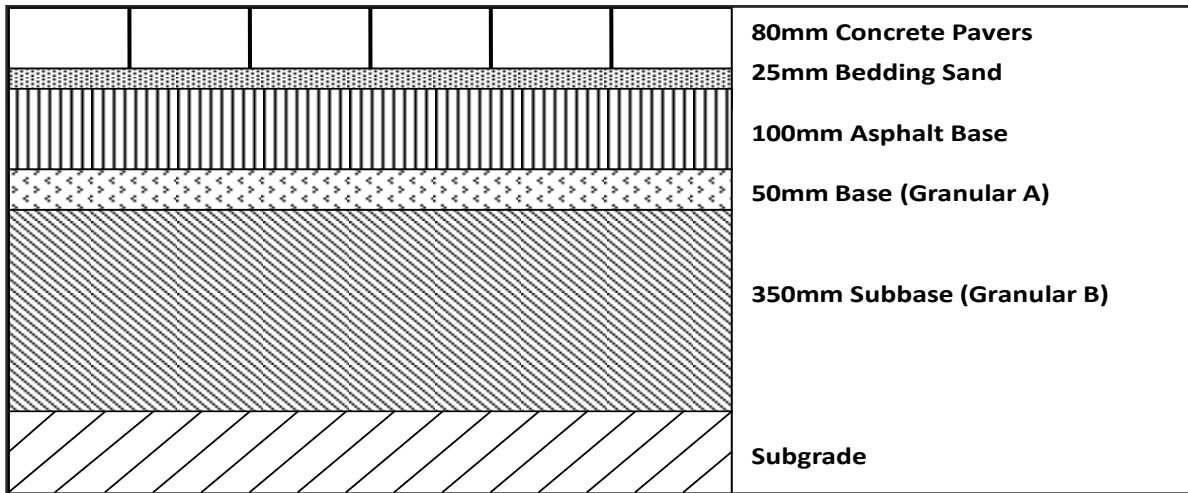
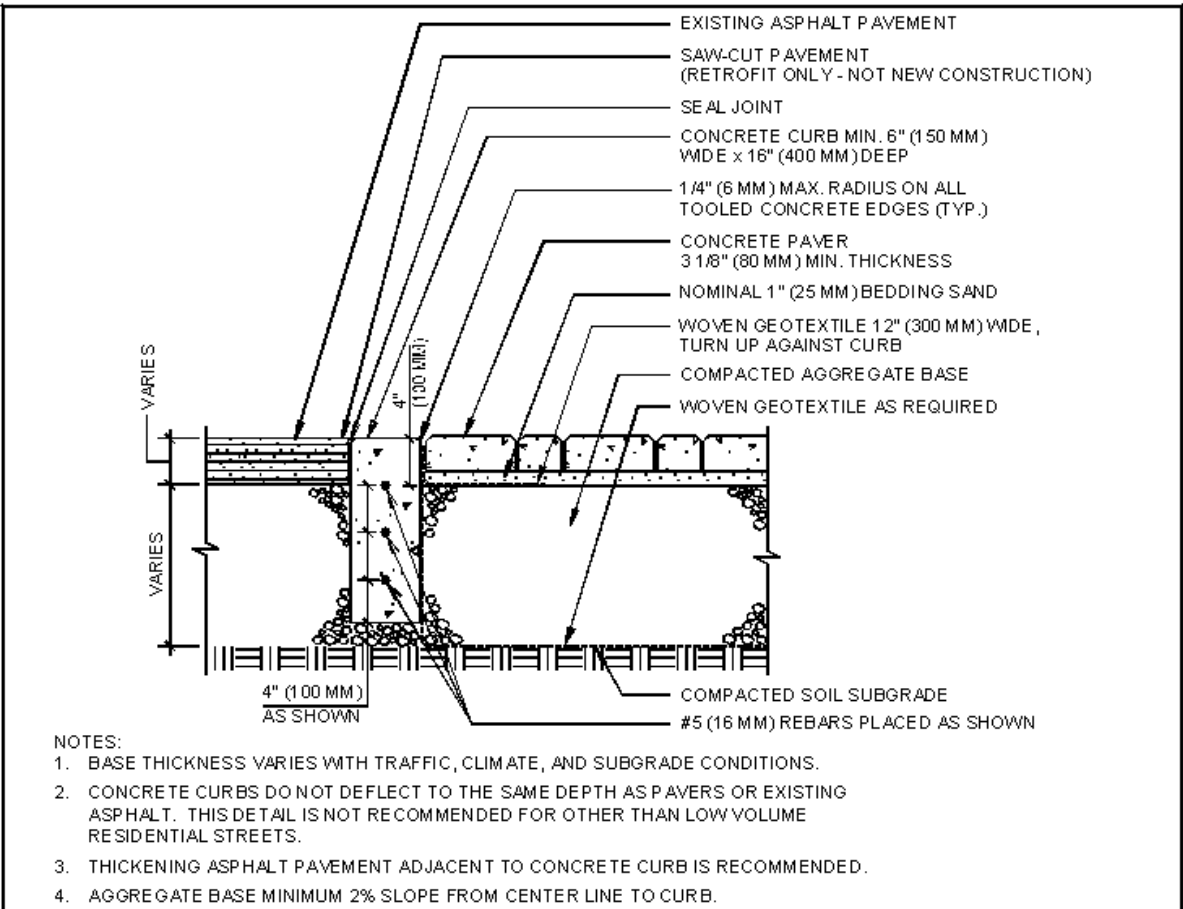
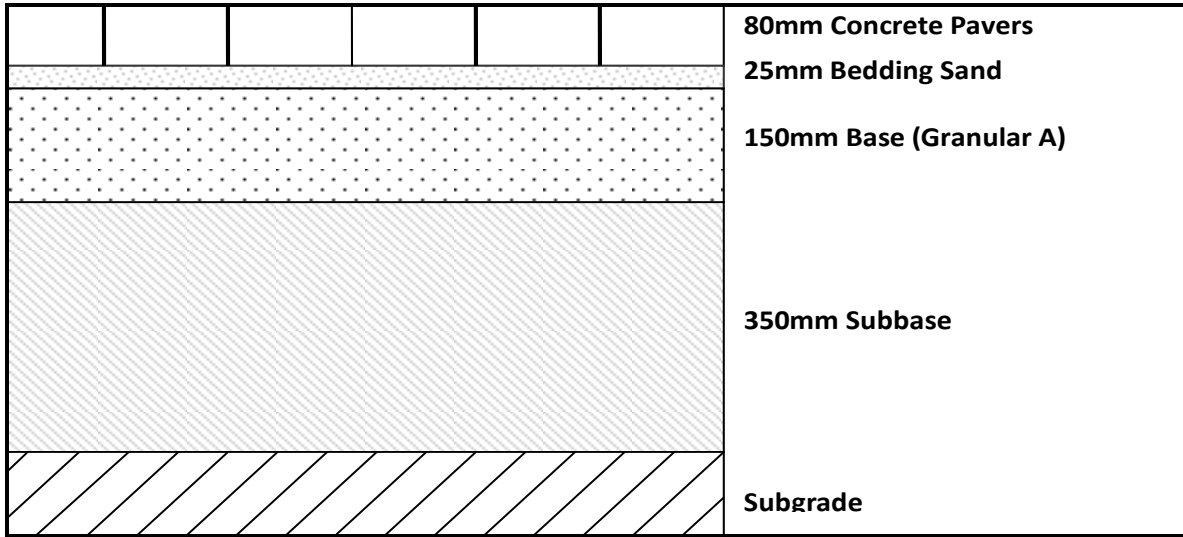


Figure 28: SSABAH Crosswalk Section



<b>CROSSWALK ON COMPACTED AGGREGATE BASE</b> <b>ICPI/U OF W RESEARCH PROJECT</b>	DRAWING NO. X - B
	SCALE NO SCALE

**Figure 29: SSGBCH Crosswalk Section**

### 3.1.2.2 Construction Phase

The construction of the CPATT interlocking concrete crosswalks at the UW ring road was also carried out by Ross Yantzi's Pavestone Plus Limited and the interlocking concrete pavestone were also supplied by NAVA STONE in Cambridge, Ontario. The entire construction phase lasted approximately one month. Each of the crosswalks is 2.635 m in width and concrete base crosswalks are 11.25 m and asphalt base and aggregate base are 12.50 m in length. The sand set crosswalk over concrete base is installed at station 2+010 Northbound, bituminous set over concrete base is at station 2+010 Southbound, the sand set over asphalt is at station 1+140 and the sand set over aggregate base is at station 1+095. Table 3 below summarizes the construction activities.

**Table 3: Summary of Construction**

<b>Crosswalk</b>	<b>Date</b>	<b>Construction Activity</b>
<b>1 (SSCBCH)</b>	July 23, 2007	Excavation of subbase for concrete base, moisture and temperature probes installation
	July 23, 2007	Compaction of subbase course and formworks for curbs and headers
	July 24, 29, 2007	Reinforcement rebars and drainage pipes placement
	July 24, 2007	Strain gauges installation and concrete placement
	July 27, 2007	Non woven geotextile installation and spreading and screeding of bedding sand
	July 27-31, 2007	Installation of ICP
	July 31, 2007	Spreading and sweeping of joint sands and final compaction
<b>2 (BSCBCH)</b>	July 25, 2007	Excavation of subgrade for concrete base, moisture probes and temperature probes installation
	July 25, 2007	Compaction of subbase course and formworks for curbs and headers
	July 25, 2007	Reinforcement rebars and drainage pipes placement
	July 26, 2007	Strain gauges installation and concrete placement
	August 1, 2007	Non woven geotextile installation and spreading and screeding of bituminous sand

	August 1, 2007	Placement of ICP
	August 1, 2007	Spreading and sweeping of joint sands and final compaction
<b>3</b> <b>(SSABAH)</b>	July 24, 2007	Excavation of subbase and moisture probes and temperature probes installation
	July 24, 2007	Compaction of subbase course
	July 25, 2007	Installation of strain gauges, asphalt (HL4) paving
	August 24, 2007	Installation of Aluminium angle edge restraint
	August 24, 2007	Non woven geotextile installation and spreading and screeding of bedding sand
	August 24, 2007	Installation of ICP
	August 24, 2007	Spreading and sweeping of joint sands and final compaction
<b>4</b> <b>(SSGBCH)</b>	July 26, 2007	Excavation of subbase and installation of moisture and temperature probes
	July 27, 2007	Compaction of subbase course and formworks for curbs and headers
	July 28, 2007	Concrete placement for curbs and headers
	June 31, 2007	Non woven geotextile installation and spreading and screeding of bedding sand
	June 31, 2007	Installation of ICP
	June 31, 2007	Spreading and sweeping of joint sands and final compaction

### **3.1.2.2.1 Base Construction**

Within the four crosswalk test sections, SSCBCH and BSCBCH have a concrete base underneath the ICP while SSABAH has an asphalt base and SSGBCH has an aggregate base underneath the ICP.

The SSCBCH was constructed first. After the final compaction of the subbase with a 20 kN/ 4500 lbs vibrating plate compactor, wooden forms were installed around the perimeter of the crosswalk for curbs and headers. Welded wire fabric having mesh size of 150 mm/150 mm was placed and high early concrete with 200 mm thickness was placed as shown in Figure 31. The concrete base of BSCBCH was constructed on July 26, 2006. The construction procedure is similar to the SSCBCH.



**Figure 30: Formworks, Drainage Pipes and Reinforcement Bars for SSCBCH Section**

The length of the concrete base sections is 11.25 m and the width is 2.635 m including the headers on both sides as shown in Figure 30. The thickness of the concrete bases is 200 mm. Each base has curb and headers around the perimeter, the width of the curb/header is 150 mm. Exposed concrete headers edges are trimmed to 3 mm radius to reduce the likelihood of chipping. The curing agent was applied after the initial setting of the concrete.

Prior to the concrete placement, twenty four ABS pipes with diameter of 75 mm and length of 300 mm were installed perpendicular to the road surface at the lowest level of the base course. Since the road base is constructed with a two percent slope towards the edge, four pipes were installed along the two outer edges of the bases and sixteen pipes were placed longitudinally along the inner side of the crosswalk. The pipes are filled with pea gravel and covered with non woven geotextile to prevent the loss of bedding materials. Their purpose is to remove excess water from the base course. The distance between adjacent drainage pipes (centre to centre) is approximately 60 cm and the first drainage pipe of each set is 20 cm offset from the edge of the base.



**Figure 31: Concrete Placement on SSCBCH Section**

The construction of SSABAH base was carried out on July 25, 2007 in two 50 mm lifts of HL4. The total of 16 tonnes of HL4 was spread, screeded, and compacted with a 20 kN plate compactor as shown in Figure 33. The air temperature during this operation ranged from 28°C to 33°C. The mix temperature on arrival to the site was 148°C and 126°C before compaction of the first lift. The mix was prepared at Cambridge Asphalt Supply of Steed and Evans Limited.

The SSABAH also has two concrete curbs similar to the concrete bases along the two edges that are parallel to the ring road. Two sets of four ABS pipes were placed along the outer edges of the base and filled with pea gravel and covered with geotextile. The distance between adjacent drainage pipes (centre to centre) is 60 cm and the first drainage pipe of each set is 20 cm offset from the edge of the base.

The construction of SSGBCH base of was done on July 26 2007, and the following the installation of moisture and temperature probes in subbase, 150 mm thick Granular A base course was placed and compacted with a 20 kN plate compactor. The concrete curbs and headers were built using the high early concrete.



**Figure 32: Concrete Base Section**



**Figure 33: Asphalt Base Construction**

#### ***3.1.2.2.2 Bedding Material Placement***

Prior to placing the interlocking concrete pavers, a layer of bedding material was placed in the base of each section. Gradation of the bedding sand is provided in Table 2. For SSCBCH, SSABAH and SSGBCH, a layer of non woven geotextile was placed in the constructed base and a layer of bedding sand with thickness of 25 mm was spread and screeded on top of the non woven geotextile.



**Figure 34: Granular Base Construction**

For SSABAH, an L-shaped aluminum angle was installed on top of the asphalt base and along the cut pavement edge. The aluminum angle is 9.5 cm wide and 9.5 cm high and 6 mm thick. Nails and screws were drilled alternatively through the aluminum angle and into the asphalt base in every 60 cm to fasten the edge restraint onto the base. On top of the angle plate and the asphalt base, a similar layer of non woven geotextile and bedding sand as crosswalk one were placed.

For BSCBCH, the concrete base surface was prepared with an emulsified asphalt tack coat. A hot-sand asphalt mix was brought to the site and spread and compacted to 25 mm thick layers. After the asphalt cooled, a thin coating of asphalt-neoprene adhesive was applied across the surface.

#### ***3.1.2.2.3 ICP Installation***

Installation was carried out in an identical manner to the test sections at the CPATT test track started from the corner with securing 45° string lines on the bedding course as shown in Figure 35. Edge pavers are saw-cut to fit against the sailor and shoulder courses. The sailor and shoulder are interlocking concrete pavers were placed in such a way that each section has three sides (one long side and two short sides) with sailor course and one long side with soldier course. After the installation, the surface was compacted with a vibratory plate roller to compact the bedding sand, seat the pavers in it and force the bedding sand into the joints at the bottom of the pavers. The final elevation of the surface course was kept 6 mm above the adjacent asphalt pavement to accommodate any future settlement.

#### ***3.1.2.2.4 Jointing Sand Placement and Final Compaction***

After initial compaction of the pavers, dry joint sand was spread on the surface and compacted with a vibratory compactor to ensure that the spaces between pavers are filled. During compaction, the pavement is transformed from a loose collection of pavers to an interlocking system capable of spreading vertical loads horizontally.



**Figure 35: Interlocking Concrete Pavers Placement**

#### ***3.1.2.2.5 Quality Control and Assurance***

Extensive sampling was performed throughout the construction of the research project. Samples were taken from the original Granular A and Granular B and HL4. Fifteen concrete cylinders were casted to perform the laboratory Compressive Strength Testing.

During the concrete placement, fifteen 100 mm x 200 mm concrete cylinders from each concrete mix were made. Two cylinders from each section were crushed on compressive strength testing equipment on 1 day, 2 day, 3 day, 7 day, 14 day, and 28 days after placement. As shown in Figure 37, the 28 day compressive strength for cylinders from both base sections did meet the 28 days compressive strength requirement (32 MPa).

In addition to extracting samples, mix temperature of the HL4 and sand asphalt were measured during the placement and before compaction. Slump (Figure 36) and air-void testing were also carried out for every batch of the concrete.



**Figure 36: On Site Concrete Slump Testing**

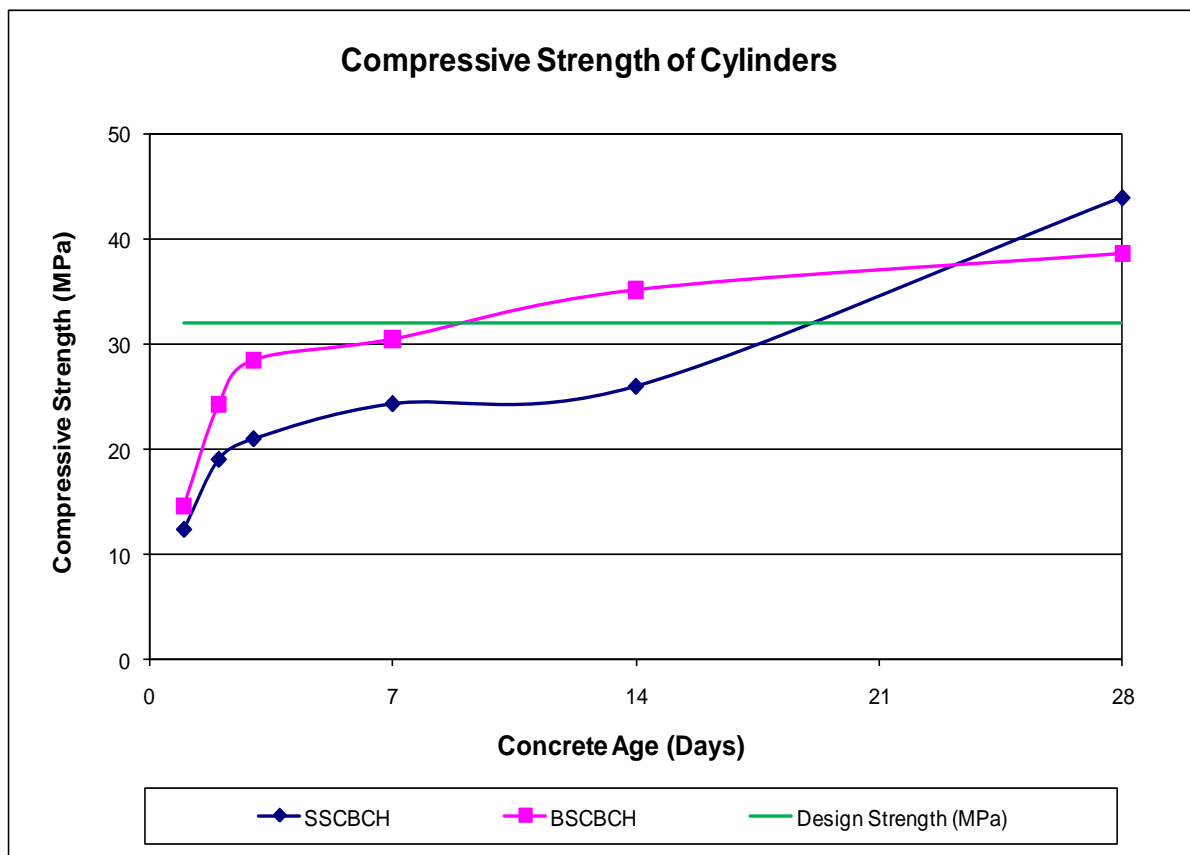


**Figure 37: Compressive Stress Testing Results**

## Chapter 4

### Instrumentation

Pavement instrumentation is crucial to understanding material performance in the field, as well as pavement system response to loading and environment. The goal of instrumentation is to assess the in-situ performance related to stress, strain, temperature and moisture. Sensors installed in pavement sections are divided into two categories. Temperature and TDR probes are installed to measure environmental responses whereas pressure cells and strain gauges are embedded to capture loading responses. The instrumentation details at two project locations are described in sections 4.1 and 4.2 respectively.

#### 4.1 CPATT Test Track

The sensors were installed during construction of the project. Four different type of sensors namely vibrating wire strain gauges, earth pressure cells, temperature and moisture probes are installed to determine the change of horizontal strain in asphalt and concrete bases, vertical earth pressure in base and subbase and temperature and moisture variation at different elevation in subbase as shown in Figure 46, 47, 48 and 49. The sensors cables were collected at a junction point and fed into a 100 mm ABS conduit. The conduit is buried in a shallow trench and routed to the data logger box. Table 4 summarizes the purpose and locations of the sensors.

**Table 4: Summary of Instrumentation**

Crosswalk	Sensor	Qty	Location	Purpose
<b>1 (SSCBCH)</b>	Concrete Strain Gauge (VWSGE)	2	50 mm and 150 mm from top of concrete base at 1.15 m offset from road edge	Measure change of strain in concrete
	Earth Pressure Cells (LPTPCO9-V)	2	Bottom of concrete base and at 250 mm from bottom of base at 1.6 m offset from road edge	Measure vertical stress in base and subbase
	Thermistor (TH0003-250-2)	2	50 mm and 250 mm from bottom of concrete base at 1.4 m offset from road edge	Measure the change of temperature
	Moisture Probes	2	100 mm and 250 mm from top of	Measure in-situ

	(6005L40WGL60 60 cm)		concrete base at 3 m offset from road edge	moisture content
<b>2</b> <b>(SSABAH)</b>	Asphalt Strain Gauge (VWSGEA)	3	Bottom of the asphalt base at 1.1 m, 2.2 m and 3.3 m offset from road edge	Measure the change of strain in the asphalt
	Earth Pressure Cells (LPTPC09-V)	2	Bottom of concrete base and at 250 mm from bottom of base at 1.6 m offset from road edge	Measure vertical stress in base and subbase
	Thermistor (TH0003-250-2)	2	50 mm and 250 mm from bottom of concrete base at 1.4 m offset from road edge	Measure the change of temperature
	Moisture Probes (6005L40WGL60 60 cm)	2	100 mm and 250 mm from top of concrete base at 3 m offset from road edge	Measure in-situ moisture content
<b>3</b> <b>(BSCBCH)</b>	Concrete Strain Gauge (VWSGE)	2	50 mm and 150 mm from top of concrete base at 1.15 m offset from road edge	Measure change of strain in concrete
	Earth Pressure Cells (LPTPC09-V)	2	Bottom of concrete base and at 250 mm from bottom of base at 1.6 m offset from road edge	Measure vertical stress in base and subbase
	Thermistor (TH0003-250-2)	2	50 mm and 250 mm from bottom of concrete base at 1.4 m offset from road edge	Measure the change of temperature
	Moisture Probes (6005L40WGL60 60 cm)	2	100 mm and 250 mm from top of concrete base at 3 m offset from road edge	Measure in-situ moisture content

#### 4.1.1 Moisture Probe

A moisture probe is a device consisting of three 600 mm long stainless steel rods for measuring moisture content as shown in Figure 38. Two probes are installed horizontally in each section at 100 mm and at 250 mm from the top of the subbase and at 3 m offset from the road edge.

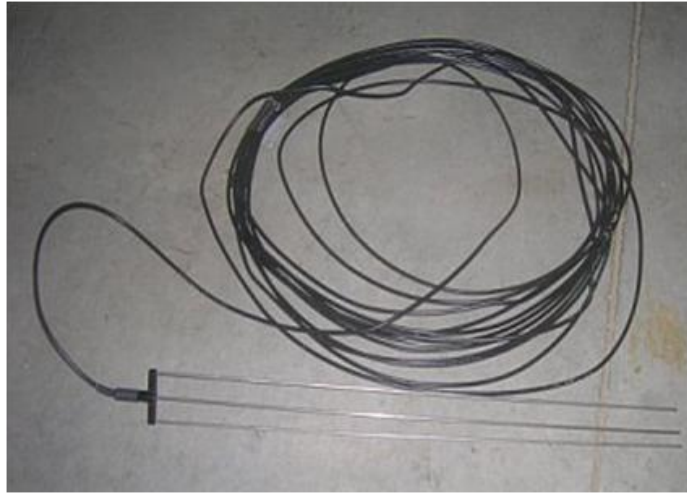


**Figure 38: Moisture Probes**

To install a moisture probe, a cavity of 700 mm x 200 mm x 300 mm is excavated into the subbase to accommodate the moisture probe. A cable trench of 200 mm wide and 250 mm deep running from the cavity to the edge of pavement was also excavated as shown in Figure 39. This trench is used to run the cables of pressure cells and temperature probe as well. All sharp stones fragments were removed from the cavity and the trench. The cavity and the trench were filled with 5 mm sand layer and the probes and cables were placed. After placing the sensors and cables the trench was filled with sand and sub base materials and compacted with a marshal hammer to ensure the density. Similarly, the second probe is installed at 150 mm above the first probe and filled with sand and compacted with a marshal hammer.



**Figure 39: Moisture Probes Installation**

### 4.1.2 Earth Pressure Cells

Earth Pressure Cells, a device to measure the vertical stress are constructed from two circular stainless steel plates, welded together around their periphery. An annulus exists between the plates, which is filled with de-aired glycol. The cell is connected via a stainless tube to a transducer forming a closed hydraulic system. As stress is exerted on the surface of the cell, it pressurizes the fluid within the cell, which in turn is measured by the pressure transducer.

Two pressure cells are installed horizontally in each section at the bottom of the concrete/asphalt base and at 250mm from the top of the sub base at 1.6 m offset from the road edge.

To install pressure cells, a cavity of 700 mm x 300 mm x 300 mm is excavated into the sub-base to accommodate the pressure cells. Cable trench excavated for moisture probes cables is used to run the pressure cells cables as well. All sharp stones fragments were removed from the cavity and the trench. The cavity and the trench were filled with 5 mm sand layer and the pressure cells and cables were placed as shown in Figure 40. After placing the pressure cells and cables, the trench was filled with sand and sub base materials and compacted with a marshal hammer to ensure the density. Similarly, the second cell is installed at 250 mm above the first cell and filled with sand and compacted with a marshal hammer.



**Figure 40: Earth Pressure Cells Installation**

### 4.1.3 Temperature Probe

Temperature probes are installed to measure temperature variation at different elevations within the pavement structure. The temperature probe consists of two thermistors at the distance of 200 mm are

installed vertically in the sub base in each section. The thermistors are located at 50 mm and 250 mm from the top of the sub base at 1.4 m offset from the road edge.

To install the temperature probes, a cavity of 300 mm x 300 mm x 600mm is excavated into the subbase as shown in Figure 41. All sharp stones fragments were removed from the cavity and the trench. The cavity and the trench were filled with 5 mm sand layer and the probes and cables were placed. After placing the temperature probe and the cables, the trench was filled with sand and subbase materials and compacted with a marshal hammer to ensure the density.



**Figure 41: Temperature Probe Installation**

#### **4.1.4 Vibrating Wire Strain Gauges**

Two types of strain gauges are installed to measure a strain in asphalt and concrete bases as shown in Figures 42 and 43 respectively. Three asphalt strain gauges are placed at the bottom of the asphalt base at 1.1 m, 2.2 m and 3.3 m offsets from the road edge. Alternatively, concrete strain gauges are installed at the depth of 50 mm and 150 mm from the top of the concrete base at 1.15 m offset from the road edge.

A HMA pad was placed at the asphalt strain gauges locations. After asphalt cooled, the strain gauges are hand placed and gently pressed into the mix as shown in Figure 44. A shallow cable trench was excavated and routed the cables to the edge. The backfill then was filled with sand and compacted with the marshal hammer



**Figure 42: Vibrating Wire Asphalt Strain Gauge**



**Figure 43: Vibrating Wire Concrete Strain Gauge**

Concrete strain gauges are attached with U-shaped chairs and the chairs were driven into the ground and tied together to prevent from moving as shown in Figure 45. A shallow cable trench was excavated and routed the cables to the edge. The backfill then was filled with sand and compacted with the marshal hammer.



**Figure 44: Vibrating Wire Asphalt Strain Gauge Installation**

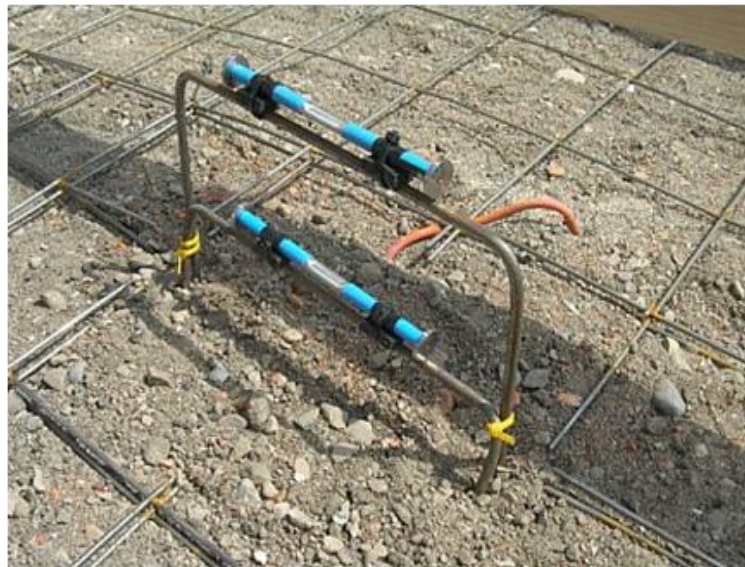


**Figure 45: Vibrating Wire Concrete Strain Gauge Installation**

Profile views of each type of crosswalk showing the various locations of sensors are presented in Figures 46, 47, 48 and 49 respectively.

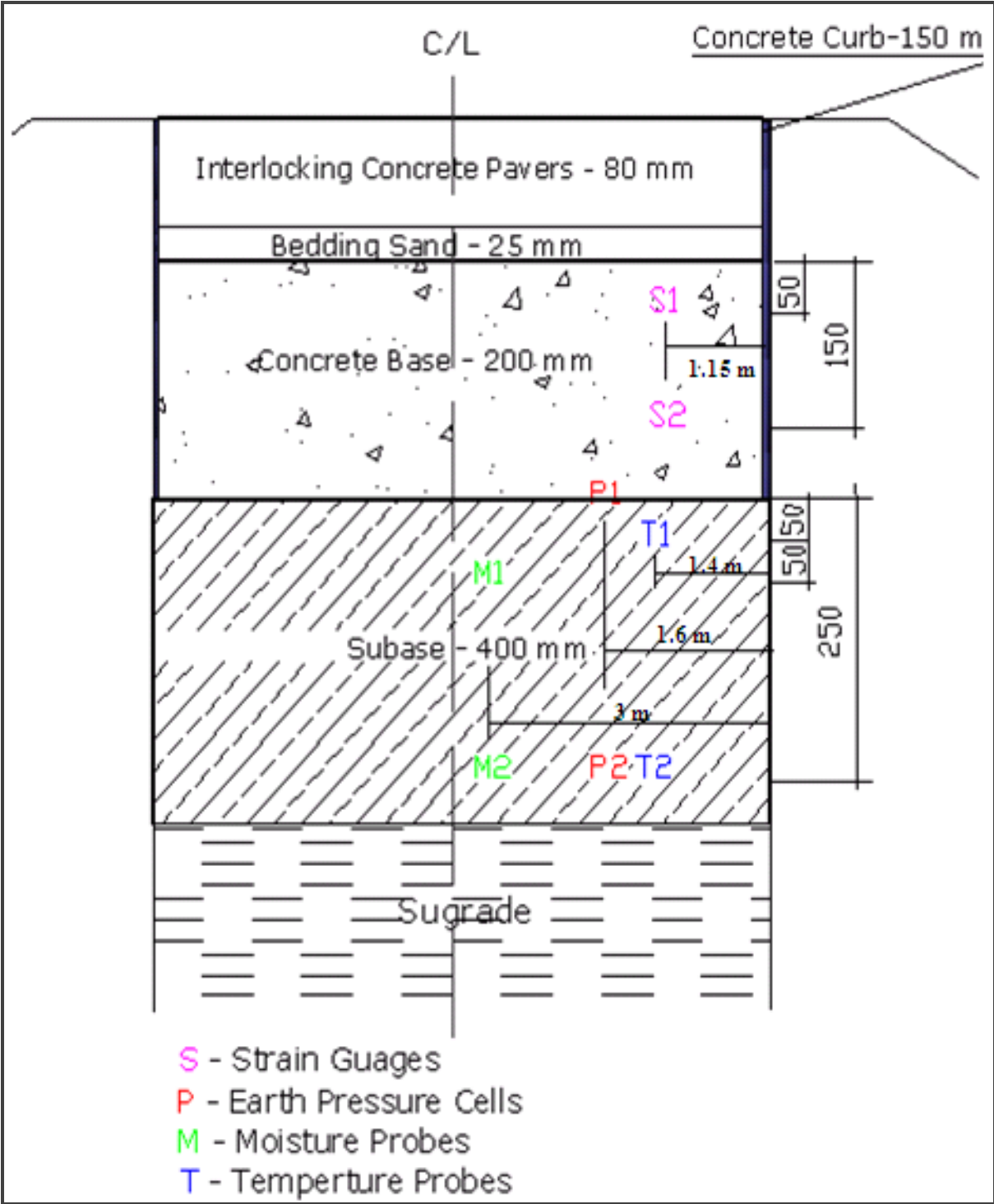


Figure 46: Profile View of Instrumented SSCBCH

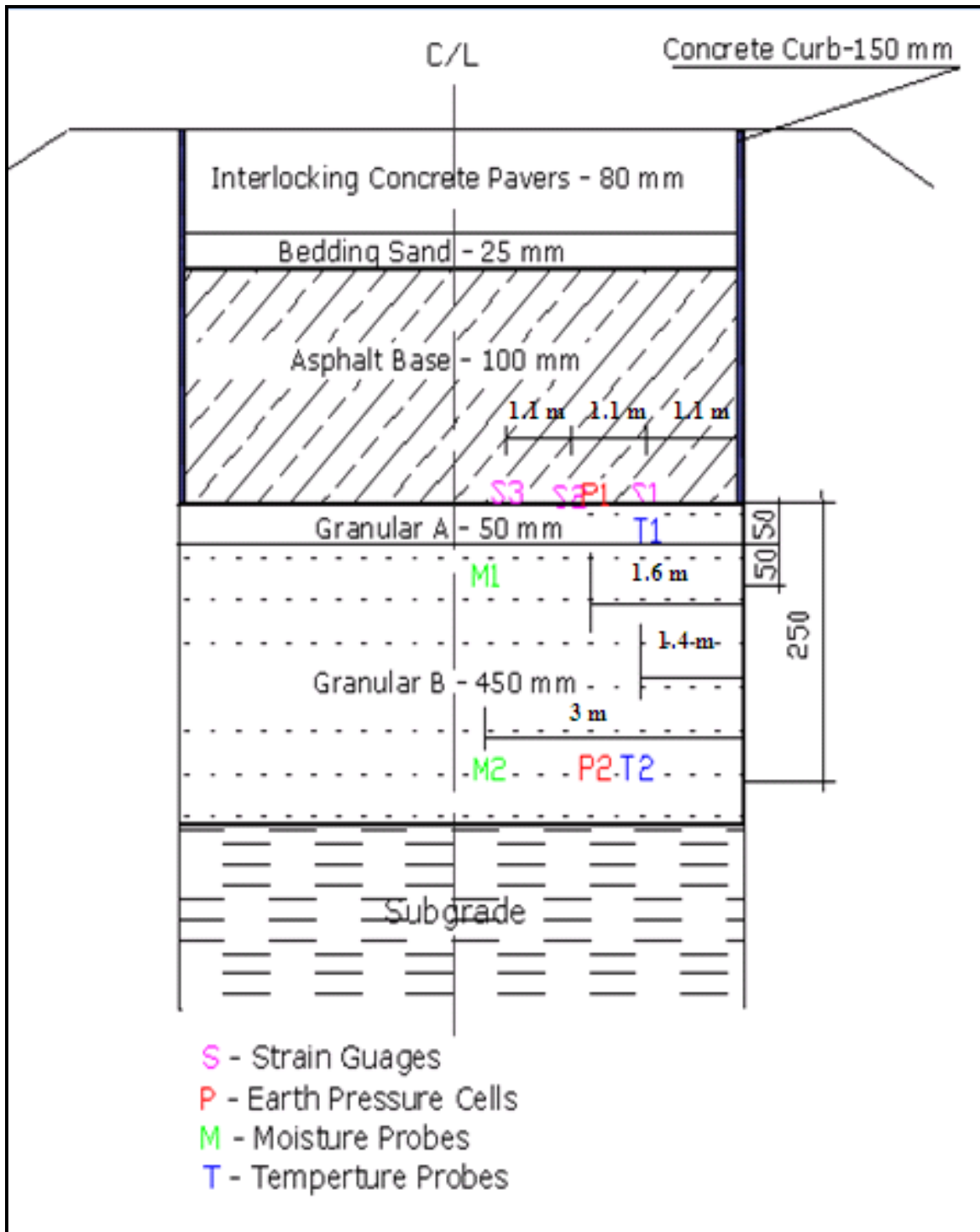


Figure 47: Instrumented View of SSABSH

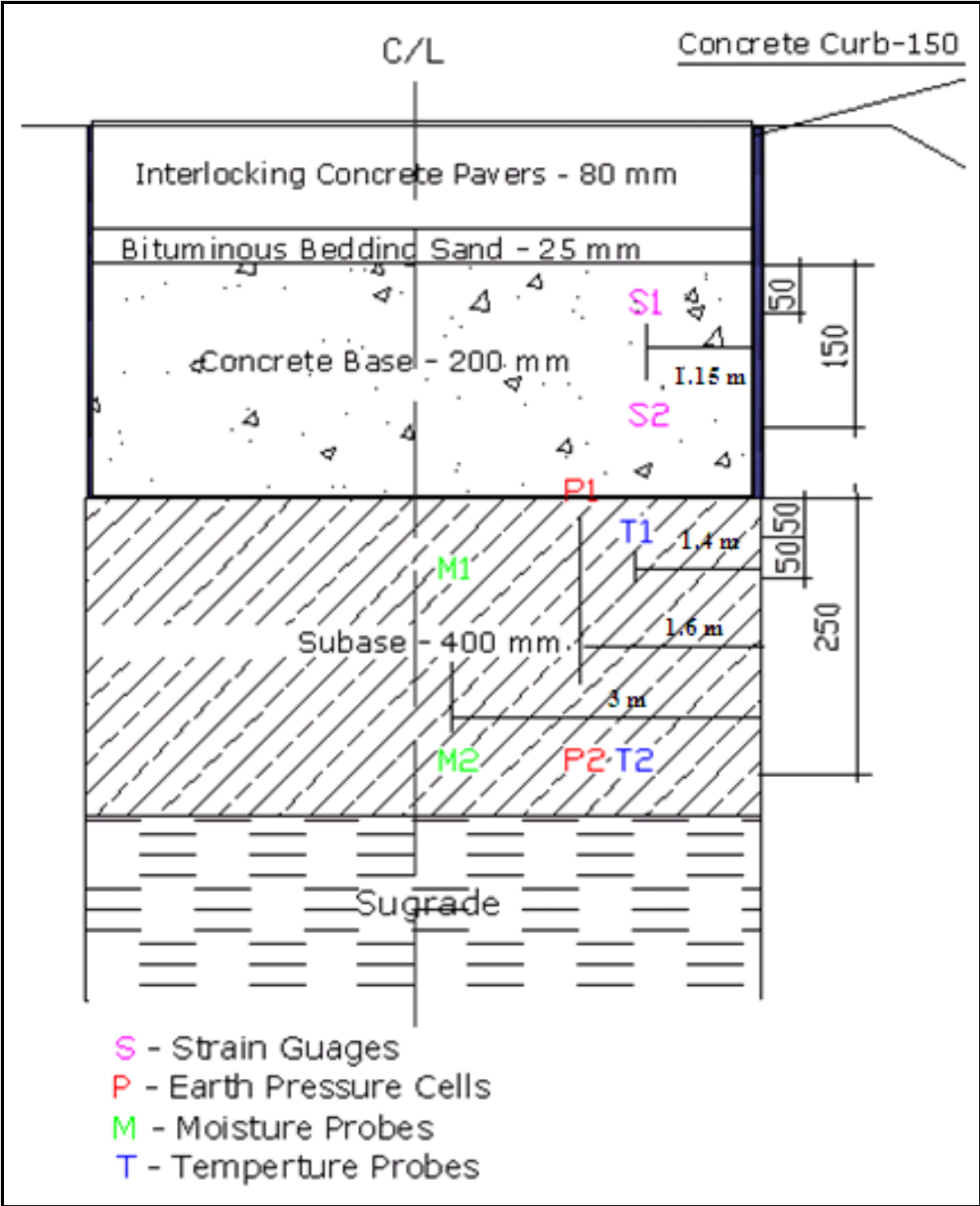


Figure 48: Profile View of Instrumented BSCBCH

#### 4.1.5 Data logger Installation

Several 100 mm diameter ABS conduits were used to route the cables to the data logger. A 50 cm wide trench was excavated along the road embankment and the conduits were laid and buried with the excavated materials. The Data logger is installed at 8.5 m west of middle crosswalk section near the fence. Figure 49 shows the plan view of conduits and data logger layout.

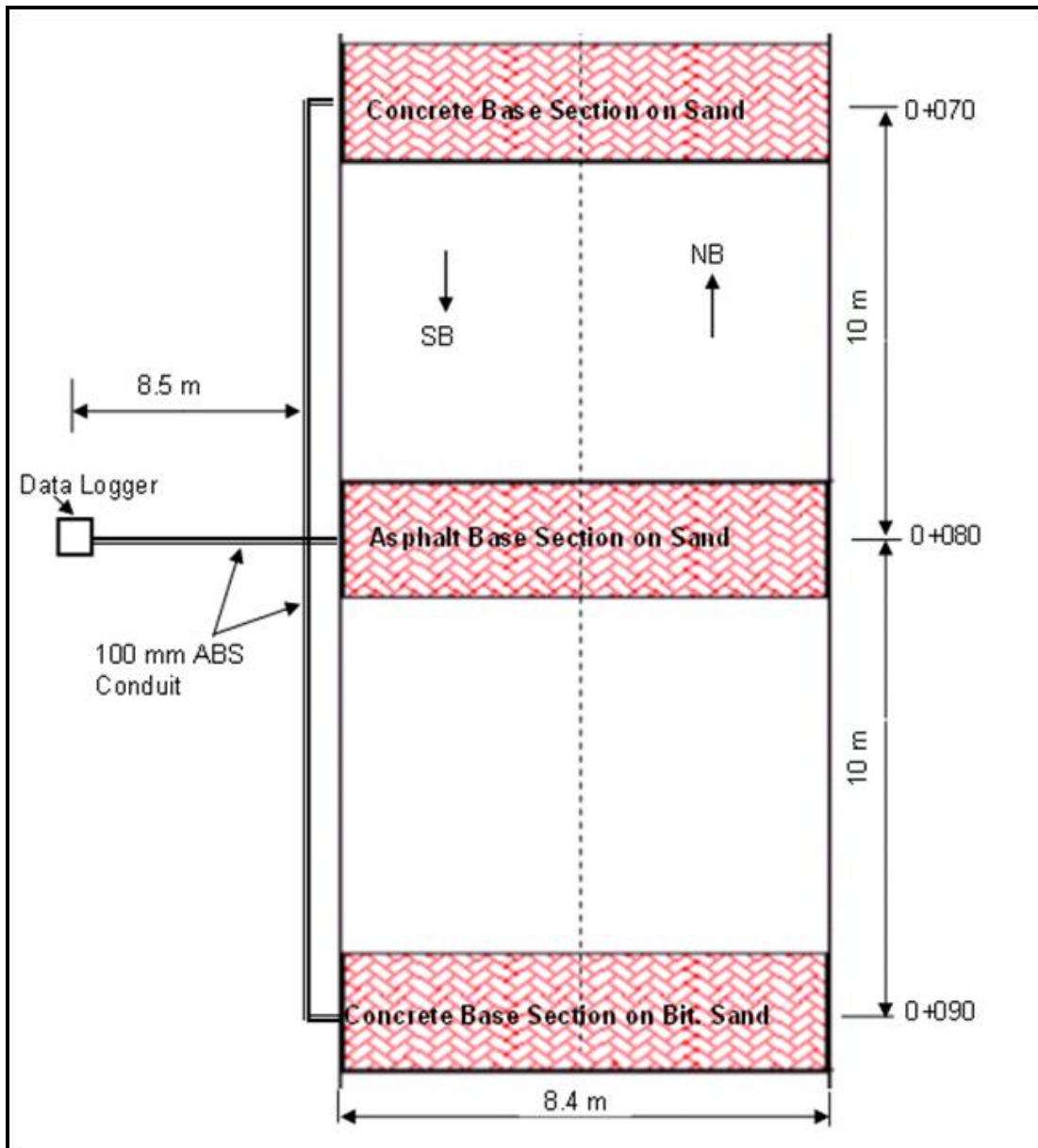


Figure 49: Conduit and Data Logger Layout

## 4.2 University of Waterloo Ring Road

At the ring road, three different types of sensors namely vibrating wire strain gauges, temperature profiles and moisture probes were installed in SSCBCH, BSCBCH and SSABAH sections as shown in Figures 50, 51 and 52. In contrast, only two types of sensors namely moisture and temperature probes are used in SSGBCH as shown in Figure 53. The sensors are installed in an identical manner as discussed in previous section. Table 5 details the summary of instrumentation at this location.

**Table 5: Summary of Instrumentation**

<b>Crosswalk</b>	<b>Sensor</b>	<b>Qty</b>	<b>Location</b>
<b>1 (SSCBCH)</b>	Concrete Strain Gauge (VWSGE)	2	50 mm and 150 mm from top of concrete base at 1.15 m offset from road edge
	Thermistor (THO003-250-2)	2	50 mm and 250 mm from bottom of concrete base at 1.4 m offset from road edge
	Moisture Probes (LPTPCO9-V)	2	100 mm and 250 mm from top of concrete base at 3m offset from road edge.
<b>2 (BSCBCH)</b>	Concrete Strain Gauge (VWSGE)	2	50 mm and 150 mm from top of concrete base at 1.15 m offset from road edge
	Thermistor (THO003-250-2)	2	50 mm and 250 mm from bottom of concrete base at 1.4 m offset from road edge
	Moisture Probes (LPTPCO9-V)	2	100 mm and 250 mm from top of concrete base at 3 m offset from road edge.
<b>3 (SSAHAB)</b>	Asphalt Strain Gauge (VWSGEA)	3	Bottom of the asphalt base at 1.1 m, 2.2 m and 3.3 m offset from road edge
	Thermistor (THO003-250-2)	2	50 mm and 250 mm from bottom of concrete base at 1.4 m offset from road edge
	Moisture Probes (LPTPCO9-V)	2	100 mm and 250 mm from top of concrete base at 3 m offset from road edge
<b>4 (SSCHAB)</b>	Thermistor (THO003-250-2)	2	50 mm and 250 mm from bottom of concrete base at 1.4 m offset from road edge
	Moisture Probes (LPTPCO9-V)	2	100 mm and 250 mm from the top of the concrete base at 3 m offset from road edge

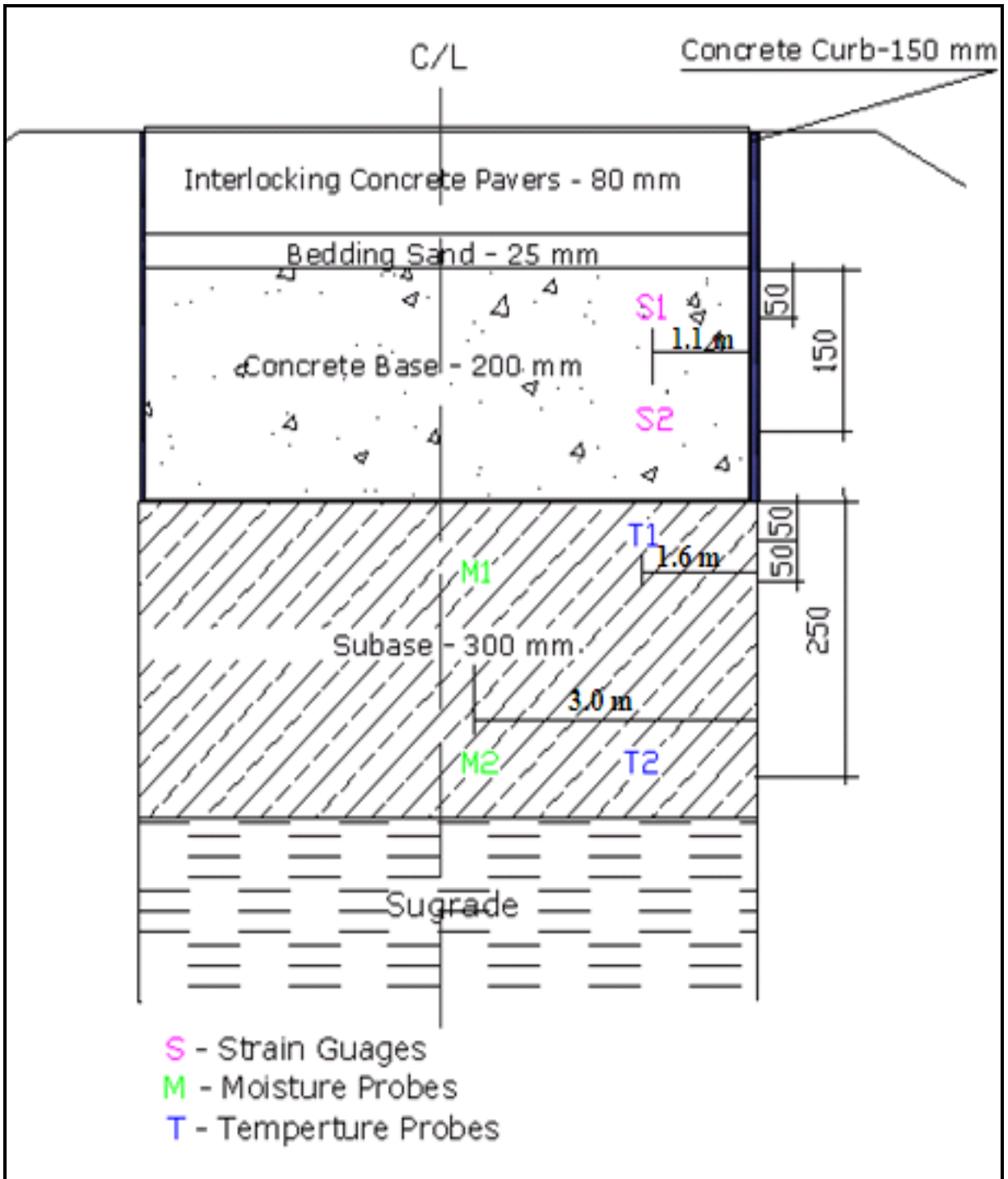


Figure 50: Profile View of Instrumented SSCBCH

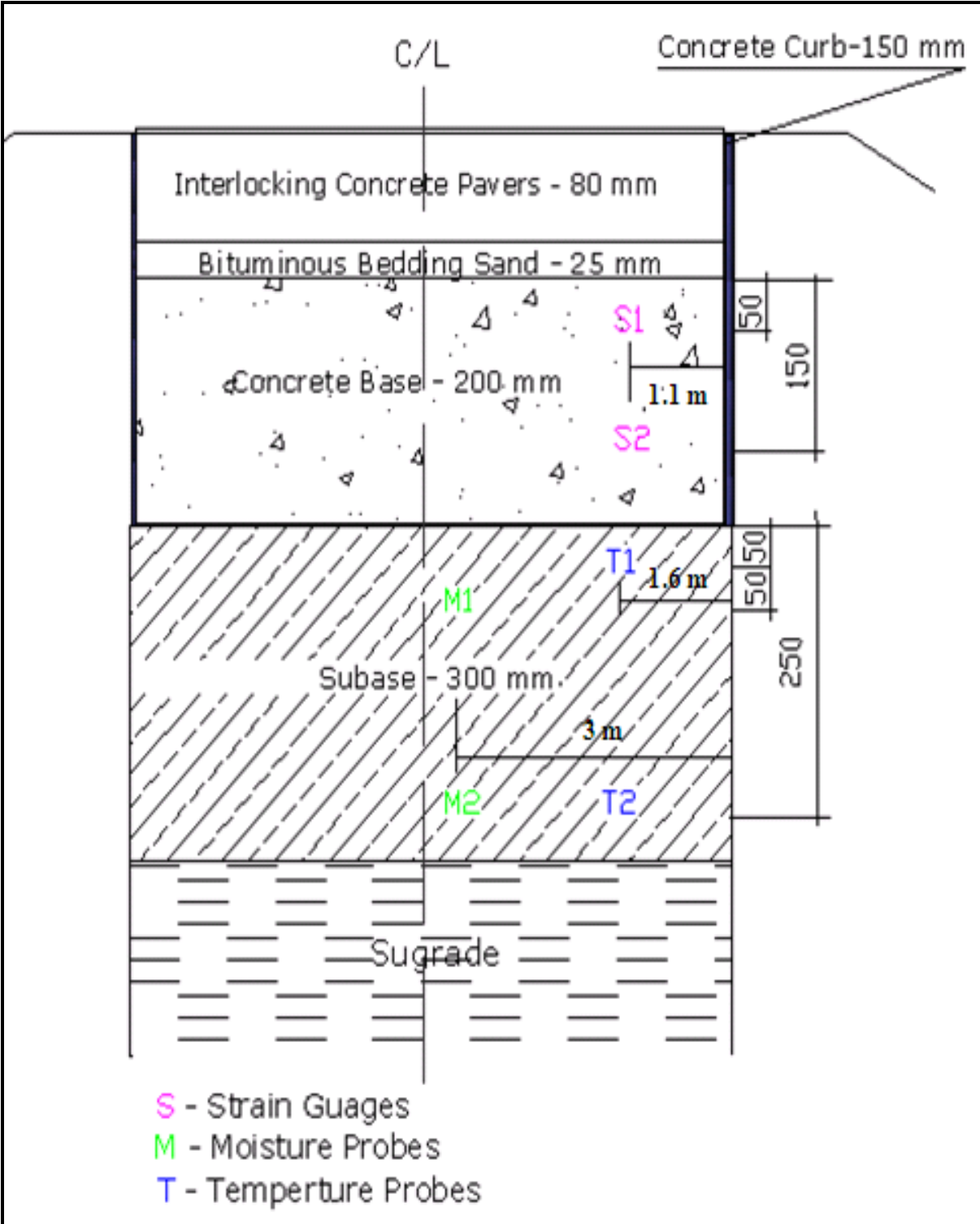


Figure 51: Profile View of Instrumented BSCBCH

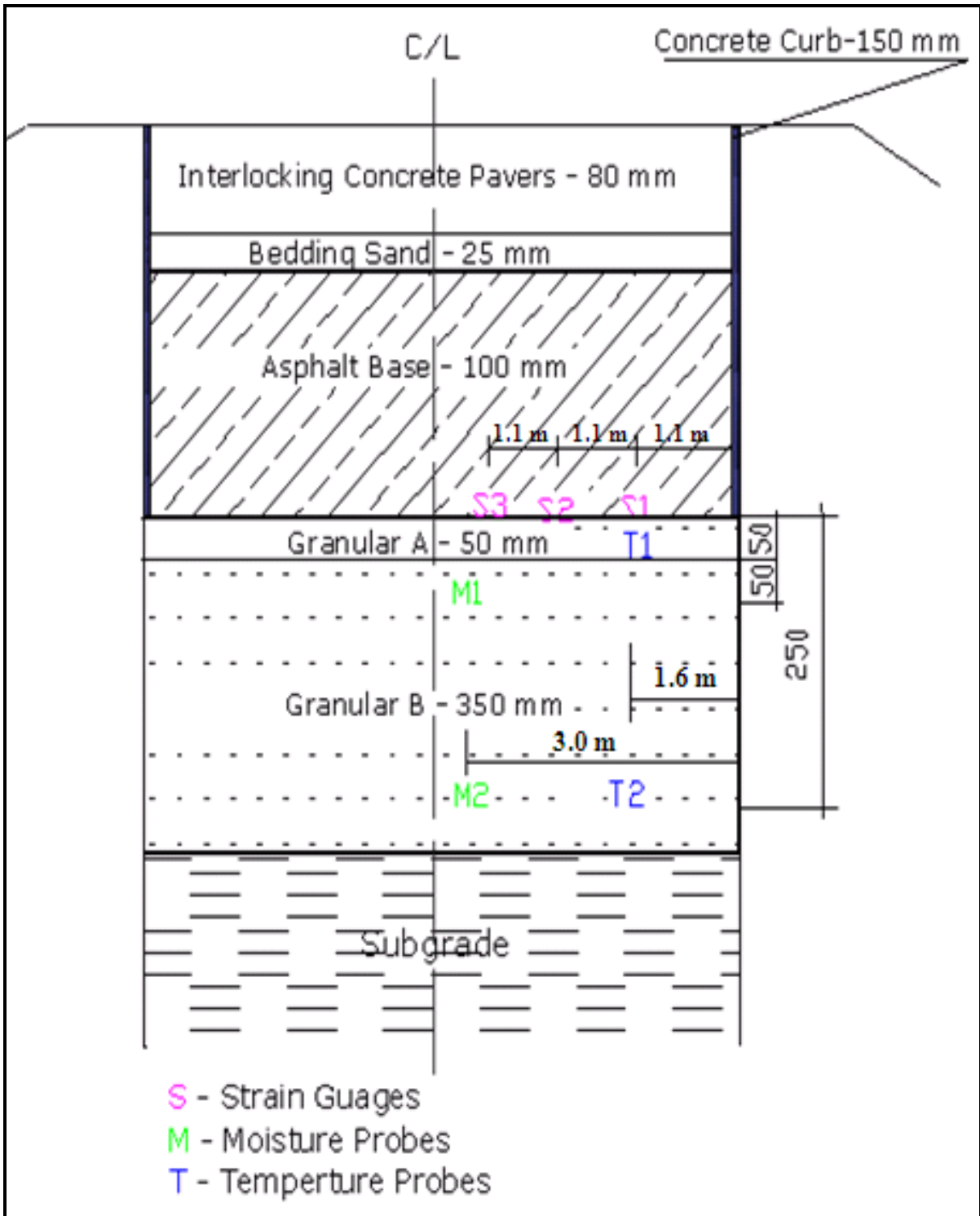


Figure 52: Profile View of Instrumented SSABAH

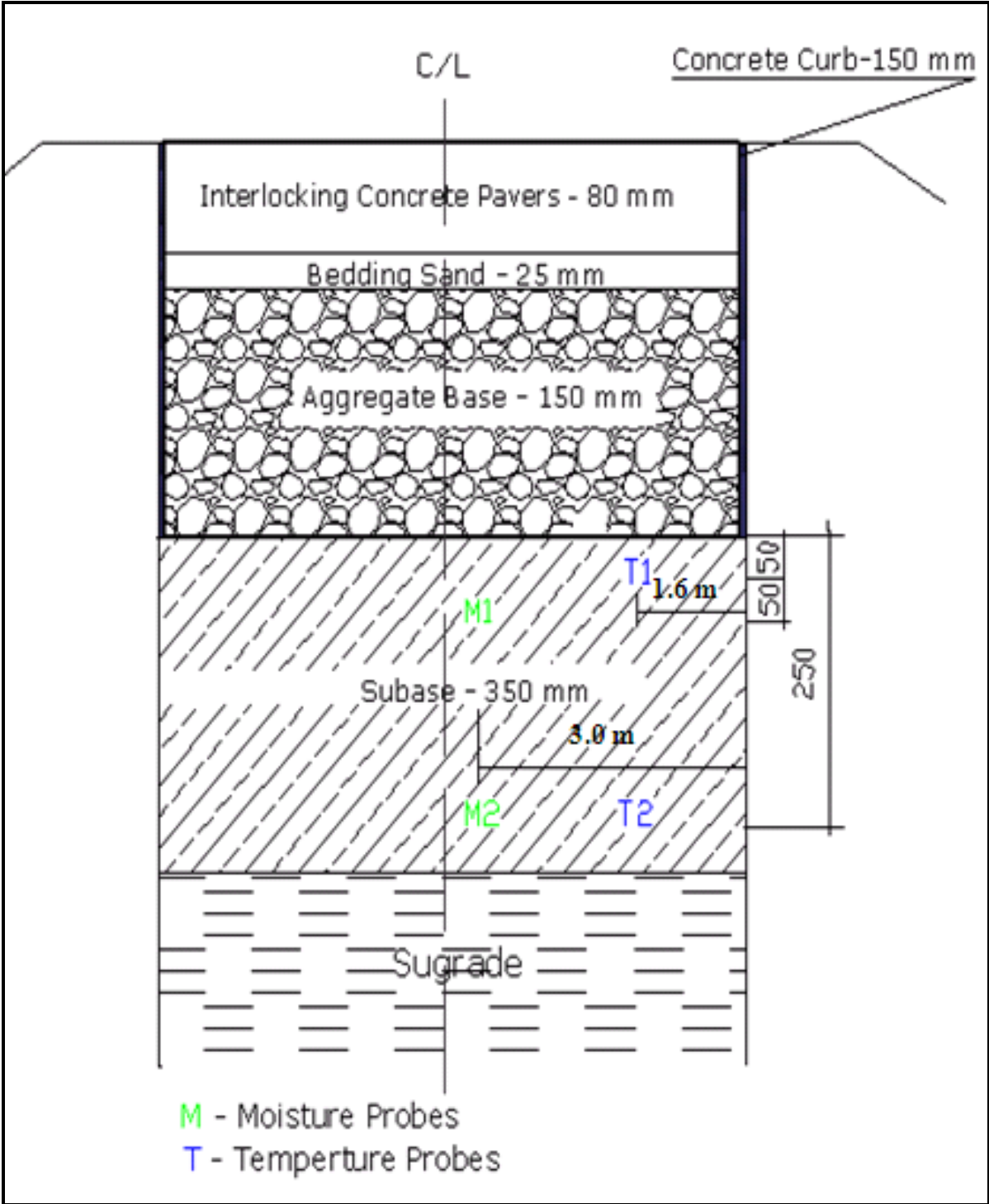


Figure 53: Profile View of Instrumented SSGBCH

### 4.2.1 Data Logger Installation

ABS conduits with the diameter of 75 mm were placed to route the cables from each crosswalk section to the collection point as shown in Figure 54 and a 100mm diameter conduit was installed to route all cables to the data logger from the collection point. The data logger is installed in between SSCBCH and BSCBCH on the road island. The data logger box is housed in a traffic cabinet which is placed on an existing concrete sidewalk and fastened with bolts.

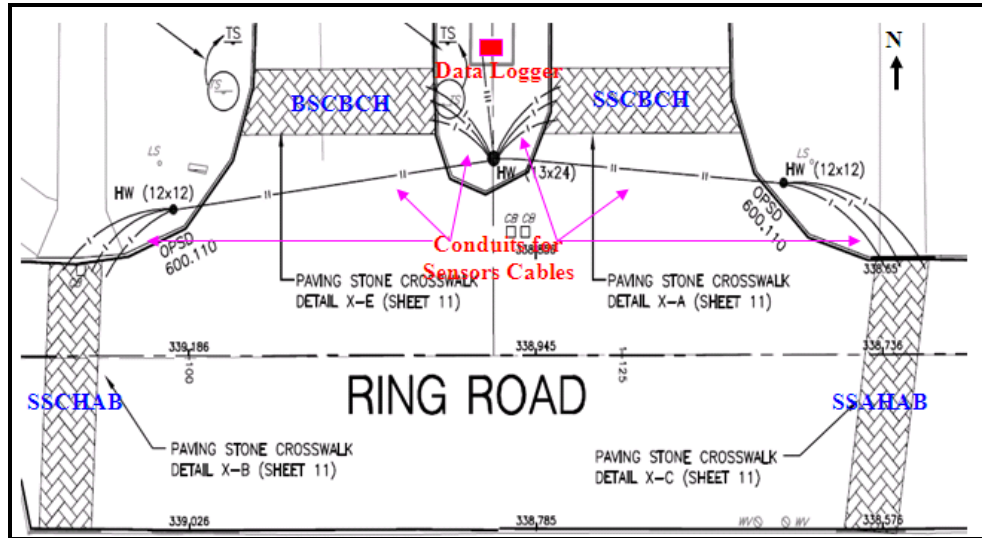


Figure 54: Conduits and Data Logger Layout

### 4.3 Sensors Validation

After installation, all sensors were tested for functionality by connecting to the data logger as shown in Figure 55. All of them were working normally during the testing.



Figure 55: Sensors Functionality Validation

## **Chapter 5**

### **Data Analysis**

#### **5.1 Data Collection**

Five different types of data as summarized in following sections were collected for the analysis. The data collection from installed sensors involved using a direct wire which sends data from the data logger using the Logger Net software to a laptop computer. Logger Net is a software that writes and compiles monitoring programs to transfer the program to the data logger and to retrieve the data by direct wires.

##### **5.1.1 Traffic**

Traffic data (AADT, vehicle type distribution, axle weight data for each vehicle type) at test track is obtained from Region of Waterloo Waste Management automation system. The CPATT test track encounters heavy truck loading primarily loaded garbage trucks. Traffic design loading for crosswalk projects is based on the AASHTO design procedure is represented using Equivalent Single Axle Load (ESAL) concept. It is calculated that there is approximately 150,000 ESAL/year.

The University of Waterloo Ring Road has traffic similar to a typical urban road with approximately 10% truck and 5% bus traffic. The annual calculated ESALs for the entire intersection is approximately 26,000 a year which is based on previous reports. The traffic distribution in the intersection is divided into two parts and the total ESALs for each crosswalk section is considered 13,000 ESALs/year.

##### **5.1.2 Horizontal Strain**

Horizontal Strain data was collected from August 15, 2007 to May 14, 2008 at the test track and from November 20, 2007 to May 14, 2008 at the ring road at four hours interval.

The strain gauge can measure actual strain changes due to changes in moisture content of the concrete and stresses from traffic loading. Thermal correction factor is used to adjust change in strain due to temperature changes. The following equation is used to convert measured resonance reading into change of strain. The temperature data was also collected from vibrating wire strain gauges.

$$\varepsilon_t = (S_n - S_0) * GF + (T_n - T_0) * (TC_{c/a} - TC_s) \quad (1)$$

Where,  $\varepsilon_t$  = True strain (microstrain)

$S_n$  = Current resonance reading

$S_0$  = Initial resonance reading

GF = 1, Gauge factor for strain gauges model VWSGEA and VWSGE

$T_n$  = Current temperature reading (°C)

$T_0$  = Initial temperature reading (°C)

$TC_{c/a}$  = Thermal Coefficient of Concrete/Asphalt,

$TC_s$  = Thermal Coefficient of Steel

A negative value indicates compressive strain and a positive value indicates tensile strain in above equation.

### 5.1.3 Vertical Stress

Vertical stress data was collected from August 15, 2007 to May 14, 2008 at the test track at four hours interval. No Earth Pressure Cells were installed in crosswalk sections located at the Ring Road. The following equation is used to calculate the change of vertical stress-state. The temperature data was also collected from vibrating wire Earth Pressure Cells.

$$\sigma = E * (P_n - P_0) * 10^{-6} \quad (2)$$

Where,  $\sigma$  = Vertical stress (MPa)

E = Elastic Modulus of material where the pressure cell is placed (MPa)

$P_n$  = Current pressure reading

$P_0$  = Initial pressure reading

A negative value indicates compressive stress and a positive value indicates tensile stress in above equation.

### 5.1.4 Temperature

Temperature data was collected from August 15, 2007 to May 14, 2008 at the test track and from November 20, 2007 to May 14, 2008 at the ring road at four hours interval. The data was also collected from strain gauges and Earth Pressure Cells.

### **5.1.5 Moisture**

Moisture data was collected from August 15, 2007 to May 14, 2008 at the test track and from November 20, 2007 to May 14, 2008 at the ring road on a weekly basis.

## **5.2 Pavement Response**

The pavement response of each section is carried out on the basis of accumulated horizontal strain in base and vertical stress in subbase. The performance of each crosswalk section in terms of accumulated strain and stress over time is discussed in the following sections.

### **5.2.1 Test Track**

The accumulation of stress and strain in three different crosswalk design assemblies at test track over a nine months period (114,000 ESALs) and respective environmental data are presented. Trendlines of stress and strain accumulations are influenced by variations in environmental conditions i.e. temperature, rainfall and moisture.

#### **5.2.1.1 Crosswalk One – SSCBCH**

Figure 56 shows the accumulation of vertical stress and moisture variation in subbase layer in SSCBCH from August, 2008 to the end of May, 2008. During this period 114,000 ESALs was observed. It can be seen that the formation of stress is not only affected by traffic loading but also by moisture variation. Tensile vertical stress is formed on the top of the subbase as well as at 250 mm below the subbase. The maximum amount of tensile stress is in March due to the effect of thawing of the pavement layers. No compressive stress is formed during this period which is a main contributor to rutting in granular layers.

Figure 57 shows the accumulation of strain in the concrete base of SSCBCH in the period of nine months since August, 2007. It can be seen that temperature variation has a direct impact to the formation of strain. High tensile strain is formed during winter when the temperature is below 0<sup>0</sup> Celsius. As temperature increases the tensile strain decreases in the concrete.

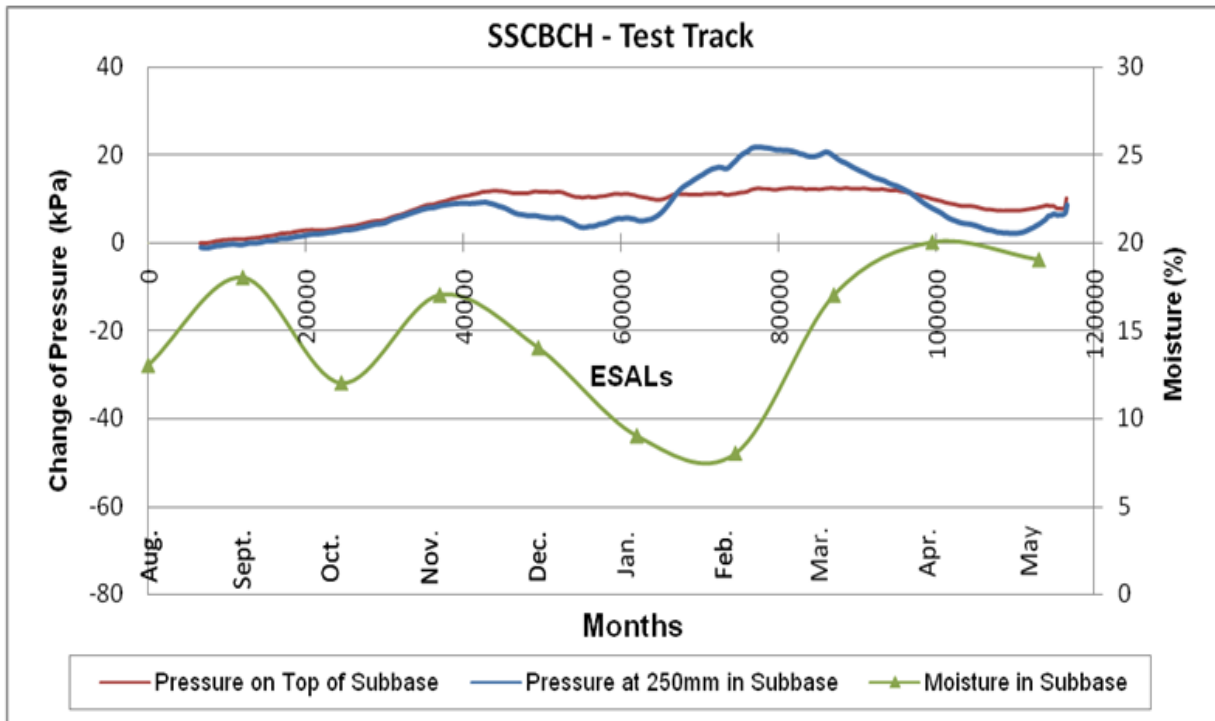


Figure 56: Measured Vertical Stress and Moisture Variation in Subbase of SSCBCH

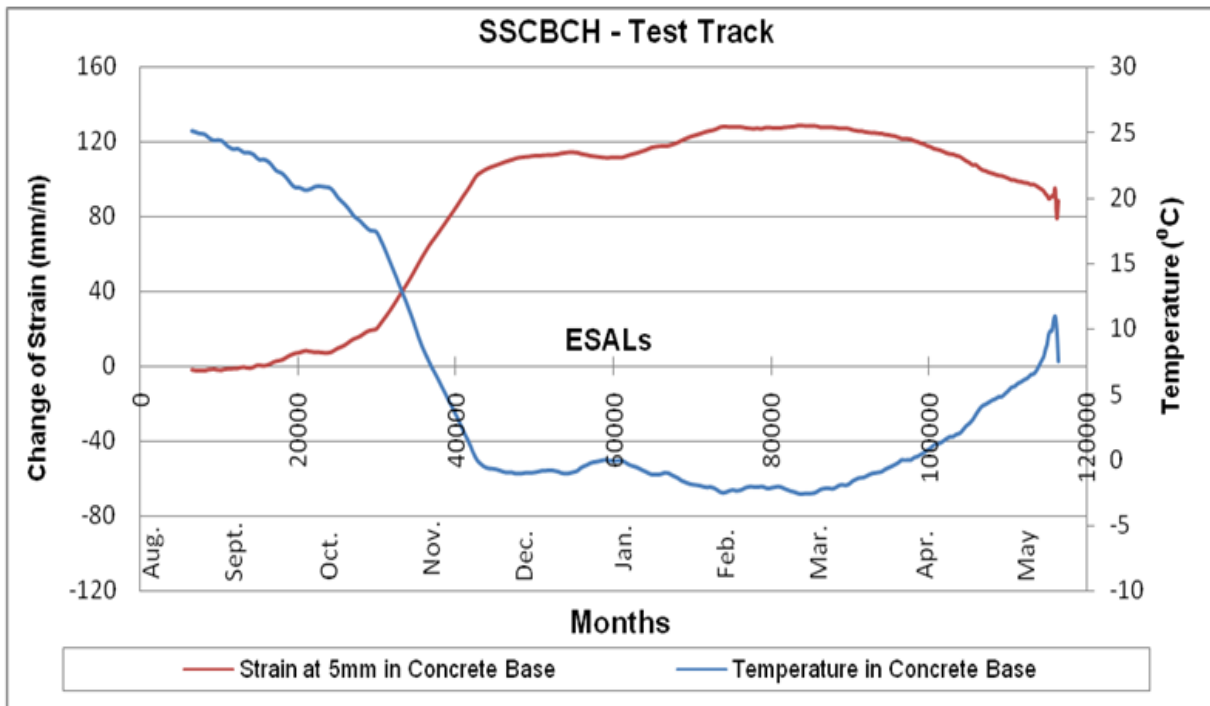
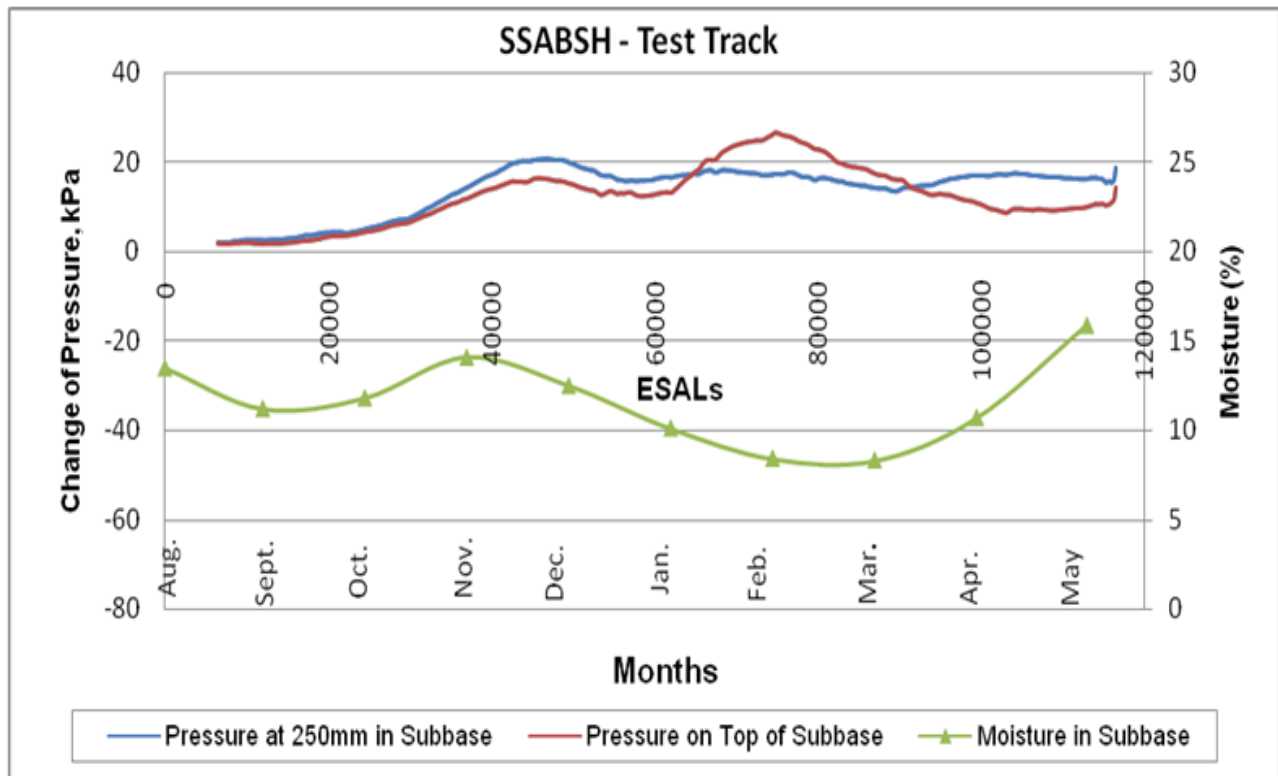


Figure 57: Accumulation of Horizontal Strain and Temperature Variation in Base of SSCBCH

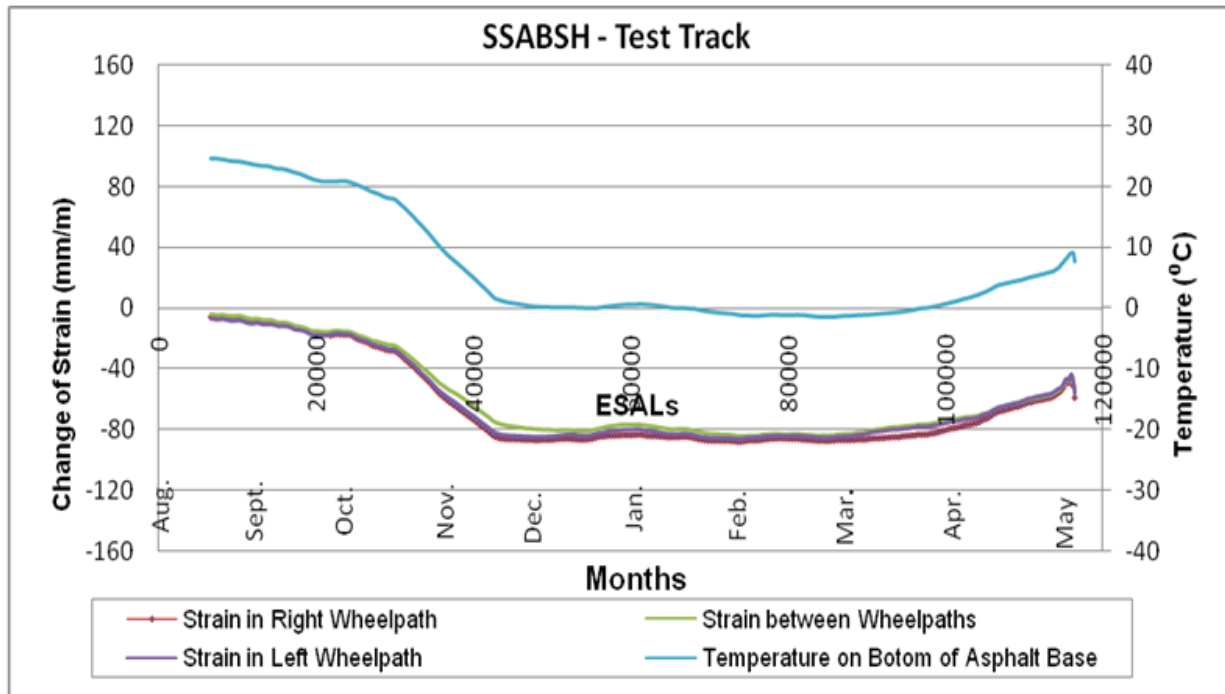
### 5.2.1.2 Crosswalk Two – SSABAH

Figure 58 shows the accumulation of vertical stress and moisture variation in subbase layer in SSABSH at test track from August, 2008 to May, 2008. It can be seen that the formation of stress is affected by moisture variation. Tensile vertical stress is formed on the top of the subbase as well as at 250 mm below in the subbase. The maximum amount of tensile stress is formed in late February because granular layers start thawing in late February. No compressive stress is formed during this period. This stress can be a main contributor to rutting in granular layers.

Figure 59 shows the accumulation of strain at the bottom of the asphalt layer in SSABSH in this period. It can be seen that temperature has a direct impact on the formation of strain. High compressive strains are formed during winter when the temperature is below 0<sup>0</sup> Celsius. As the temperature increases, the tensile strain increases at the bottom of the asphalt base. It is likely to form tensile strain when the temperature is above 15<sup>0</sup> Celsius which is a main contributor of fatigue cracking in asphalt layer.



**Figure 58: Accumulated Vertical Stress and Moisture Variation in Subbase of SSABSH**



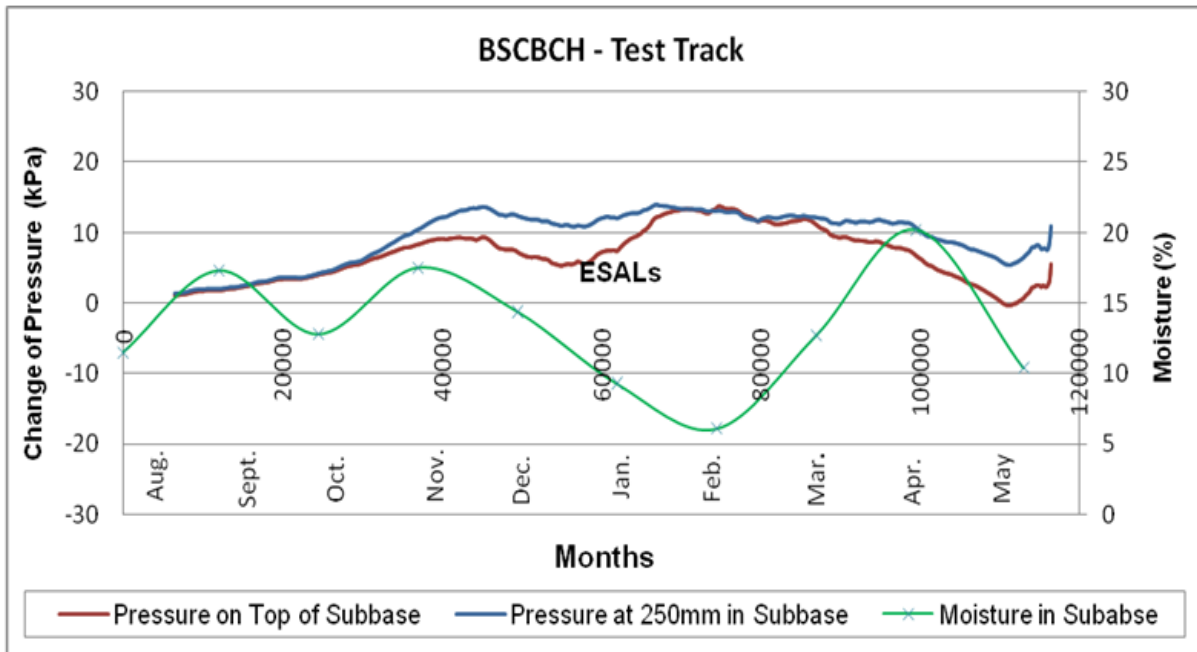
**Figure 59: Accumulated Horizontal Strain and Temperature Variation in Base of SSABSH**

### 5.2.1.3 Crosswalk Three – BSCBCH

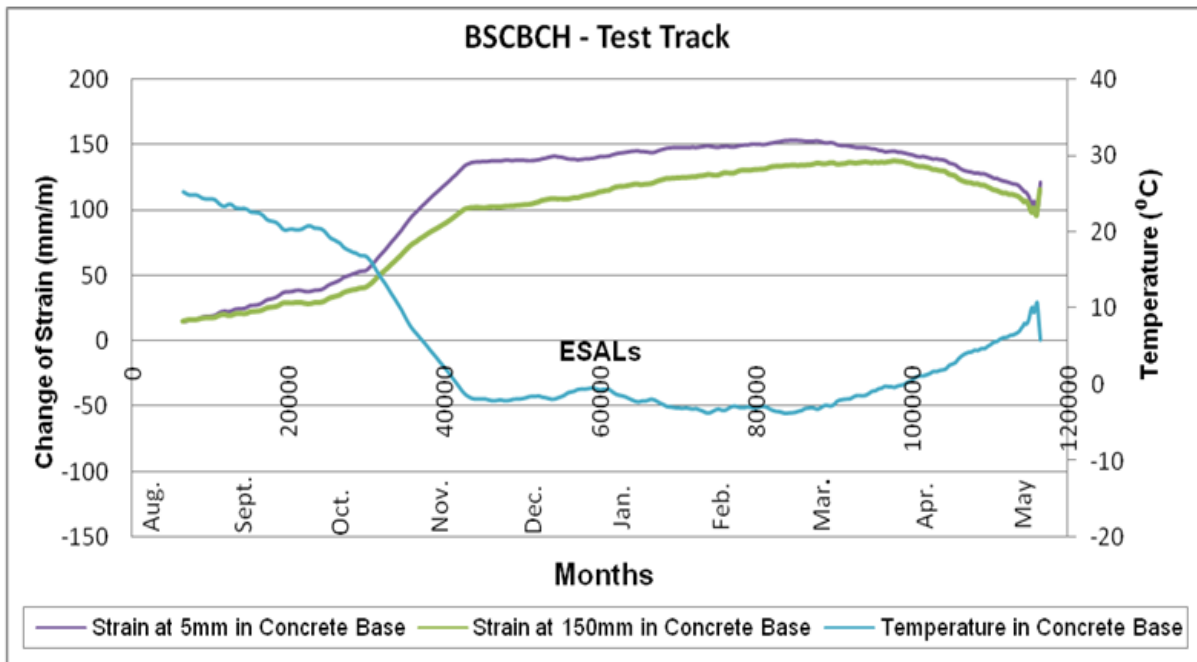
Figure 60 shows the accumulation of vertical stress and moisture variation in subbase layer in BSCBCH. It can be seen that the formation of stress is affected by moisture variation. Tensile vertical stress is formed on the top of the subbase as well as at 250 mm below in the subbase. The trend shows that tensile stresses increases as moisture content increases. No compressive stress is formed during this period which is a main contributor to rutting in the granular layers.

Figure 61 shows the accumulation of strain in the concrete base of the BSCBCH crosswalk section from August, 2007 to May 2008. It can be seen that temperature has a direct impact on the formation of strain. High tensile strain is formed during winter when the temperature is below 0<sup>0</sup> Celsius. As the temperature increases the tensile strain decreases in the concrete.

Figure 62 and 63 show the stress and strain accumulation in all test sections at test track. Maximum vertical stress is found in the subbase of SSABSH. Similarly, maximum tensile strain is formed in BSCBCH and the maximum compressive strain is formed in SSABSH in this period.



**Figure 60: Accumulation of Vertical Stress in Subbase of BSCBCH**



**Figure 61: Accumulation of Horizontal Strain in Base of BSCBCH**

At the test track, when the three sections are compared as shown in Figure 62 and Figure 63, the stresses and strains are observed as follows: the maximum observed stress for all sections is measured in the asphalt base section (SSABSH) followed by sand set concrete base (SSCBCH) and bituminous

set concrete base (BSCBCH) crosswalks. The maximum strain is observed in the bituminous set concrete base crosswalk (BSCBCH) followed by sand set concrete base (SSCBCH) and sand set asphalt base (SSABSH) crosswalks.

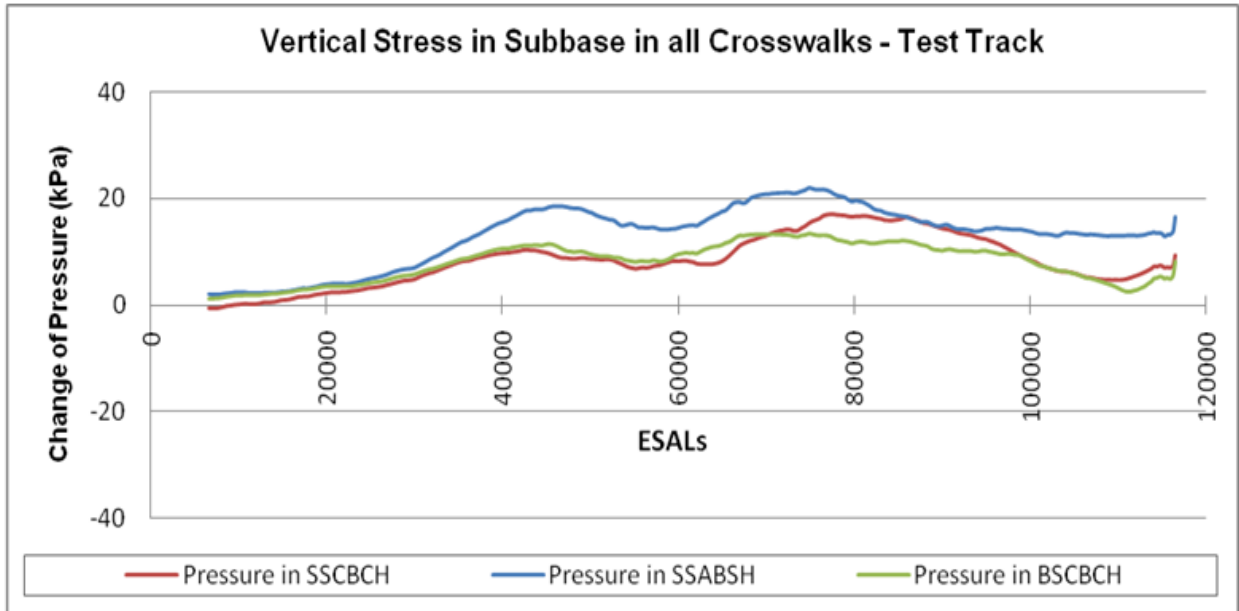


Figure 62: Accumulated Vertical Stress in Subbase in All Crosswalks

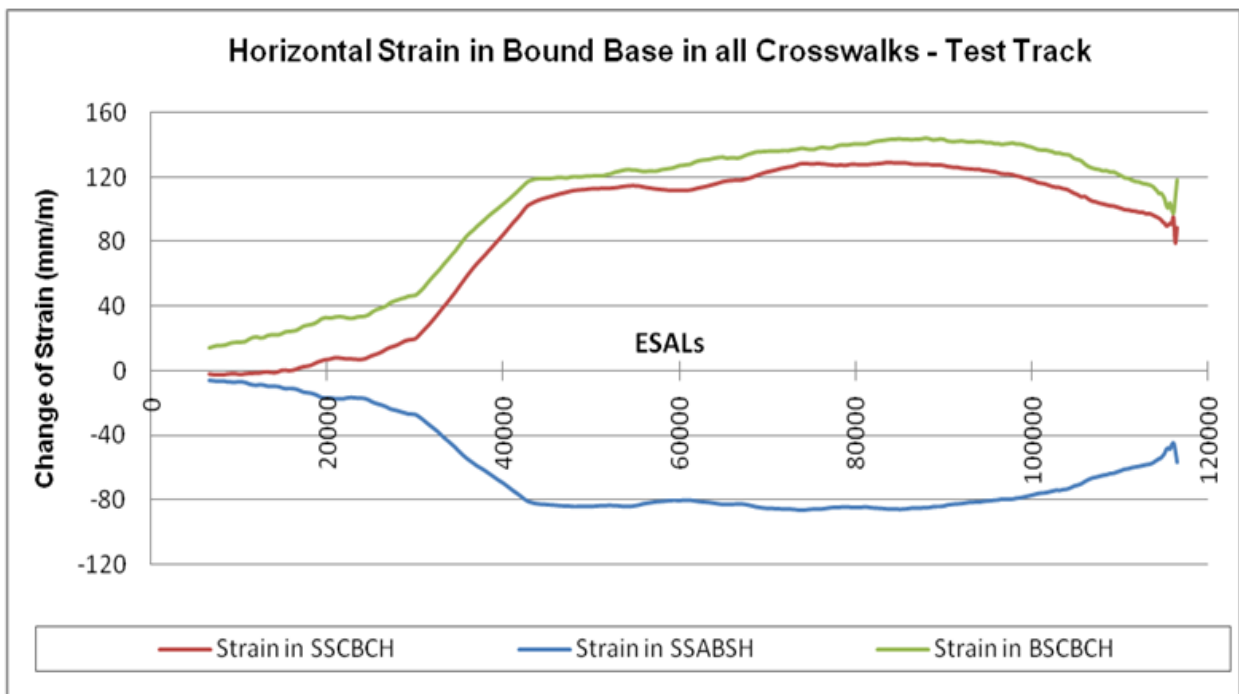


Figure 63: Accumulated Horizontal Strain in Base in All Crosswalks

## 5.2.2 UW Ring Road

The accumulation strain in three different crosswalk design assemblies at UW ring road over six months period (13,000 ESALs) and the respective environmental data are presented. Trendlines of strain accumulations are influenced by variations in environmental conditions i.e. temperature, rainfall and moisture.

### 5.2.2.1 Crosswalk One - SSCBCH

Figure 64 shows the accumulation of strain in the concrete base layer of SSCBCH at ring road from November 2007 to May 2008. It can be seen that temperature has direct impact on the formation of strain. High tensile strain is formed during winter when the temperature is below 0 Celsius. As temperature increases the tensile strain decreases and compressive strain increases. When the concrete temperature was above 6<sup>o</sup> Celsius, compressive strain started forming and reached 45 microstrains when the temperature is 20<sup>o</sup> Celsius.

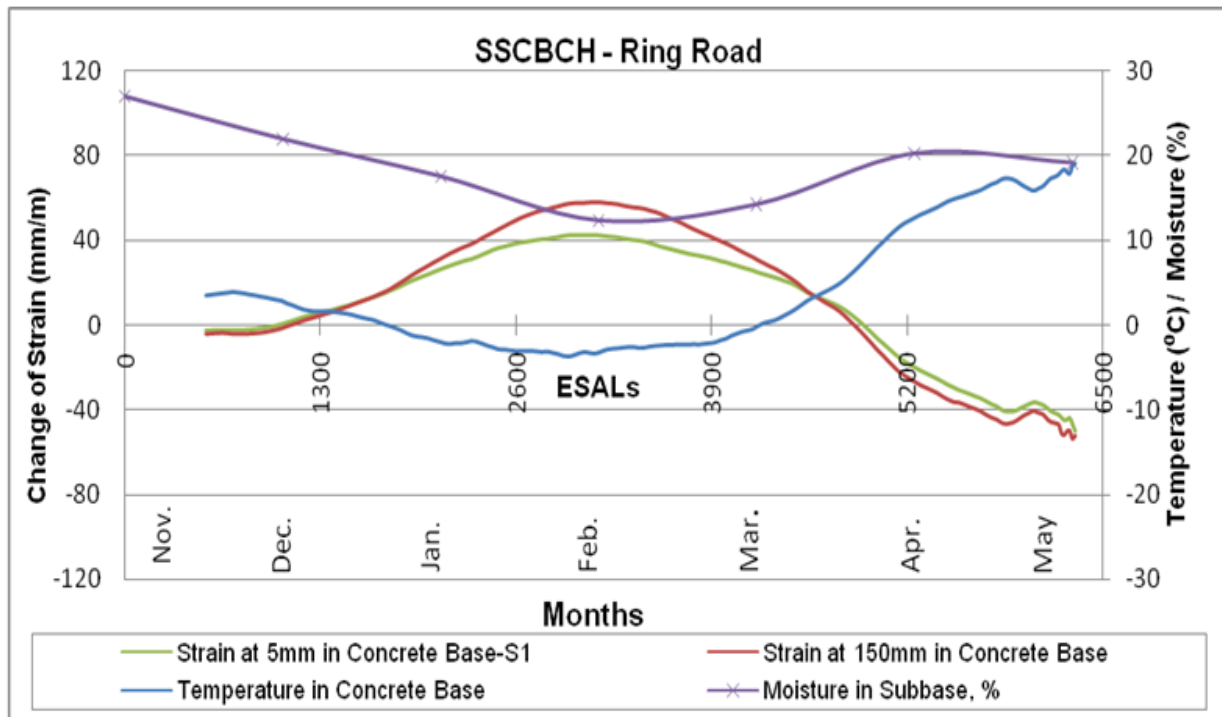


**Figure 64: Accumulated Horizontal Strain and Temperature and Moisture Variation in SSCBCH**

### 5.2.2.2 Crosswalk Two - BSCBCH

Figure 65 shows the accumulation of strain in concrete base of BSCBCH in the period of six months since November 20, 2007. It can be seen that temperature has direct impact to the formation of strain. High tensile strain is formed during winter when the temperature is below 0<sup>0</sup> Celsius. As temperature increases the tensile strain decreases and compressive strain increases. When the concrete temperature was above 6<sup>0</sup> Celsius, compressive strain started forming and reached 35 microstrains at the bottom and 70 at the top of the concrete base.

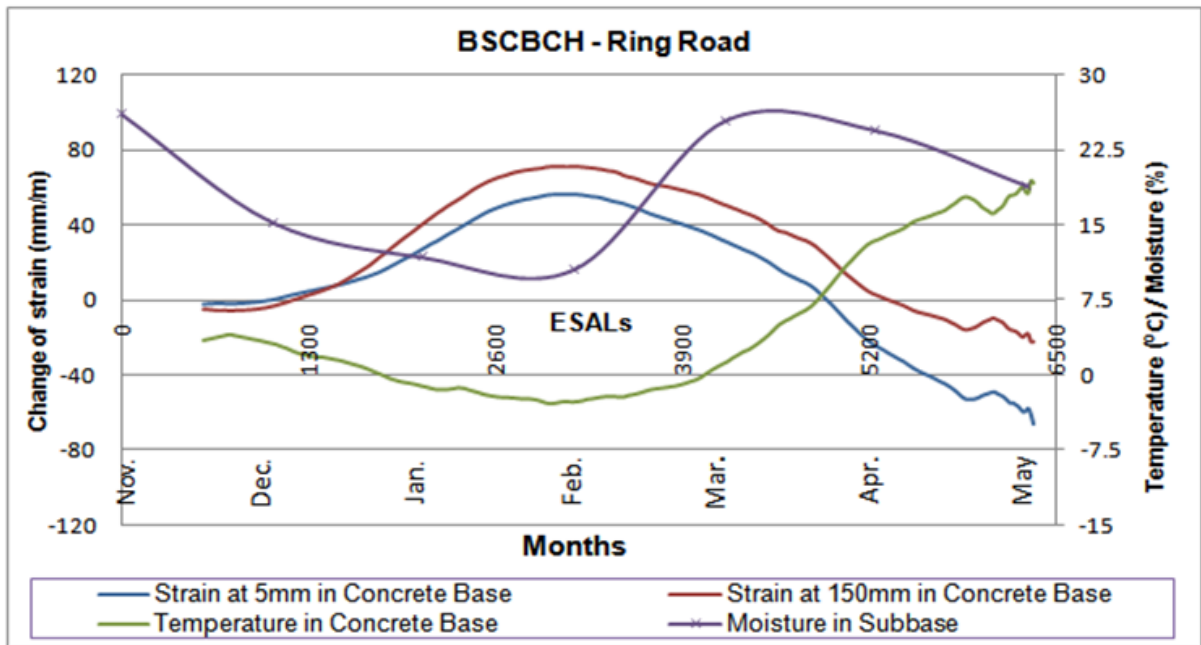
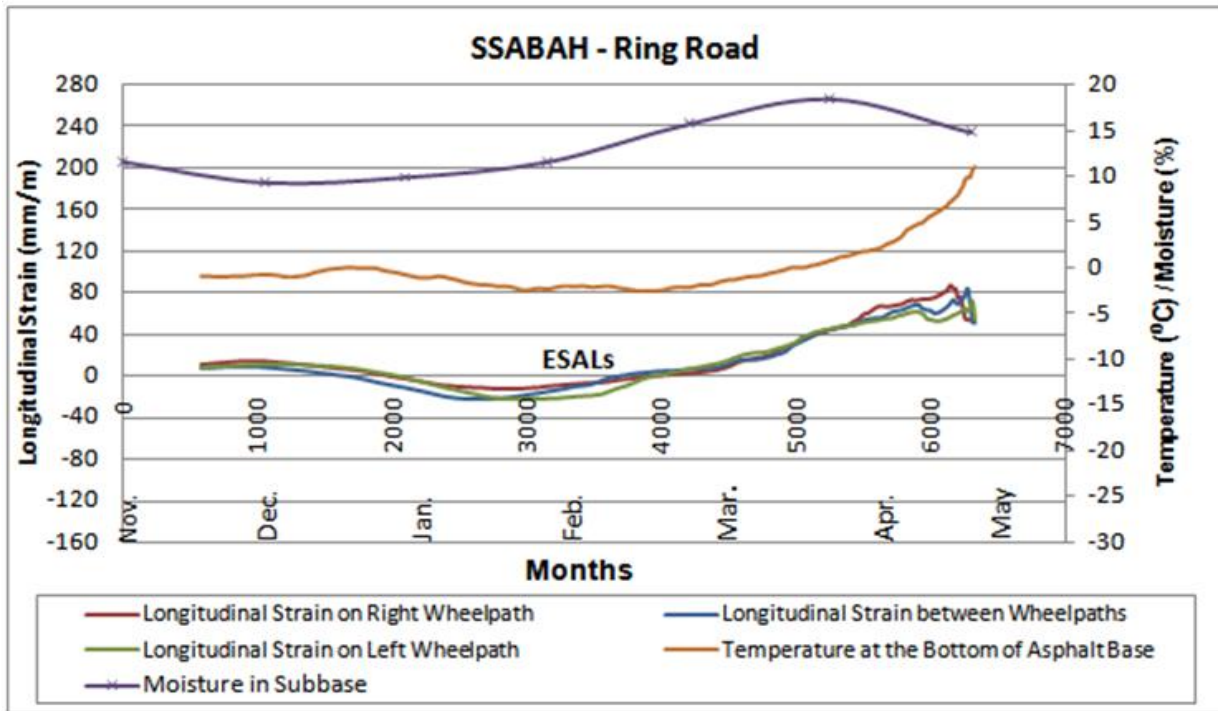


**Figure 65: Accumulated Horizontal Strain and Temperature and Moisture Variation in BSCBCH**

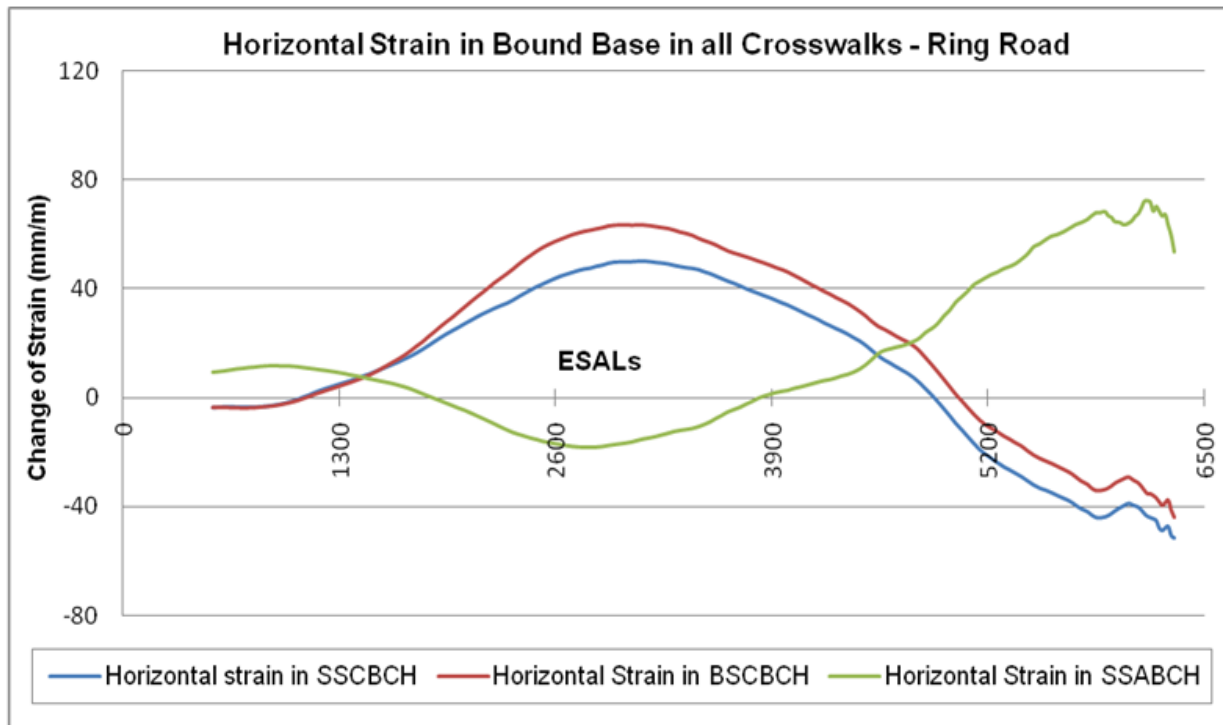
### 5.2.2.3 Crosswalk Three - SSABAH

Figure 66 shows the accumulation of strain at the bottom of the asphalt base layer of the SSABAH from November 2007 to May 2008. It can be seen that temperature has direct impact on the formation of strain. High compressive strain is formed during the winter when the temperature is below 0<sup>0</sup> Celsius. Tensile strain forms as the temperature increases and reaches a maximum of 80 microstrains in May. This is seen to be a main contributor to fatigue cracking.

Figure 67 shows the strain accumulation in all test sections at ring road. Maximum tensile strain is observed in SSABAH and the maximum compressive strain is formed in SSCBCH in this period.



**Figure 66: Accumulated Horizontal Strain and Temperature and Moisture Variation in SSABAH**



**Figure 67: Accumulated Horizontal Strain in All Crosswalk Sections**

### 5.3 Prediction Models

The load distribution and failure modes of flexible asphalt and interlocking concrete pavement are very similar. The pavement carries load as a flexible pavement and pavement failure primarily through rutting in the layers under the block surface. The major failure modes for the asphalt and concrete base courses are fatigue cracking, rutting and low temperature cracking.

Having defined the characteristics of the individual pavement materials it becomes necessary to examine the overall response of the pavement to traffic and environment. The pavement responses analysis included the tensile strain on the bottom of the asphalt concrete base layer, tensile strain in concrete base course and the vertical compressive stress in granular subbase courses. Fatigue of concrete is typically manifested in the form of cracking and can be the result of secondary stresses like curling, where expansion and contraction result in a temperature gradient across the depth of a rigid slab. Fatigue cracking in asphalt pavements is also related to horizontal tensile stresses induced in the asphalt layers by daily temperature cycles and the traffic. In general, cracking compromises the integrity of the pavement structure and results in reduction of performance. Rutting is related to vertical compressive stresses in granular layers or vertical compressive strain at the top of the subgrade. These two criteria are adopted to assess the in service performance of the pavement and to develop the prediction models for each section:

#### 1) *Fatigue Failure Criterion*

In the case of concrete base, the following failure criterion proposed by Bryan Shackel is adopted to calculate the maximum allowable tensile strain to failure and its corresponding ESALs:

$$\epsilon_t = \left[ \frac{993,500 * f_c}{E^{1.022} * N^{0.0502}} \right] \quad (3)$$

Where,  $\epsilon_t$  – Tensile strain in concrete base (microstrain)  
 $f_c$  – Compressive strength of concrete base (MPa)  
 $E$  – Elastic modulus of concrete base (MPa)  
 $N$  – Number of load repetitions to failure (ESALs)

In the case of asphalt base, the following criterion proposed by Asphalt Institute is adopted:

$$N_f = 2.83 * 10^{-6} \left[ \frac{10^6}{\varepsilon_t} \right]^6 \quad (4)$$

Where,  $\varepsilon_t$  – Tensile strain on the bottom of asphalt base (microstrain)  
 N – Number of load repetitions to failure (ESALs)

## 2) *Rutting Failure Criterion*

The following Danish stress criterion is used on subbase layers:

$$\sigma_f = K * \left[ \frac{N}{10^6} \right]^{(-\frac{1}{a})} * \left[ \frac{E}{E'} \right]^b \quad (5)$$

Where,  $\sigma_f$  – Permissible Stress (MPa)  
 K, a, b – Materials and environment constants  
 N – Number of load repetitions to failure (ESALs)  
 E – Elastic modulus of the material (MPa)  
 E' – Reference modulus (MPa)

### 5.3.1 CPATT Test Track

Remaining life of each crosswalk section for both fatigue cracking and rutting criteria is calculated in ESALs by comparing above mentioned empirical models with the models developed by using observed stress and strain data. MATLAB<sup>®</sup> rstoool is used to fit the curve into the observed data and the method root mean square error is used to determine the best fit model.

#### 5.3.1.1 Crosswalk One – SSCBCH

The maximum allowable stress in subbase layer to relate rutting and the maximum horizontal strain in base to relate fatigue cracking is compared with empirical model and the maximum allowable ESAL is calculated as illustrated in Figure 68 and 69. The maximum allowable horizontal strain in concrete base for this section is 321 microstrains and the fatigue life is 757,280 ESALs. Similarly, maximum allowable vertical stress in subbase layer is 108 kPa and the rutting life is 2,091,900 ESALs.

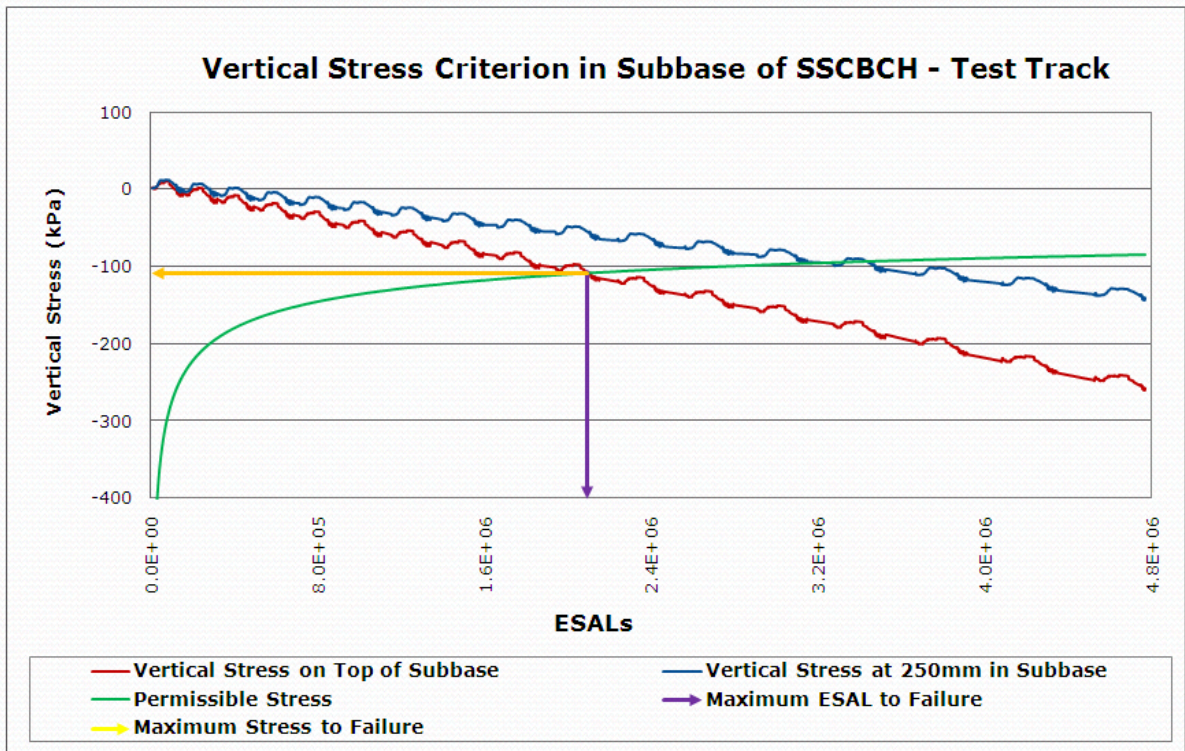


Figure 68: Vertical Stress Prediction Model of SSCBCH

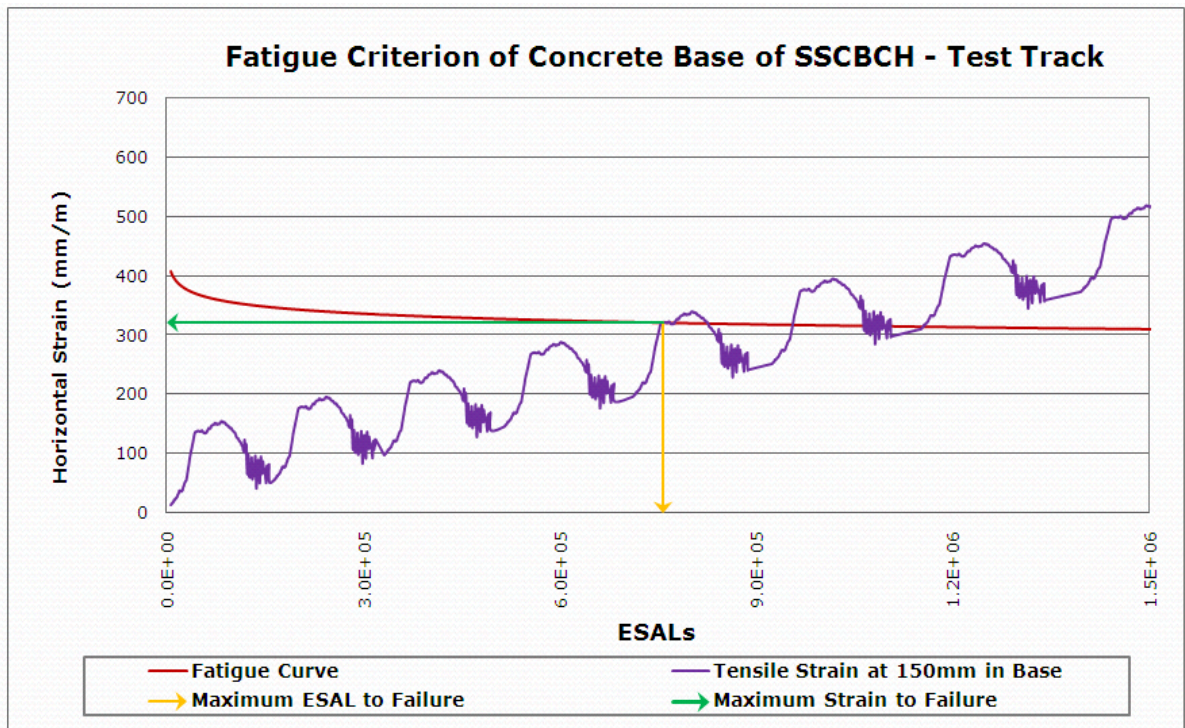


Figure 69: Fatigue Cracking Prediction Model of SSCBCH

### 5.3.1.2 Crosswalk Two – SSABSH

The maximum allowable stress in subbase layer and the maximum horizontal strain on bottom of asphalt base is compared with empirical model and the maximum allowable ESAL is calculated as illustrated in Figure 70 and 71. The maximum allowable horizontal strain on the bottom of asphalt base is 186 microstrains and the fatigue life is 1,552,230 ESALs. Similarly, maximum allowable vertical stress in subbase layer is 108 kPa and the rutting life is 2,101,840 ESALs.

### 5.3.1.3 Crosswalk Three – BSCBCH

The maximum allowable stress in subbase layer and the maximum horizontal strain on bottom of asphalt base is compared with empirical model and maximum allowable ESAL is calculated as illustrated in Figure 72 and 73. The maximum allowable horizontal strain on the bottom of asphalt base is 343 microstrains and the fatigue life is 965,590 ESALs. Similarly, maximum allowable vertical stress in subbase layer is 108 kPa and the rutting life is 2,107,100 ESALs.

Table 6 summaries the permissible ESALs, stress and strain of all sections for both failure criteria.

**Table 6: Summary of Permissible ESLAs, Stress and Strain**

<b>Fatigue Criterion</b>		
<i>Crosswalks</i>	<i>Permissible ESALs</i>	<i>Permissible Strain (mm/m)</i>
SSCBCH	757,280	321
SSABSH	1,552,230	186
BSCBCH	965,590	343
<b>Vertical Stress Criteria</b>		
<i>Crosswalks</i>	<i>Permissible ESALs</i>	<i>Permissible Stress (kPa)</i>
SSCBCH	2,09,1900	108
SSABSH	2,101840	108
BSCBCH	2,107,100	108

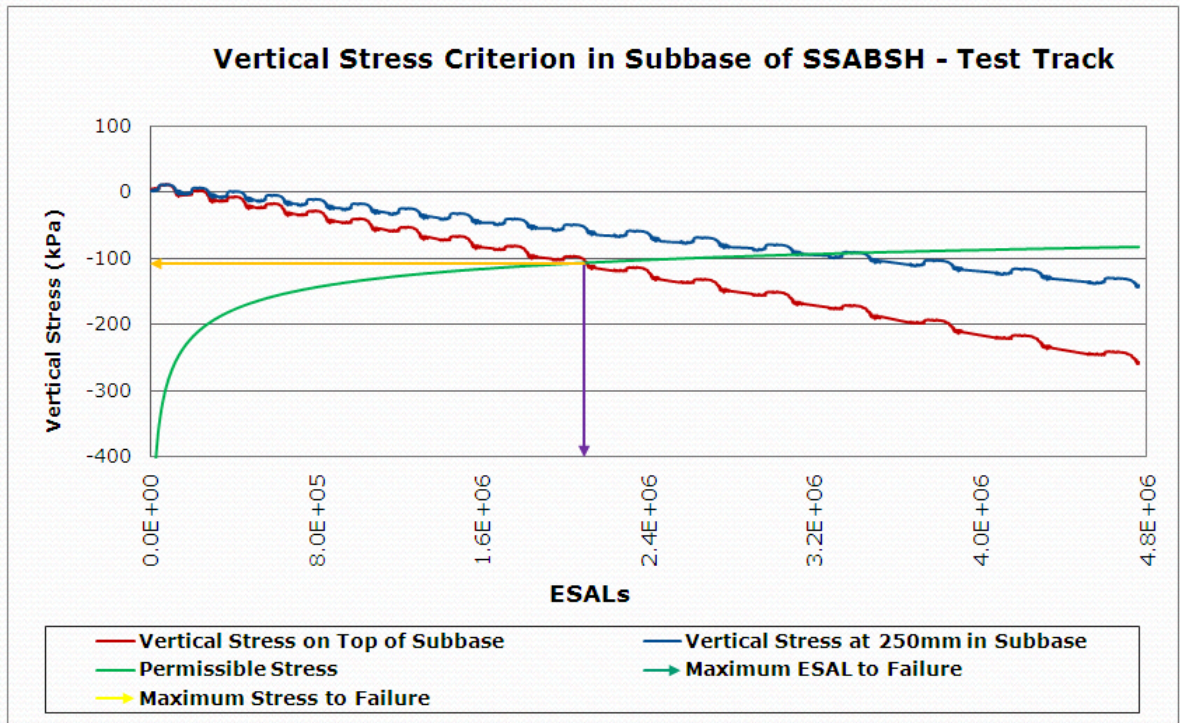


Figure 70: Vertical Stress Prediction Model of SSABSH

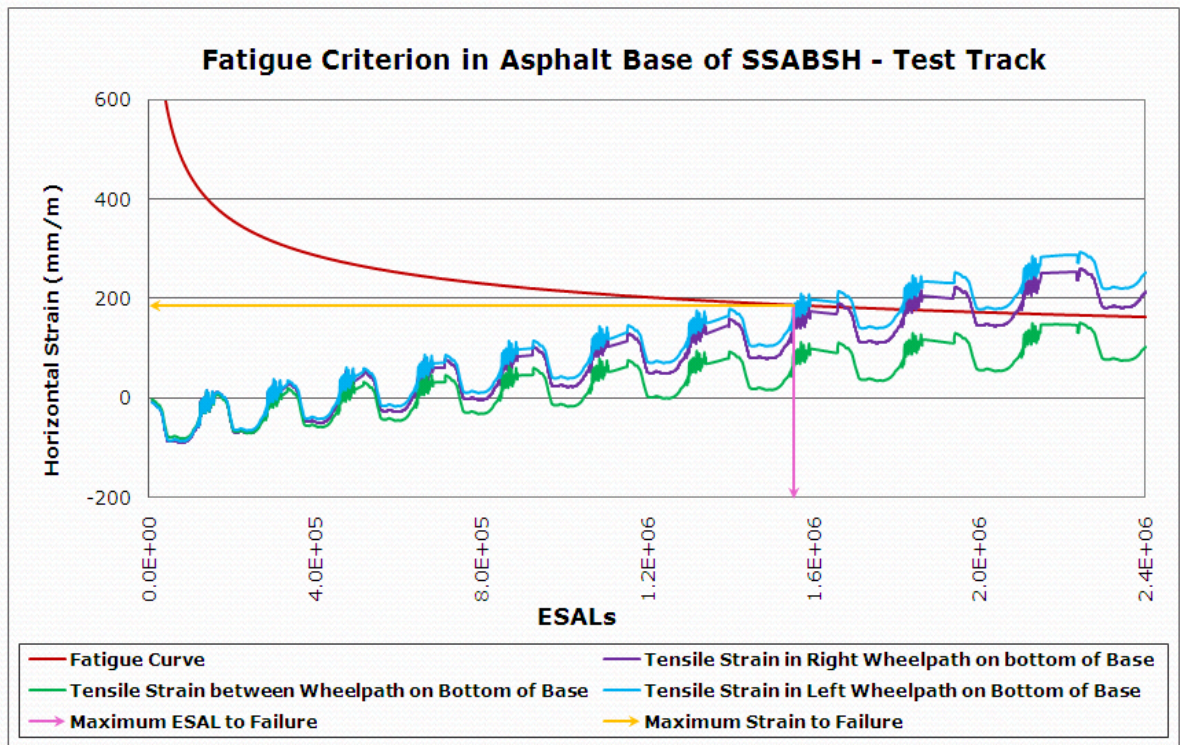


Figure 71: Fatigue Cracking Prediction Model of SSABSH

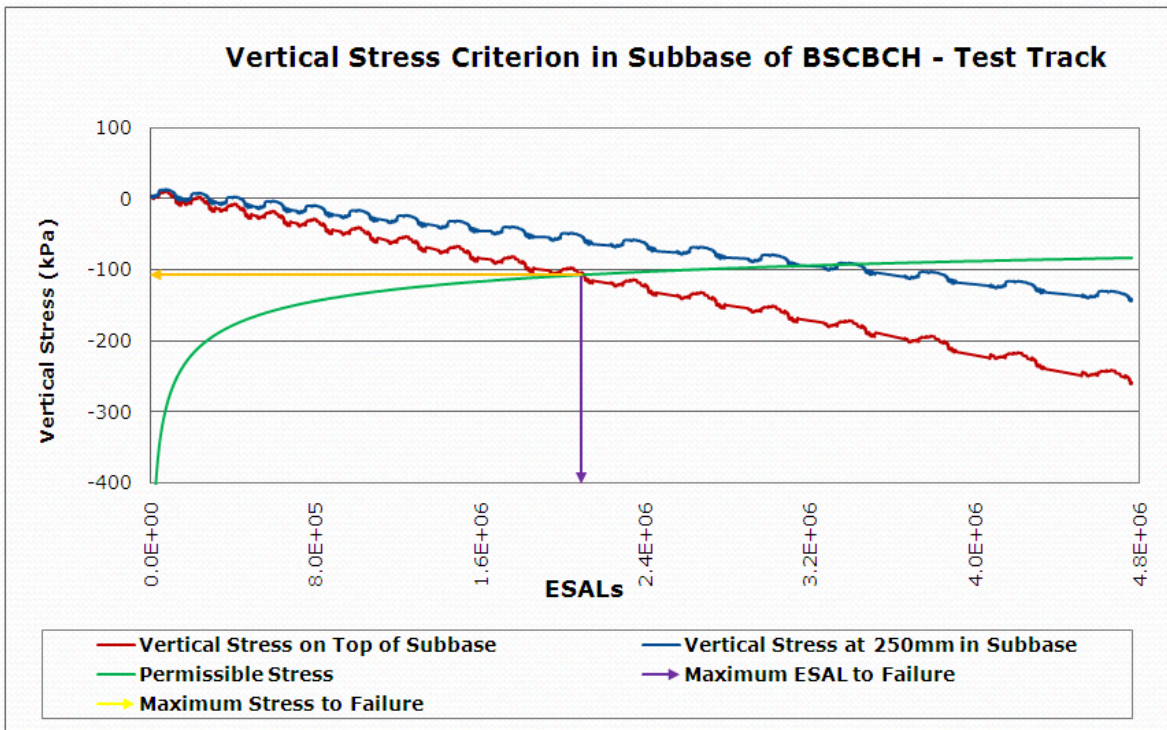


Figure 72: Vertical Stress Prediction Model of BSCBCH

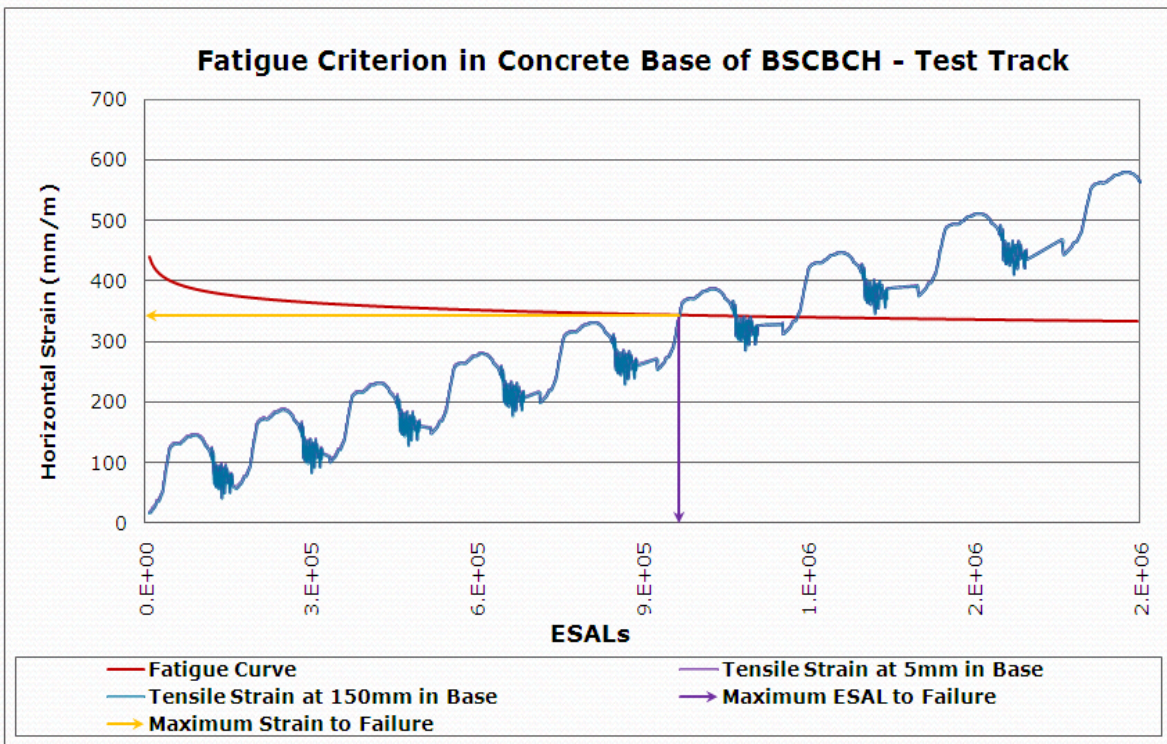


Figure 73: Fatigue Cracking Prediction Model of BSCBCH

### 5.3.2 UW Ring Road

Since no pressure cells were installed at this location, remaining life of three crosswalk sections is calculated in ESALs only for fatigue cracking failure criterion by comparing empirical models with the models developed by using observed strain data. MATLAB<sup>®</sup> rstool is used to fit the curve into the observed strain data and the method root mean square error is used to determine the best fit model.

Performance evaluation of granular base crosswalk (SSGBCH) is carried out by using ICPI Distress Evaluation Guide and is discussed in Chapter 6.

#### 5.3.2.1 Crosswalk One – SSCBCH

The maximum allowable horizontal strain in concrete base to relate fatigue cracking is compared with empirical model and the maximum allowable ESAL is calculated as illustrated in Figure 74. The maximum allowable horizontal strain in concrete base for this section is 652 microstrains and the fatigue life is 97,790 ESALs.

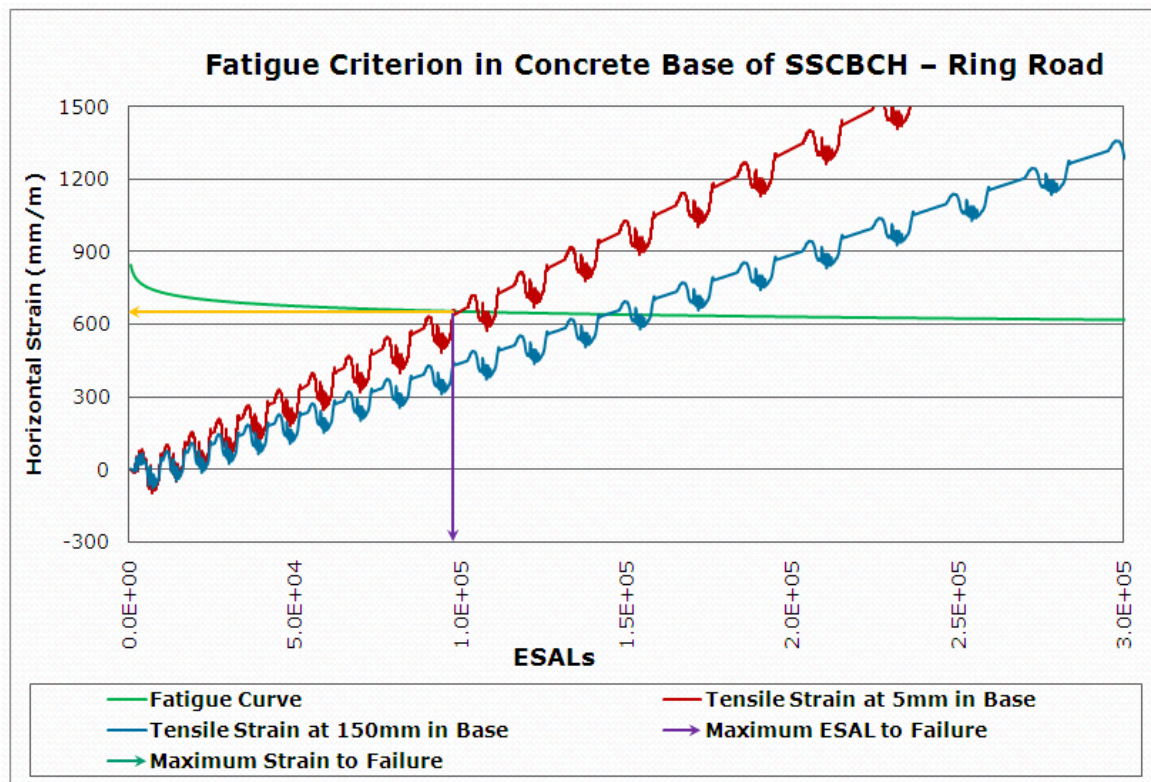
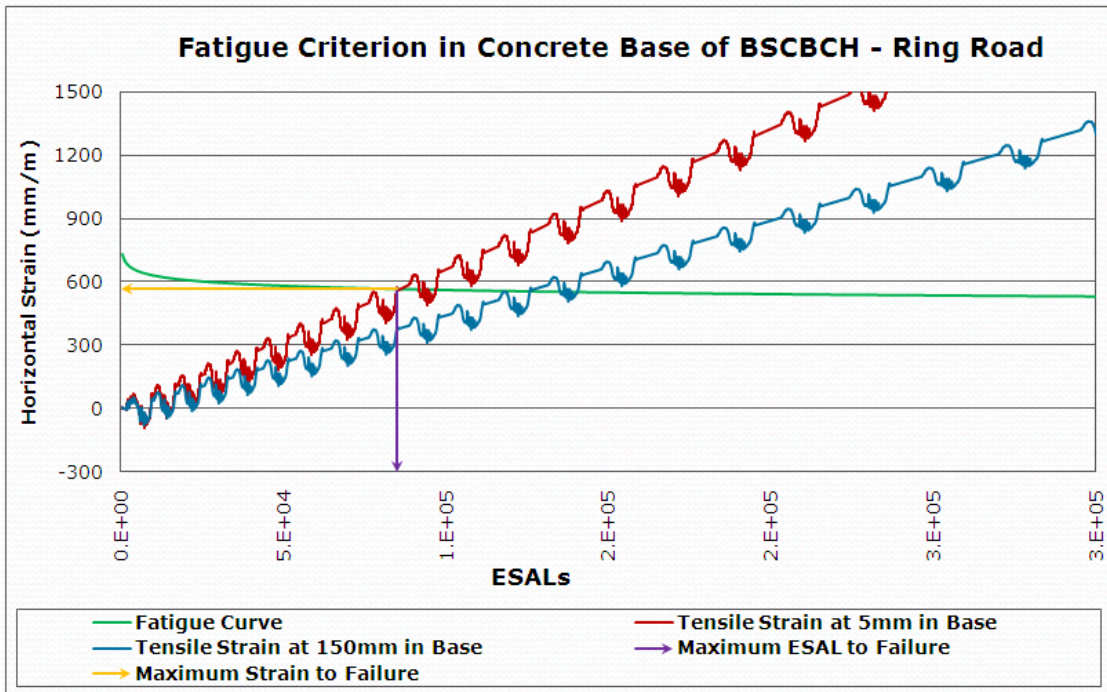


Figure 74: Fatigue Cracking Prediction Model for SSCBCH

### 5.3.2.2 Crosswalk Two – BSCBCH

The maximum allowable horizontal strain in concrete base to relate fatigue cracking is compared with empirical model and the maximum allowable ESAL is calculated as illustrated in Figure 75. The maximum allowable horizontal strain in concrete base for this section is 570 microstrains and the fatigue life is 85,040 ESALs.



**Figure 75: Fatigue Cracking Prediction Model of BSCBCH**

### 5.3.2.3 Crosswalk Three – SSABAH

The maximum allowable horizontal strain in concrete base to relate fatigue cracking is compared with empirical model and the maximum allowable ESAL is calculated as illustrated in Figure 75. The maximum allowable horizontal strain in concrete base for this section is 570 microstrains and the fatigue life is 85,040 ESALs.

Table 7 summaries the permissible ESALs and strain of three sections for fatigue cracking failure criterion.

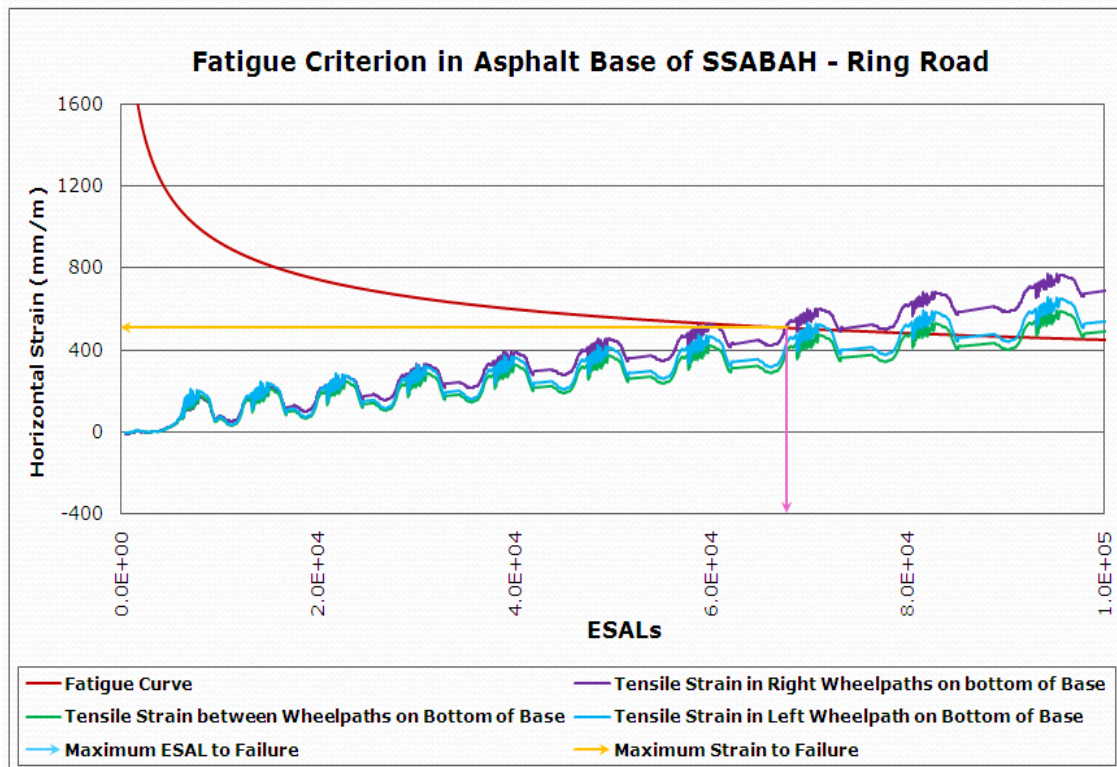


**Figure 76: Fatigue Cracking Prediction Model of SSABAH**

**Table 7: Summary of Permissible ESALs and Strain**

<b>Fatigue Criterion</b>		
<i>Crosswalks</i>	<i>Permissible ESALs</i>	<i>Permissible Strain (mm/m)</i>
SSCBCH	97,790	652
SSABAH	67,680	507
BSCBCH	85,040	570

## Chapter 6

### Pavement Distress Condition Evaluation

Distress condition surveys were carried out on a regular basis on accordance with Interlocking Concrete Block Pavement Distress Guide developed by ICPI (ICPI, 2008). The guide is based on the Pavement Condition Index (PCI) methodology and was modeled on the U.S. Army of Corps of Engineers MicroPAVER distress guide as published by ASTM. The PCI is a numerical indicator that evaluates the present condition of the pavement based on the surface distress. The type and severity of pavement is assessed by visual inspection of each crosswalk section surface condition of the pavement. The PCI does not measure the structural capacity nor does it provide direct measurement of skid resistance or roughness. The structural capacity of each section is evaluated by measuring strains, stresses, temperature and moisture at different locations in the pavement.

The following distresses are measured and evaluated for each crosswalk sections. The individual type of damage is rated separately with both degree and extent of the damaged being assessed. The observations and findings are presented in Table 6 and 7. Transverse and Longitudinal profiles are also plotted where significant visible distresses are found and presented in Figure 29-42. The degree of distress is rated high, medium, or low based on PCI numerical indicator.

- Damaged Pavers
- Depressions
- Edge Restraint
- Excessive Joint Width
- Faulting
- Heave
- Horizontal Creep
- Joint Sand Loss/Pumping
- Missing Pavers
- Patching
- Rutting

**Damaged Pavers** include the distresses like a chip, crack or spall on the pavers and are measured in square meters of surface area. Random individual cracks are only counted to evaluate the section in general.

**Depression** is the pavement surfaces that have elevations lower than surrounding areas is considered as depressions. The depressions are measured with 1.2m straight-edge and expressed in square meters.

**Edge Restraint** is constructed to resist lateral movement of the blocks, minimize loss of joint and bedding sand, and prevent block rotational movement. Concrete cast in situ headers/curbs and iron/aluminum angle rods are types of edge restraints in the research projects. The severity is measured in terms of the horizontal movement of the pavement edge in linear. Random cracks in the concrete headers are also considered for the evaluation.

**Excessive Joint Width** is a distress in which joints between pavers are widened. The joint between individual blocks are maintained 3mm during the construction to be filled with joint sands. When the width is widened the blocks become less stiff and can lead to overstressing the underlying layers and may show the signs of rotation. This is measured in square meters of the surface area.

**Faulting** is caused settlement of bedding sand or pumping of the bedding or joint sand. The distress usually associated with more severe distresses such as settlement, heave, rutting etc. Faulting is measured in square meters of the surface area and rated on the basis of elevation difference.

**Heaves** are caused by differential frost heave of the underlying layers and can be associated with rutting and settlement. The maximum height of heave defines the severity. The heaves areas of the pavement surface are measured in square meters by a straight-edge.

**Horizontal Creep** is the longitudinal or lateral movement of the pavement blocks caused by traffic loading. The distress is measured in square meters and the severity is defined the deviation on the blocks from the original position.

**Joint Sand Loss/Pumping** is caused by rain, pumping under traffic loading etc. This can contribute to pavement failure by permitting water to enter the underlying layers of the structure. Joint sands provide the structural interlock necessary for stresses to be distributed among adjacent

blocks. The distress is measured in square meters of surface area and severity is defined by the depth of sand loss measured from the bottom of the chamfer.

**Missing Pavers** is caused by disintegration or removal of the concrete blocks. The distress can let water seep into the underlying layers and also affects the ride quality. Missing pavers are measured in square meters of the surface area. The severity is evaluated by degree of distress.

**Patching** is done by reinstating the missing pavers and measured in square meters.

**Rutting** is a surface deformation in the wheelpath caused by traffic loading. The deformed area of the pavement surface is measured by straight-edge. The depressions are measured in square meters. The maximum rut depth defines the severity.

Visual distress survey is performed for each section of both project locations. Transverse and Longitudinal profile were also measured and plotted as shown in Figures 77- 86. The degree of distress is rated high, medium, or low based on a visual inspection. Table 6 and 7 summarise the distress condition evaluation of test track and ring road crosswalk sections respectively.

**Table 8: Summary of Pavement Condition Evaluation in Test Track Sections**

<b>Distress Types</b>	<b>Crosswalk 1 (SSCBCH)</b>	<b>Crosswalk 2 (SSABAH)</b>	<b>Crosswalk 3 (BSCBCH)</b>
Damaged Pavers	Low - 5 pavers are edge broken in the right wheelpath of south bound lane adjacent to the north concrete header.	Low - 3 pavers are edge broken in the right wheelpath of south bound lane adjacent to the north concrete header.	No distress

depressions	<p>Medium - Maximum depth of the depression is 19 mm in right wheelpath of southbound lane.</p> <p>Medium - Maximum depth of the depression is 17 mm in left wheelpath of southbound lane.</p> <p>The total depression area is 1.5 m<sup>2</sup>.</p>	<p>Medium - Maximum depth of the depression is 23 mm in right wheelpath of southbound lane.</p> <p>Medium - Maximum depth of the depression is 18 mm in left wheelpath of southbound lane.</p> <p>Low - Maximum depth of the depression is 12 mm in right wheelpath and 5 mm in left wheelpath of northbound lane.</p> <p>The total depression area is 1.7 m<sup>2</sup>.</p>	No distress
Edge Restraint	No distress	No distress	No distress
Excessive Joint Width	No distress	Low – 8 mm joint width between angle header and soldier course in right wheelpath is 0.5 m <sup>2</sup> of southbound lane.	No distress
Faulting	No distress	No distress	No distress
Heaves	No distress	No distress	No distress
Horizontal Creep	No distress	No distress	No distress
Joint Sand Loss/Pumping	Low - Joint sand loss in 0.4 m <sup>2</sup> in right wheelpath.	Low - Joint sand loss in 0.9 m <sup>2</sup> in right wheelpath.	No distress
Missing Pavers	No distress	No distress	No distress

Rutting	<p>Medium - Maximum rut depth is 19 mm in right wheelpath of southbound lane.</p> <p>Medium - Maximum rut depth is 17 mm in left wheelpath of southbound lane.</p> <p>The total rutting area is 1.5 m<sup>2</sup>.</p>	<p>Medium - Maximum rut depth is 23 mm in right wheelpath of southbound lane.</p> <p>Medium - Maximum rut depth is 18 mm in left wheelpath of southbound lane.</p> <p>Low - Maximum rut depth is 12 mm in right wheelpath and 5 mm in left wheelpath of northbound lane.</p> <p>The total rutting area is 2.2 m<sup>2</sup>.</p>	No distress
Other Distresses	Low - Cracks in asphalt surface adjacent to the south concrete header on southbound lane	No distress	Low - Cracks in asphalt surface adjacent to the south concrete header on both lanes.
PCI	68	59	100
PCI Rating	Good	Good	Excellent
Pavement age	9 months	9 months	9 months
Total ESALS	114,000	114,000	114,000

According to the visual survey and PCI rating, it is observed that BSCBCH outperformed two other sections at this site. It can be seen in Figure 77 - 82 that SSCBCH and SSABSH crosswalks experienced deformations and ruttings at the beginning of section in both wheelpaths on loaded southbound lane. The unloaded northbound lane experienced low deformations and ruttings in comparison to loaded southbound lane.

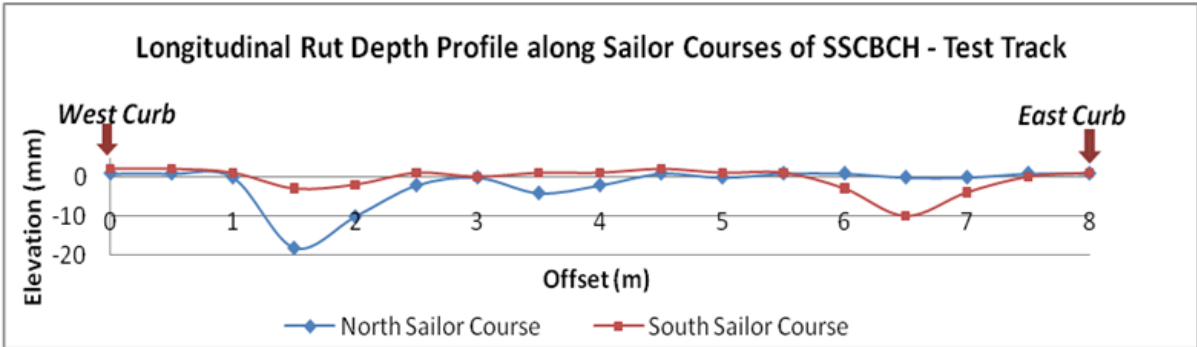


**Figure 77: Rut Profile along Sailor Course in SSCBCH**

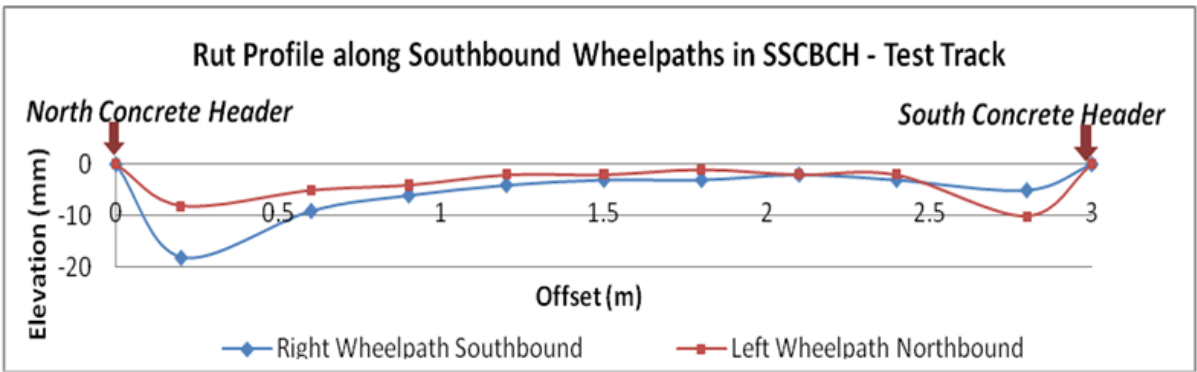


**Figure 78: Rut Profile along Southbound Wheelpath in SSCBCH**



**Figure 79: Depressions, Ruttings and Joint Sand Loss and in SSCBCH**

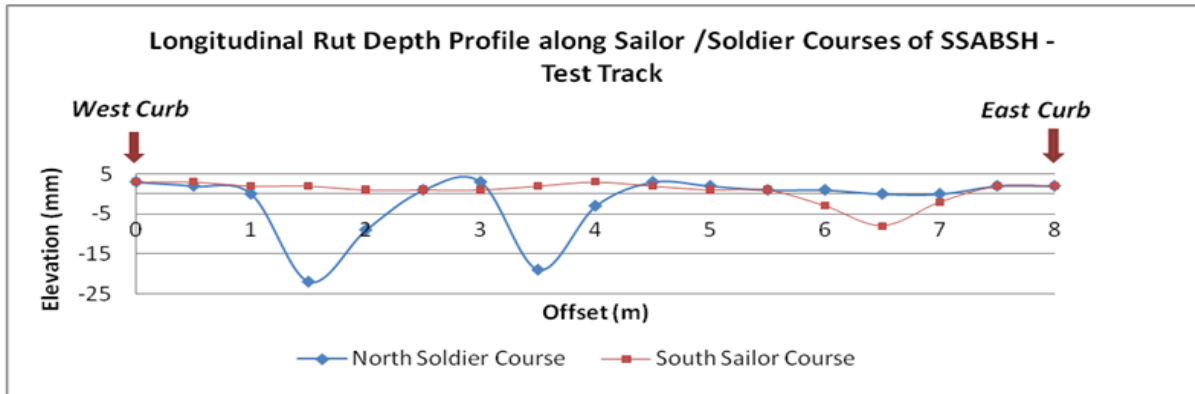


**Figure 80: Longitudinal Profile along Sailor and Soldier Courses in SSABSH**

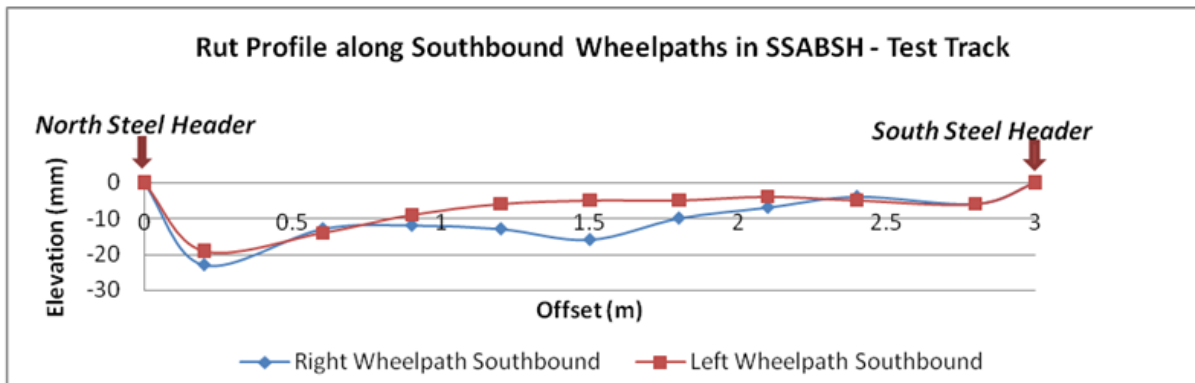


**Figure 81: Rut Profile in Southbound Wheelpath in SSABSH**

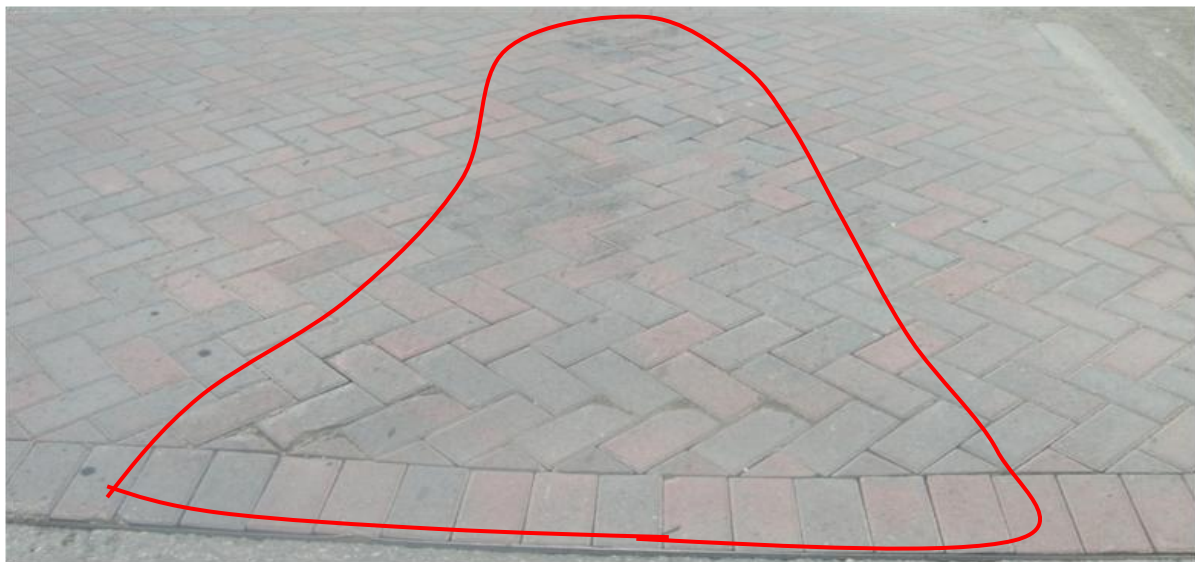


**Figure 82: Depressions, Ruttings and Joint Sand Loss in SSABSH**

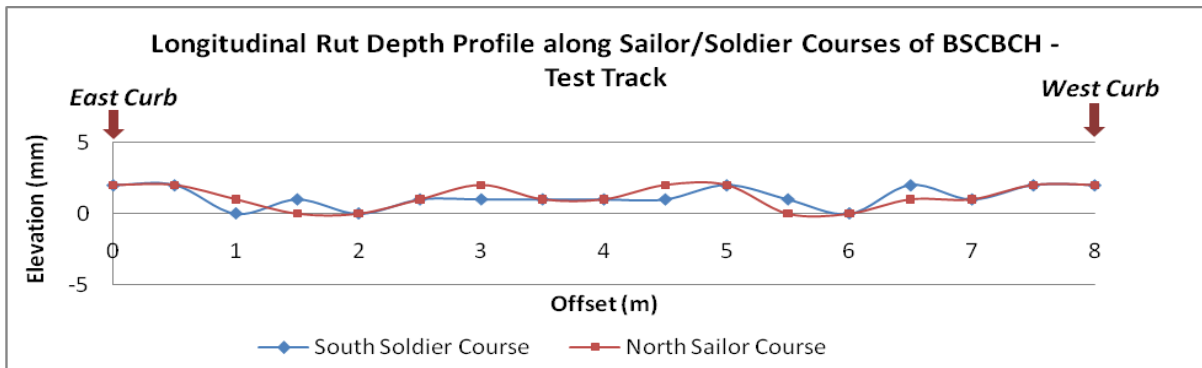


**Figure 83: Rut Profile along Sailor and Soldier Courses in BSCBCH**

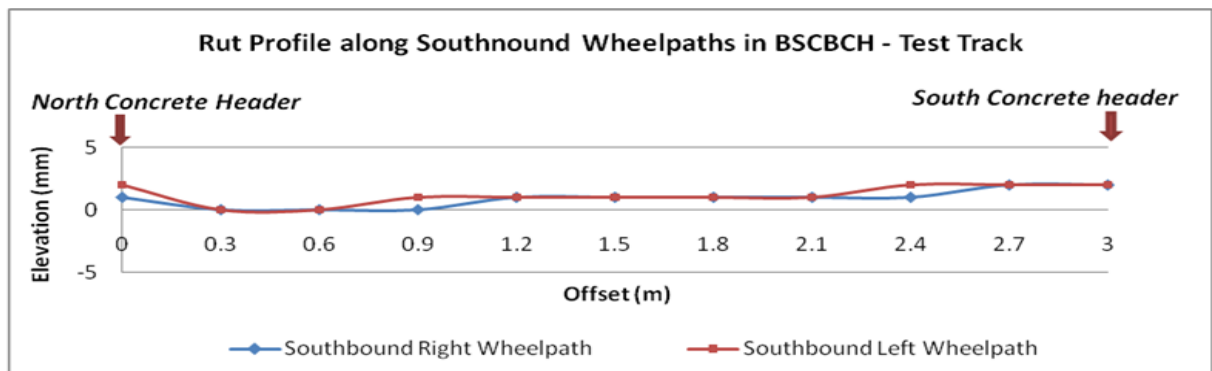


**Figure 84: Rut Profile in Southbound Wheelpath in BSCBCH**



**Figure 85: No Distresses in BSCBCH**

**Table 9: Summary of Pavement Condition Evaluation in Ring Road Sections**

<b>Distress Types</b>	<b>Crosswalk 1 (SSCBCH)</b>	<b>Crosswalk 2 (BSCBCH)</b>	<b>Crosswalk 3 (SSABAH)</b>	<b>Crosswalk 4 (SSGBCH)</b>
Damaged Pavers	Low - 9 individual pavers are edge broken at sailor course in the both wheelpaths of northbound lane.	Low - 3 pavers are edge broken in the right wheelpath of westbound lane	No distress	No distress
Depressions	High - Maximum depth of the depression is 33mm in left wheelpath at sailor course of northbound lane.  Medium - Maximum depth of the depression is 27 mm in right wheelpath at sailor course on northbound lane.  The total depression area is 12 m <sup>2</sup> .	No distress	Medium-Maximum depth of the depression is 17 mm in left wheelpath of northbound lane.  Low - Maximum depth of the depression is 13 mm in right wheelpath on northbound lane.  The total depression area is 1.8 m <sup>2</sup> .	Low - Maximum depression is 10 mm in left wheelpath of eastbound lane.  Low - Maximum depth of depression is 8 mm in right wheelpath on westbound lane.  The total area of depression is 3 m <sup>2</sup> .
Edge Restraint	No distress	No distress	No distress	No distress
Excessive Joint Width	No distress	No distress	Low – 9 mm average joint width between iron angle header and	

			soldier course on eastbound lane.	
Faulting	No distress	No distress	No distress	No distress
Heaves	Low - Maximum 14 mm heave in 4.6 m <sup>2</sup> area	No distress	Low- 5 mm maximum heave in 0.8 m <sup>2</sup> area	No distress
Horizontal Creep	Low – 6 mm deviation of sailor course pavers from its original position in 1.2 m <sup>2</sup> area.	No distress	No distress	No distress
Joint Sand Loss/Pumping	Medium - Joint sand loss in 4.8 m <sup>2</sup> in both wheelpaths and at the center.	No distress	Low - Joint sand loss in 1.2 m <sup>2</sup> in both wheelpaths on westbound lane.	Low - Joint sand loss in 1.0 m <sup>2</sup> in right wheelpath on westbound lane.
Missing pavers	No distress	No distress	No distress	No distress
Patches	No distress	No distress	No distress	No distress
Rutting	High - Maximum rut depth is 33 mm in left wheelpath.  Medium - Maximum rut depth is 17 mm in right wheelpath.  The total rutting area is 6 m <sup>2</sup> .	No distress	Medium - Maximum rut depth is 17 mm in left wheelpath of northbound lane.  Low - Maximum rut depth is 13 mm in right wheelpath of northbound lane.  The total rutting area is 2.2 m <sup>2</sup> .	No distress
Other Distress	Cracks in asphalt	Cracks in	No Distress	Minor cracks in east

	surface adjacent to the south concrete header at the center of the crosswalk section	asphalt surface adjacent to the concrete header		concrete header in 2m length near catch basin
PCI	41	100	76	83
PCI Rating	Fair	Excellent	Very Good	Very Good
Pavement age	7 months	7 months	7 months	7 months
Total ESALS	6,400	6,400	6,400	6,400

According to the visual survey and PCI rating, it is observed that BSCBCH outperformed three other sections at this site. It can be seen in Figures 87 - 97 that SSCBCH, SSABAH and SSGBCH crosswalks experienced deformations and ruttings and no visual distresses are observed in BSCBCH crosswalk at UW Ring Road.

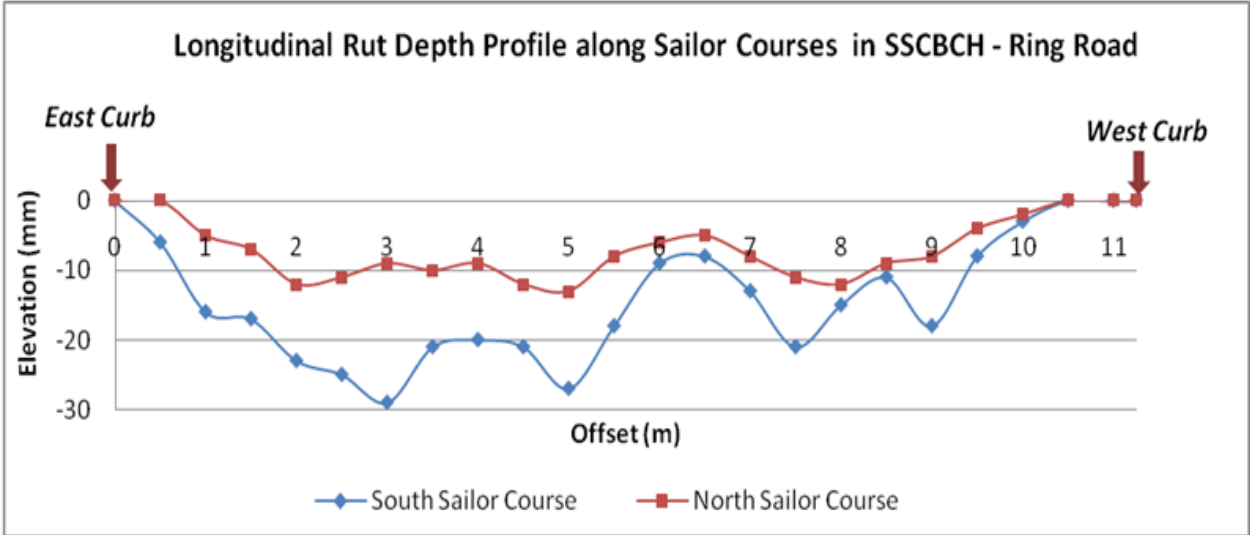


**Figure 86: Rut Profile along Sailor Courses in SSCBCH**

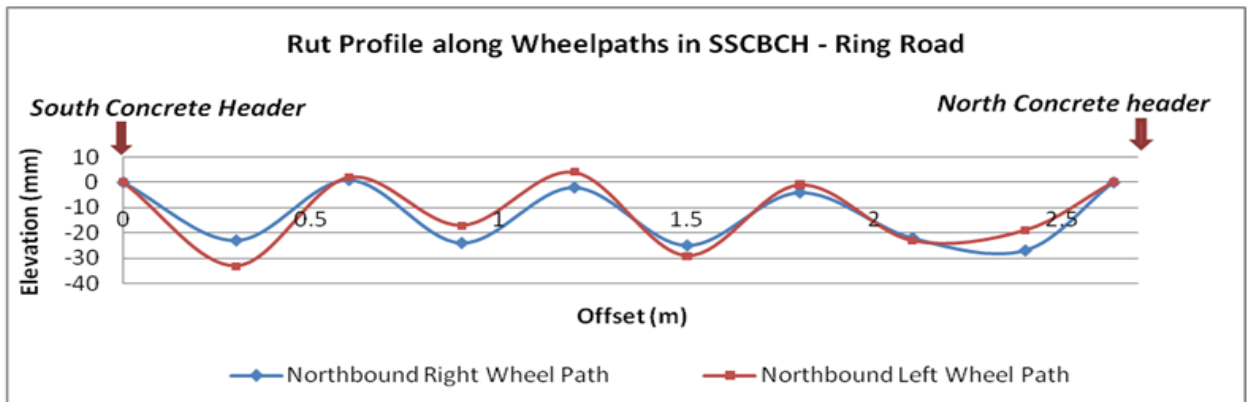


**Figure 87: Rut Profile in Wheelpaths in SSCBCH**



**Figure 88: Depressions, Ruttings and Heaves in SSCBCH**

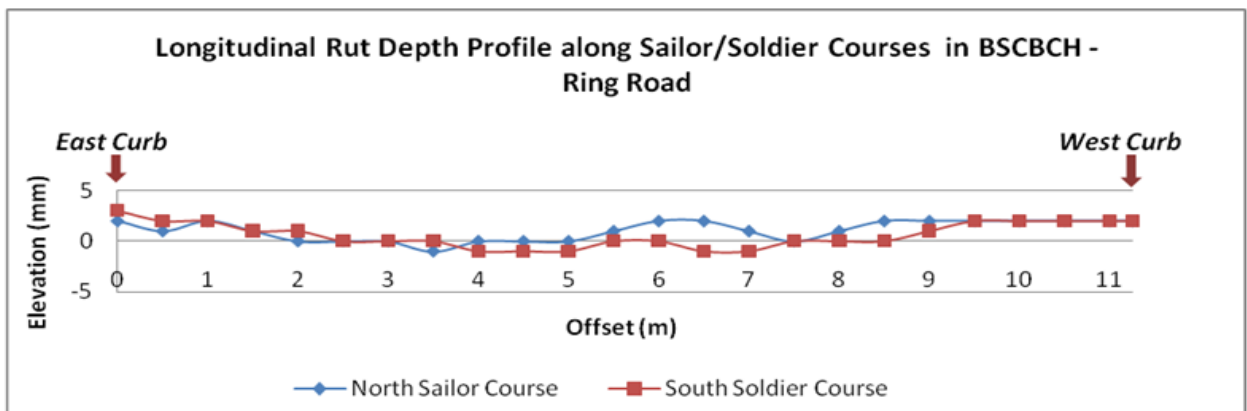


**Figure 89: Profile along Sailor and Soldier Courses in BSCBCH**

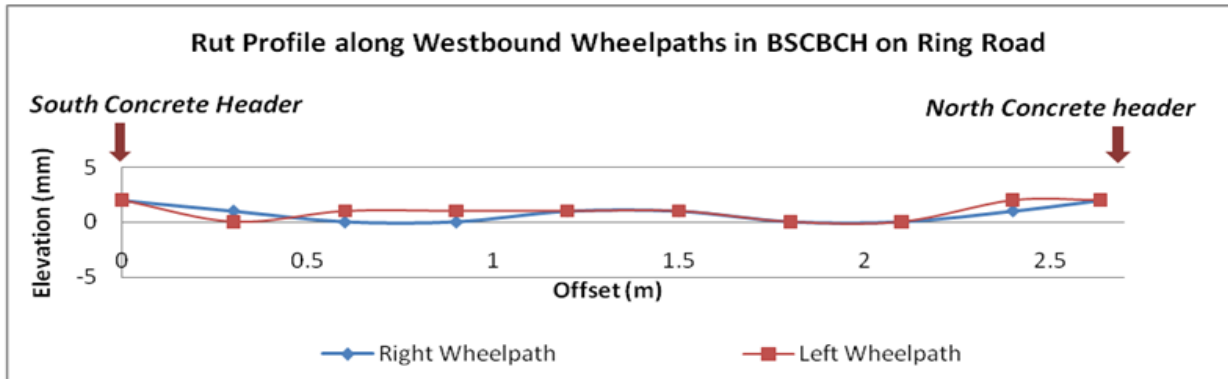


Figure 90: Rut Profile in Wheelpaths in BSCBCH



Figure 91: No Visual Distresses in BSCBCH

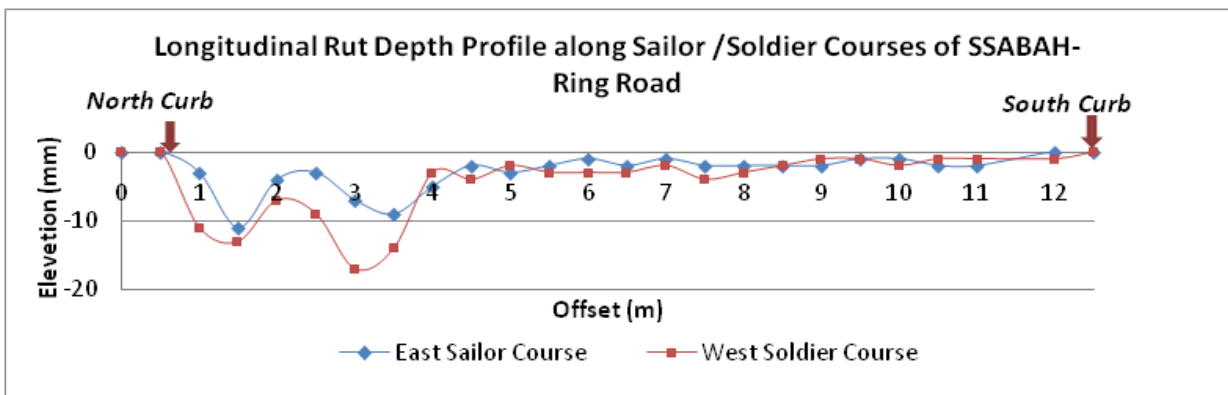


Figure 92: Rut Profile along Sailor and Soldier Courses in SSABAH

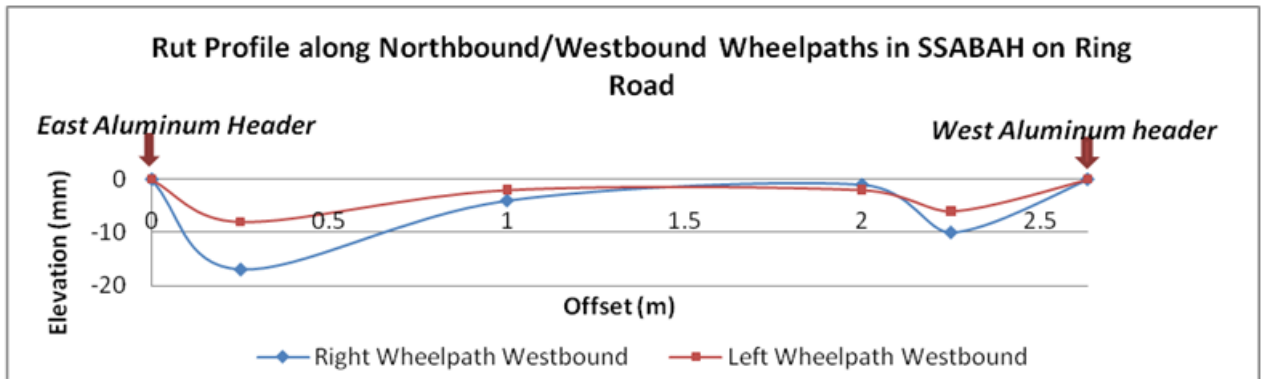


Figure 93: Rut Profile in Wheelpaths in SSABAH

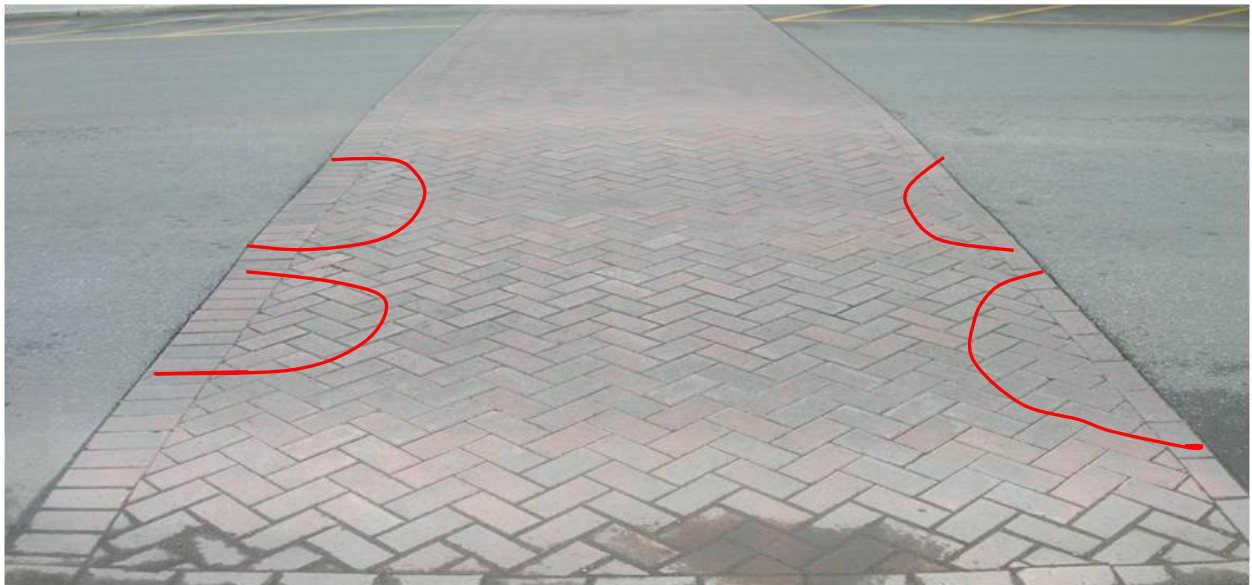
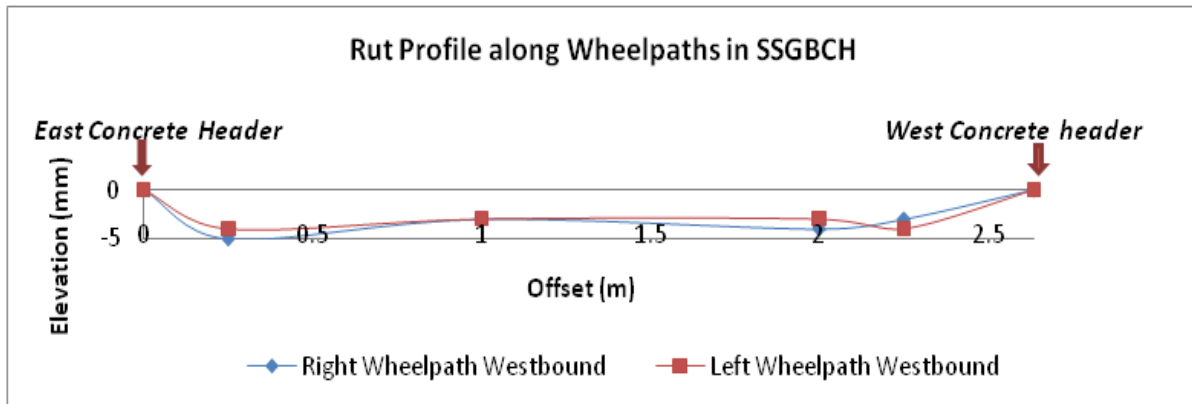


Figure 94: Depressions and Ruttings in SSABAH



Figure 95: Rut Profile in Sailor and Soldier Courses in SSGBCH



**Figure 96: Rut Profile in Wheelpaths in SGBCH**



**Figure 97: Uniform Deformations and Cracks on Concrete Headers in SGBCH**

## Chapter 7

### Conclusions and Recommendations

#### 7.1 Conclusions

- Seven test sections were built at two sites in Waterloo to assess the structural performance of four different interlocking concrete pavement crosswalk design assemblies under two different loading scenarios.
- Six sections are instrumented with mechanical and environmental sensors whereas aggregate base section on ring road has only environmental sensors.
- The pavement behavior under 114,000 ESALs repetitions at test track site and under 6400 ESALs on ring road site is studied. The CPATT test track encounters heavy truck loading primarily loaded garbage trucks with maximum load up to 56,000 kg (6 axles) while the UW ring road traffic is similar to a typical urban road with approximately 10% truck and 5% bus traffic.
- At the test track, the stresses and strains are observed as follows: the maximum observed stress for all sections is measured in the asphalt base section (SSABSH) followed by sand set concrete base (SSCBCH) and bituminous set concrete base (BSCBCH) crosswalks. This observed trend is also consistent with the distress observations and measurements. The maximum strain is observed in the bituminous set concrete base crosswalk (BSCBCH) followed by sand set concrete base (SSCBCH) and sand set asphalt base (SSABSH) crosswalks. Since the maximum strain value is well below the allowable strain from typical models, there is no indication at this time of unserviceable fatigue cracking in the sections. The fatigue cracking occurs when the maximum tensile strain exceeds the maximum allowable strain.
- At the ring road, the strains are observed as follows: Maximum observed tensile strain for all test sections is found in the bituminous set concrete base (BSCBCH) section followed by sand set concrete base (SSCBCH) and sand set asphalt base (SSABAH) crosswalks. The maximum tensile strain has not exceeded the maximum allowable strain. Therefore no unserviceable fatigue cracking has occurred in the sections in this period. This observed trend is not consistent with the distress observations and measurements. It is observed that, the

lowest performance is of the concrete base sand set (SSCBCH) crosswalk and this is suspected to be do inadequate surface drainage design which caused severe ponding of surface water runoff on this crosswalk in the spring. Horizontal creep is also observed in this section where the half-cut paver sailor course in the loaded direction.

- The pavement prediction models are calibrated with the observed strain and stress accumulation and compared with empirical models.
- At test track maximum permissible ESALs for fatigue cracking is 0.76, 1.55 and 0.96 million and for rutting 2.09, 2.1 and 2.1 million for SSCBCH, SSABSH and BSCBCH respectively
- At the ring road maximum permissible ESALs for fatigue cracking is 0.098, 0.068 and 0.085 million for SSCBCH, SSABAH and BSCBCH respectively
- Pavement distress data, such as measurements of permanent deformation, rutting, and cracking were collected and analyzed. PCI is calculated according to the draft ICPI distress Guide for each section. Based on the current PCI rating, bituminous set concrete base (BSCBCH) is performing the best at both sites whereas concrete base sand set (SSCBCH) at the ring road and asphalt base (SSABSH) at the test track are rated fair and good.
- Maximum deformation and rutting are observed in sand set concrete base crosswalk (SSCBCH) section on the ring road and in asphalt base section (SSABSH) at the test track respectively. The aggregate base crosswalk (SSGBCH) at the ring road was evaluated by using the draft version of ICPI Distress Manual.

## **7.2 Recommendations**

- Additional modeling of the pavement performance is needed to observe longer term trends. For this purpose, a database will be established within CPATT to regularly monitor the performance of the test sections.

## References

- AASHTO, Guide for Design of Pavement Structures, (1993). American Association of State Highway and Transportation Officials, Washington, D.C.
- A.B.N. Enterprise (2008). <http://www.abnenterprise.com>.
- Boss Paving (2008). <http://www.bosspaving.co.za>.
- Adhikari,S., Tighe,S. (2007). “Centre of Pavement and Transportation Technology Interlocking Concrete Crosswalk Construction Report.” University of Waterloo.
- Adhikari, S, Tighe S., Burak, R. (2008). “In-Situ Measurements of Interlocking Concrete Pavement Response to Vehicular Loading and Environment.” 2008 Transportation Association of Canada Annual Conference, Toronto.
- Algin, H. M., and Knapton, J. (1998). “Research into the Performance of Interlocking Paver Pavements.” Proceedings of the Institution of Civil Engineers. Transport., 129(03), 142–150.
- Beaty, A.N.S., Raymond, G.P. (1992). “Geotechnical aspects of interlocking concrete block Pavements.” Proceedings of the 45<sup>th</sup> Canadian Geotechnical Conference, pp. 41-1/41-7.
- Chua, K. M., Askree, Z., Shackel, B. (2000). “Axisymmetric Finite Element Modeling of Block Pavement Subjected to Repeated Loading.” Transportation Research Record 1730, Paper No. 00-0260.
- Clifford J.M. (1984). “A description of ‘interlock’ and ‘lock-up’ in block pavements.” Proceedings 2<sup>nd</sup> International Conference on Concrete Block Paving, pp. 50-54, Delft.
- Collop A.C., Cebon, D (1993). “A theoretical analysis of fatigue cracking of flexible pavements.” CUED/C- MECH/TR 56.
- Cronney, D., Cronney, P. (1991). “The design and performance of road Pavements.” Second Edition.

- Festa B., Giannattasio, P., Perneti, M. (1996). "Evaluation of Some Factors Influence on the Interlocking Paving System Performance." Proceedings of Fifth International Conference on Concrete Block Paving, Tel-Aviv, Israel. pp 305-314.
- Gonzalo R. Radha et.al. (1990). "Structural Design of Concrete Block Pavements." Journal of Transportation Engineering, ASCE, Vol. 116, No. 5.
- Guo, R., Prozzi, J.A. (2008). "Predicting In-Service Fatigue Life of Flexible Pavements Based on Accelerated Pavement Testing." TRB 8<sup>th</sup> Annual Meeting CD-Rom Paper revised from original submittal.
- Halil, C., Gopalakrishnan, K., Coree, B. J. (2007). "Rehabilitation of concrete pavements utilizing rubblization: a mechanistic based approach to HMA overlay thickness design." International Journal of Pavement Engineering, 9:1, pp 45 – 57.
- Houben, L.J.M., Molenaar A.A.A., Fuchs, G.H.A.M., Moll, H.O. (1984). "Analysis and Design of Concrete Block Paving Subject to Road Traffic and Heavy Industries Loading." Concrete Block Paving Proceedings, 2<sup>nd</sup> international conference, pp 86-99, Delft.
- ICPI (2007). "Bedding Sand Selection for Interlocking Concrete Pavements in Vehicular Applications." Tech Spec 17, Interlocking Concrete Pavement Institute, Washington, DC, U.S.A.
- ICPI (2007). "Interlocking Concrete Block Pavement Distress Guide." Interlocking Concrete Pavement Institute, Washington, DC, U.S.A.
- ICPI (2004). "Mechanical Installation of Interlocking Concrete Pavements." Tech Spec 11, Interlocking Concrete Pavement Institute, Washington, DC, U.S.A.
- ICPI (2003). "Structural Design of Interlocking Concrete Pavements for Roads and Parking Lots." Tech Spec 4, Interlocking Concrete Pavement Institute, Washington, DC, U.S.A.
- ICPI (1995), revised (January 2005). "Edge Restraints for Interlocking Concrete Pavements." Tech Spec 3, Interlocking Concrete Pavement Institute, Washington, DC, U.S.A.

- ICPI (1995), revised (March 2003). "Construction of Interlocking Concrete Pavements." Tech Spec 2, Interlocking Concrete Pavement Institute, Washington, DC, U.S.A.
- Judycki, J., Alenowich, W.C. (1996). "Structural Designs of Concrete Block Pavement Structures for Polish Conditions." Proceedings of Fifth International Conference on Concrete Block Paving, Tel-Aviv, Israel. pp 365-374.
- Knapton, J. and Barber, S.D. (1979) "The behavior of a concrete block pavement." Proceedings of Institution of Civil. Engineers, 66, pp. 227-292.
- Larsen, H.J.E. L., Ullidtz, P. (1998). "Development of improved mechanistic deterioration models for flexible pavements." Danish Road Institute Report 89.
- Lilley, A. (1994). "Size and Block Shape—Do They Matter?." Proc., 2nd International Workshop on Concrete Block Paving, Oslo, Norway, Norwegian Concrete Industries Association.
- Mahboub, P.E., et al. (2004). "Evaluation of Temperature Responses in Concrete Pavement." Journal of Transportation Engineering, Vol. 130, No. 3.
- Mavkin, K.C.(1978). "The Interlocking Concrete Block Pavement." Australian Road Research, Vol. 8, No.3, pp.54-57.
- Nor H.B.M., Ismail C. R. B., Mudiyo, R. (2006). "The Effect of Thickness and Laying Pattern of Paver on Concrete Block Pavement." Department of Geotechnics and Transportation, Faculty of Civil Engineering University Teknologi, Malaysia, RESEARCH VOTE NO: 75067.
- Panda, B.C., and Ghosh, A.K. (1999). "Structural modeling and design and interlocking block pavement." Indian Construction Journal 73(2), pp 123-127.
- Pavement Design and Management Guide (1997). Transportation Association of Canada, Ottawa, Ontario, 1997.
- Rollings R.S. (1984). "Corps of engineers design method for concrete block pavements." Concrete block paving procedigns, 2<sup>nd</sup> international conference, pp 147-151, Delft.
- RST Instruments (2003). Earth Pressure Cells, Instruction Manual.
- RST Instruments (2002). Vibrating Wire Strain Gauge, Instruction Manual.

- Ryntathiang T. L. (2005). "Structural Behavior of Cast In Situ Concrete Block Pavement." J. Transp. Engrg. Volume 131, Issue 9, pp. 662-668.
- Seddon, P.A. (1981). "The Behaviour of Concrete Block Paving under Repetitive Loading."
- Shackel, B. (1990). "Design and Construction of Interlocking Concrete Block Pavements." Elsevier Applied Science, London.
- Shackel, B. (1986). "Computer –aided design and analysis of concrete segmental pavements." International Workshop on Interlocking Concrete Pavements, Royal Melbourne Institute of Technology, Melbourne.
- Shackel, B. (1982). "An Experimental Investigation of Factors Influencing the Design of Interlocking Concrete Block Pavements for Roads." Proc Aust Road Res Board, 11: Part 2.
- Shackel, B. (1980). "An Experimental Investigation of the Response of Interlocking Concrete Block Paving to Simulated Traffic Loading". Aust Road Research Rpt 90, pp 11- 43.
- Shackel, B. (1980). "An Experimental Investigation of the Roles of the Bedding sand and Jointing Sands in the Performance of Interlocking Concrete Block Pavements." Concrete/Beton.
- Shackel, B. (1980). "The Design of Interlocking Concrete Block Pavements for Road Traffic." Proceedings of First International Conference on Concrete Block Paving, Newcastle, London Conc. Publishing Co.
- Shackel, B. (1979). "A Design Method for Interlocking Concrete Block Pavements." Proceedings Symposium on Precast Concrete Paving Block, Johannesburg, Concrete Society of Southern Africa.
- Shackel, B., & Arora, M.G. (1979) "The Evaluation of Interlocking Block Pavements" Proceedings of Conference on Concrete Masonry Association Sydney.
- Sharp, K.G., Grad, B.E., Armstrong, P.J. (1986). "The Australian Road Research Board's Program of Testing of Interlocking Concrete Block Pavements." International Workshop on Interlocking Concrete Pavements, Proceedings, Melbourne.
- Smith, D.R. (1996). "Achieving Excellence – Lessons from Recent Port and Airport Projects in America." Proceedings of Fifth International Conference on Concrete Block Paving, Tel-Aviv, Israel. pp 511-531.

- Syed, W. H.(2005). “The Use of Long Term Pavement Performance Data for Quantifying the Relative Effects of Structural and Environmental Factors on the Response and Performance of New Flexible Pavements.” Michingan State University.
- Thickness Design - Asphalt Pavements for Highways band Streets (1991), Manual Series No.1, Asphalt Institute.
- Tighe, S., Chung, W. (2004). “University Curriculum Interlocking Concrete Pavements, Module: Interlocking Concrete Pavements.” Developed for the Interlocking Concrete Pavement Institute,University of Waterloo.
- Timm, D., Priest, A. L., McEwen T. V. (2004), “Design and Instrumentation of the Structural Pavement Experiment at the NCAT Test Track.” NCAT Report 04-01, National Centre for Asphalt Technology, Aurban University,
- Ullitz, P. (1987). “Pavement Analysis.” Elsevier.
- Yang H. H. (1993) “Pavement Design and Analysis.” Prentice Hall, NJ, 1993.
- Ziari, H., Khabiri, M. M. (2007). “Interface Condition Influence on Prediction of Flexible Pavement Life.” Journal of Civil Engineering and Management, Vol XIII, No 1, pp 71–76.